# Technology Plan for the Terrestrial Planet Finder Interferometer

**Edited by:**

**Peter R. Lawson and Jennifer A. Dooley**

**Jet Propulsion Laboratory**
**California Institute of Technology**
**Pasadena, California**

*June 2005*

**Abstract**

The technology plan for the Terrestrial Planet Finder Interferometer (TPF-I) describes the breadth of technology development currently envisaged to enable TPF-I to search for habitable worlds around nearby stars. TPF-I is currently in Pre-Phase A (the Advanced Study Phase) of its development. For planning purposes, it is expected to enter into Phase A in 2010 and be launched sometime before 2020.

TPF-I is being developed concurrently with the Terrestrial Planet Finder Coronagraph (TPF-C), whose launch is anticipated in 2016. The missions are being designed with the capability to detect Earth-like planets should they exist in the habitable zones of Sun-like (F, G, and K) stars out to a distance of about 60 light-years. Each mission will have the starlight-suppression and spectroscopic capability to enable the characterization of extrasolar planetary atmospheres, identifying biomarkers and signs of life. TPF-C is designed as a visible-light coronagraph; TPF-I is designed as a mid-infrared formation-flying interferometer. The two missions, working together, promise to yield unambiguous detections and characterizations of Earth-like planets.

The challenges of planet detection with mid-infrared formation-flying interferometry are described within this technology plan. The approach to developing the technology is described through roadmaps that lead from our current state of the art through the different phases of mission development to launch. Technology metrics and milestones are given to measure progress. The emphasis of the plan is the development and acquisition of technology during Pre-Phase A to establish the feasibility of the mission to enter Phase A sometime around 2010. Plans beyond 2010 are outlined.

The plan contains descriptions of the development of new component technology as well as testbeds that demonstrate the viability of new techniques and technology required for the mission. Starlight-suppression (nulling) and formation-flying technology are highlighted. Although the techniques are described herein, the descriptions are only at a high-level, and tutorial material is not included. The reader is expected to have some familiarity with the principles of long-baseline, mid-infrared interferometry. Selected references to existing literature are given where relevant.

This document will be reviewed annually and updated as needed. The most recent edition is available at http://tpf.jpl.nasa.gov/ or by email request to Peter.R.Lawson@jpl.nasa.gov.

# Approvals

Prepared by: _Peter R. Lawson (signature)_ 6/23/05

Peter R. Lawson          date
TPF-I Technologist

Approved by: _Daniel R. Coulter (signature)_ 6/23/05
JPL

Daniel R. Coulter          date
Project Manager,
Terrestrial Planet Finder

Approved by: _Michael Devirian (signature)_ 6/23/05
JPL

Michael Devirian          date
Manager,
Navigator Program

Approved by: _Jakob van Zyl (signature)_ 6/29/05
JPL

Jakob van Zyl          date
Director, JPL Astronomy &
Physics Directorate

Approved by: _Z. Tsvetanov (signature)_ 06/30/05
NASA HQ

Zlatan Tsvetanov          date
Program Scientist,
Terrestrial Planet Finder

Approved by: _Lia LaPiana (signature)_ 6/30/05
NASA HQ

Lia LaPiana          date
Program Executive,
Terrestrial Planet Finder

# Summary and Highlights

Steady progress in interferometer technology has been achieved since the last development plan was published (*Technology Plan for the Terrestrial Planet Finder*, March 2003).

The most notable success has been the achievement of the goals of the Advanced Cryocooler Technology Development Program. The Lockheed Martin Advanced Technology Center cooler demonstrated breakthrough success by achieving the Advanced Cryocooler Technology Development Program performance specification of 20 mW at 6 K with 150 mW at 18 K. This development program has been now passed along to the James Webb Space Telescope as part of the Mid-Infrared Instrument (MIRI) development.



**Figure i-1.** The first robot of the Formation Control Testbed was commissioned in September 2004.

The Formation Control Testbed, shown in Fig. i-1, commissioned the first of its ground-based formation flying robots in 2004. The robot floats on air bearings above a flat floor and supports a platform on a spherical air bearing, allowing the unit to move and rotate with thrusters as if it were maneuvering in space. The second robot will be commissioned in 2005.

The Planet Detection Testbed has been commissioned since the last development plan and has demonstrated remarkable success with 4-beam nulling with a 10 μm laser to a null depth exceeding $10^{-5}$, as shown in Fig. i-2.

Also notable are significant advances in spatial filter technology, with the first samples of single-mode mid-infrared fibers delivered to JPL and now in use on the Achromatic Nulling Testbed.
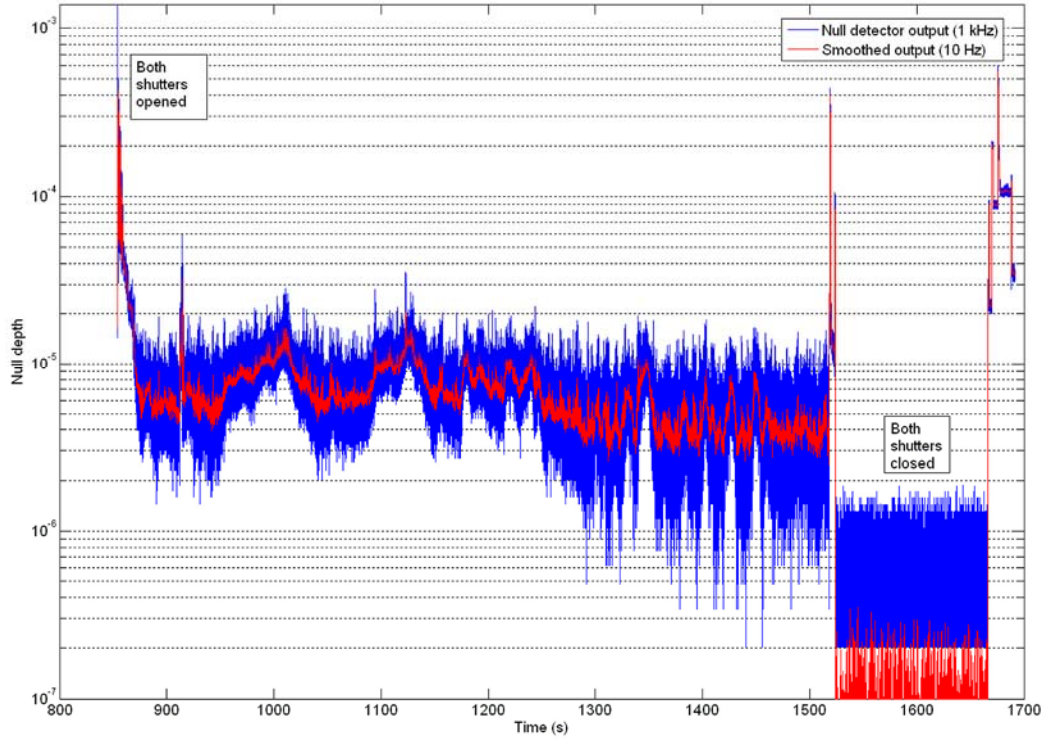


**Figure i-2.** Four-beam nulling with the Planet Detection Testbed was achieved at a level of $10^{-5}$ in May 2005.

# Acknowledgements

# Table of Contents

# 1   Introduction

The Terrestrial Planet Finder (TPF) is envisaged as a series of two space observatories: an 8-m class optical coronagraph (TPF-C), planned for launch around 2016; and a mid-infrared formation-flying interferometer (TPF-I), planned for launch sometime prior to 2020. The goal of these missions, broadly stated, is to understand the formation and evolution of planets and, ultimately, of life beyond our Solar System. These two missions provide a unifying context for all missions within NASA's Navigator Program. They are being managed by the Jet Propulsion Laboratory and supported by the Goddard Space Flight Center, on behalf of the Universe Division of NASA's Science Mission Directorate. An artist's impression of TPF-I is shown in Fig. 1-1.

## 1.1 Purpose and Scope

The primary purpose of this document is to detail the technology development activities for the Terrestrial Planet Finder Interferometer (TPF-I) that will take place in Pre-Phase A. The focus of the technology plan is therefore to lay out the scope, depth, and inter-relatedness of activities that will enable TPF-I to achieve its technology milestones, supporting its entry into Phase A. Within these pages are documented the critical component, subsystem, and system technologies and a schedule of development that includes
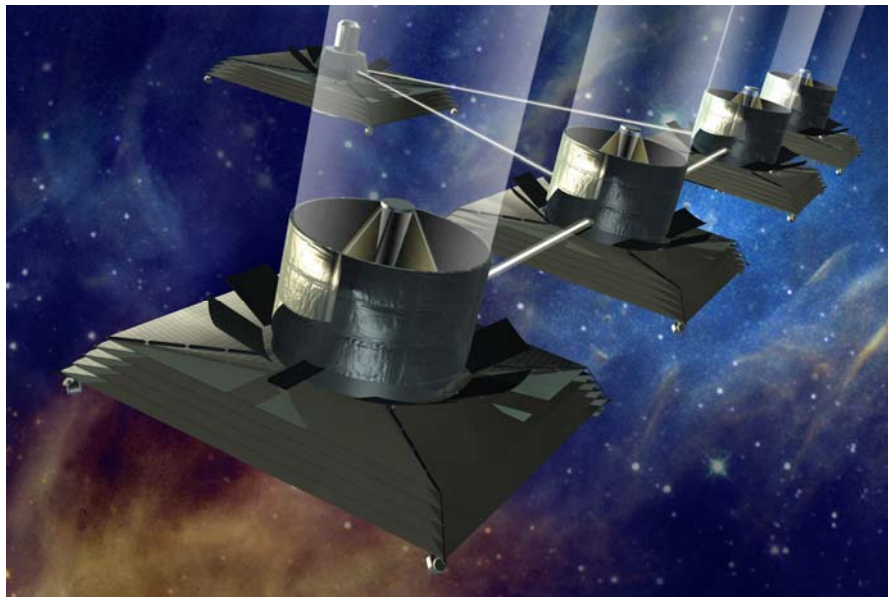


**Figure 1-1.** Artist's Impression of the Terrestrial Planet Finder Interferometer

the progression of NASA Technology Readiness Levels. Although the focus is near-term, roadmaps are presented that lead the technology development onwards towards the eventual flight system.

A previous version of the TPF Technology Plan was prepared in 2003, and at that time charted the path for the technology development for both a coronagraph and an interferometer architecture for TPF. This updated plan, focusing solely on TPF-I, expands upon the earlier document, presenting more detailed requirements and error budgets that justify the current technology goals. This information is presented with the understanding that the error budgets are subject to revision as the technology matures.

## 1.2 Science Objectives

This section describes the measurement requirements, assumptions and definitions for the detection and characterization of extrasolar planetary systems. This description is based on deliberations by the TPF Science Working Group in 2004, but includes minor revisions specifically for TPF-I. It should be kept in mind that these objectives are subject to change and will be revised by the new Science Working Group.

The major scientific objectives of TPF-I are: (1) search for and detect any Earth-like planets in the habitable zone around nearby stars; (2) characterize Earth-like planets and their atmospheres, assess habitability and search for signatures of life; (3) carry out a program of comparative planetology; and (4) enable a program of "revolutionary" general astrophysics. A mission lifetime of 5 years, possibly
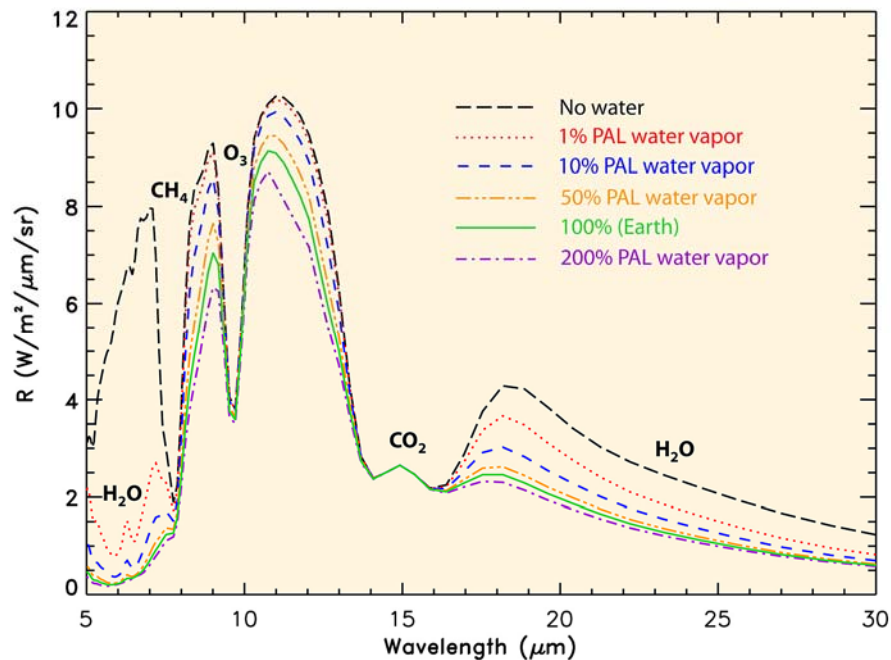


**Figure 1-2**. Appearance of Earth-like planets as seen in the mid-infrared wavelength range for a range of different planetary water abundances, shown as percentages of Earth's present atmospheric level (PAL). These synthetic spectra were generated using a planetary radiative transfer model and convolved to mimic the spectrum seen by a spectrometer with a constant wavenumber resolution of 40 cm$^{-1}$. Courtesy of G. Tinetti, V. Meadows, and D. Crisp (California Institute of Technology).

extended to 10 years, is foreseen. It is worth noting that neither the comparative planetology nor the general astrophysics programs will be considered as design drivers for the mission. These programs are intended to be carried out at little or no additional expense to the project.

The core scientific goal of TPF-I is to detect directly and characterize Earth-like planets around nearby stars. The requirements that flow down from this goal define the characteristics of the observatory design and the mission. In particular, the ability to directly detect planets implies that TPF-I must be capable of separating the planet light from the starlight. Moreover, the facility must provide a sensitivity that will enable spectroscopic measurements of the light from the planet to determine the type of planet, its gross physical properties, and its main atmospheric constituents — the ultimate goal, of course, being to assess whether life or habitable conditions exist there. TPF-I will be designed so that, with a high degree of confidence, it will be capable of detecting Earth-like planets should they exist in the habitable zones of the stars in its survey.

The habitable zone is defined as that region around a star within which liquid water may continue to exist on a planet's surface for geologically significant timescales. A planet located in the habitable zone would in principle be habitable by water-based life like our own. The location of the habitable zone is a function of stellar type and is defined here to be the range of semi-major axes corresponding to the orbits of Venus and Mars (0.7 AU to 1.5 AU) scaled according to the square-root of the luminosity of the specific star in question.

TPF-I will focus its search to Sun-like and similar stars, broadly defined as those main-sequence stars with spectral types F, G, and K, either in single systems or wide binaries. A few nearby A and M stars may be considered in addition to the primarily solar-type stars. M dwarfs closest to our Solar System (having habitable zones with the largest angular sizes) will probably also be considered candidates for TPF searches.

The TPF Science Working Group recommended in 2003 that the TPF missions (TPF-C and TPF-I) be designed so they are capable of detecting and characterizing terrestrial-type planets having a surface area as small as half the surface area of the Earth. For TPF-I, a spectral resolution of at least 20 was recommended at mid-infrared wavelengths, over a spectral band extending from 6.5 to 13 μm, and if possible out to 17 μm.

As a *minimum*, TPF-I must be able to detect planets with half the area of the Earth, and the Earth's geometric albedo or the equivalent effective temperature, searching the entire habitable zone of the core-group of stars with 90% completeness per star. Flux ratios must be measured in 3 broad wavelength bands, to 10% accuracy, for at least 50% of the detected terrestrial planets. A spectral resolution of 20 must be used for planet characterization. The spectrum must be measured—for at least 50% of the detected terrestrial planets—to give the equivalent widths of $H_2O$, and $O_3$ in the mid-infrared to an accuracy of 20%. A mission lifetime of 5 years is required as a minimum. A simulated spectrum on an Earth-like planet is shown in Fig. 1-2.

As a *goal*, TPF-I must be able to detect planets with half the area of the Earth, with Earth's geometric albedo, searching the habitable zone (HZ) of the 150 core-group stars and additional stars with 90% completeness. Flux ratios must be measured in 3 broad wavelength bands to 10% accuracy for at least 50% of the detected terrestrial planets. A spectral resolution of 40 must be used for planet
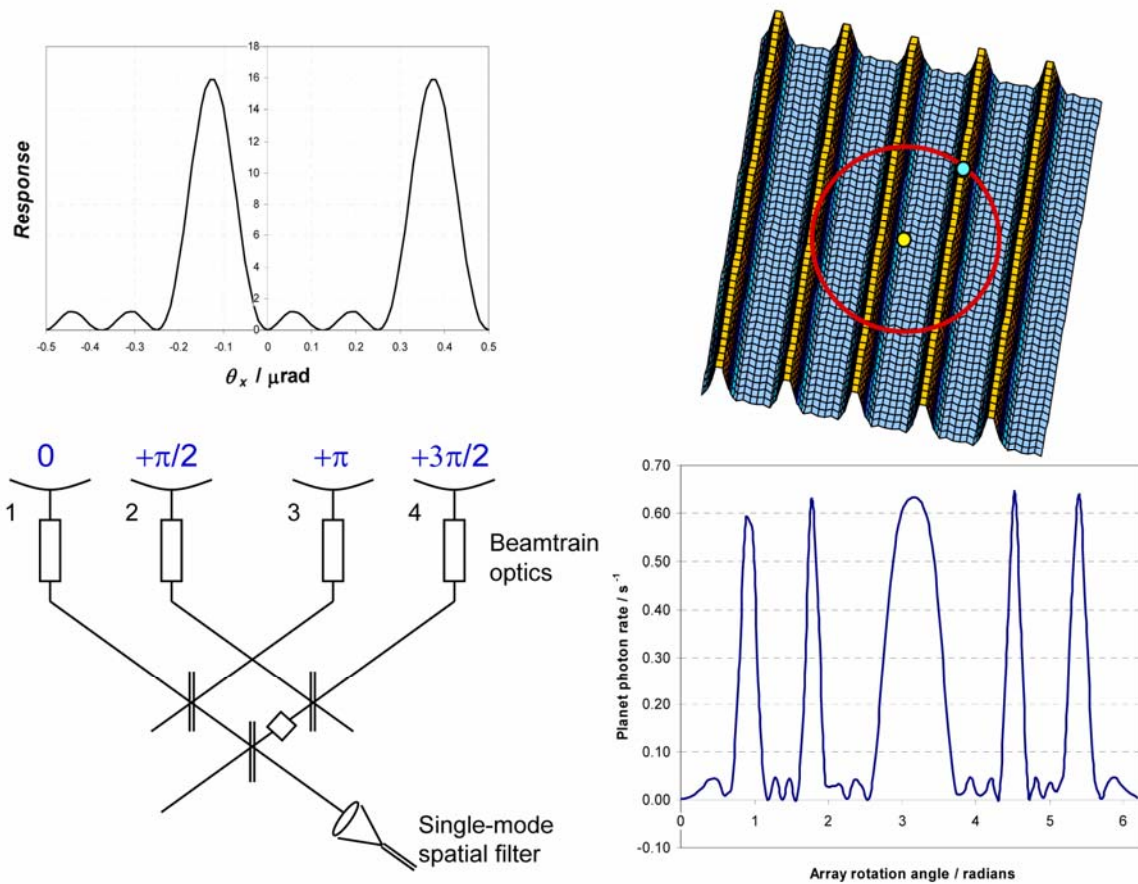
**Figure 1-3.** Planet detection with TPF-I: In this example the interferometer (bottom left) first nulls the signals from pairs 1 & 3 and 2 & 4, and then cross-combines the nulled outputs to arrive at the fringe response (top left). The null of the response is centered on the star, shown as the central dot in the fringe pattern (top right). The response due to the presence of a planet (the dot in the circle, top right), then rises and falls in a characteristic pattern (bottom right) as the fringe pattern is swept about the star.

characterization. The spectrum must be measured—for at least 50% of the detected terrestrial planets—to give the equivalent widths of $CO_2$, $H_2O$, $O_3$, and $CH_4$ in the mid-infrared to an accuracy of 20%. Further, we desire that the mission search an *extended group of stars* defined as those systems *of any type* in which all or part of the Continuously Habitable Zone (0.9–1.1 AU, scaled according to the square-root of the luminosity of the star) can be searched. An extended mission lifetime of up to 10 years is desired.

To date, the TPF Science Working Groups (SWG) have not imposed requirements for polarization sensitivity. This would be needed for example to detect features that shine in reflected (thus polarized) light in the observed planetary system. Because there have been no related science requirements, polarization in this plan is treated as a purely technical issue that could limit the depth of star suppression. Polarization is not discussed as a science tool for planet characterization.

**Caveat:** The constraints imposed by the completeness requirement were extensively discussed by the TPF-SWG in 2004 and were deemed to be overly restrictive, since they force revisits to the same stars at the expense of surveying a larger sample.

# 1.3 How TPF-I Detects Planets

TPF-I was designed as a mid-infrared observatory, in part because at longer wavelengths the contrast between star and planet is more favorable for planet detection than at visible wavelengths. However, at mid-infrared wavelengths an observatory must have a primary mirror 10 or 20 times larger to have the same angular resolution required for planet finding. The approach to building a mid-infrared observatory has therefore been to design it as an interferometer, combining the light from several individual telescopes that work in concert, obviating the need to construct such a large primary mirror. The light from the parent star would still overwhelm the light from the planet, unless the interference fringes were controlled in such a manner that the response of the interferometer is minimum in the direction of the star, but modulated by planet light in other (nearby) directions on the sky. As illustrated in Fig. 1-3, planets can then be detected by rotating the fringe pattern of the array (rotating the telescope array as a whole with respect to the star) and observing the change in amplitude of the detected light. Planets at a given distance from the star will produce a time-sequence of detected signal that is characteristic of their orbit. Mid-infrared techniques are used to minimize the background due to exozodiacal dust, and arrays that chop back and forth using two pairs of telescopes (for example the Dual-Chopped Bracewell array) are commonly presented in the literature for this reason. Although the total observing time for a given star/planet may be numbered in days, the stability of the interferometer need only to be maintained for several hours at a time. This represents the time between calibrations of the fringe tracker measurements compared to the science detector. In this regard the technology for instrument stability is similar to the TPF Coronagraph.

# 1.4 Mission Description

The current concept of the TPF-I mission begins with the launch of a single heavy-class launch vehicle from Kennedy Space Center. The complete observatory, traveling as one integrated assembly, is flown to the Sun-Earth L2 point. At the L2 point the observatory is inserted into a halo orbit. L2 was chosen over an Earth drift-away orbit like that used by the Spitzer mission because L2 offers simpler telecommunications geometry, a lower insertion energy requirement, and the option to launch ground-based spare spacecraft to the orbit after the deployment of the original formation.

Figure 1-4 depicts a concept for the **cruise stage.** The cruise stage is used to transport the formation as packaged for launch from Earth to L2. The cruise stage also protects the optics from some potential contamination sources during launch. The stage includes a separate propulsion system, solar panels, and mechanical structure. The electronics on the combiner spacecraft are used to control the cruise stage. On the way to L2 the cruise stage performs a slow "barbecue" roll to maintain a benign thermal environment for the spacecraft within its shell. After arrival at L2 the cruise stage is used to deploy the individual spacecraft of the observatory one at a time. Ground operators verify successful deployment of each spacecraft before deploying subsequent spacecraft. After all the spacecraft are deployed the formation is formed and calibration begins. Following initial calibrations, the observatory is commissioned and the prime mission begins.

Cruise Stage Enclosure Section separates to expose Collector #2 for deployment

Aft Prop Module / Collector Enclosure Section 1 separates to expose Collector #1 for deployment

Cruise Stage Position and Attitude maintained by Combiner S/C using Cruise Stage Forward RCS

Collector #1 Separates from S/C aft attach fitting, deploys with gentle spring push off

Combiner Spacecraft

Collector Spacecraft (4)

Cruise Stage

Cruise Stage sustains launch loads and provides contamination protection for optics during launch and cruise phases

**Figure 1-4.** Cruise Stage

Table 1-1 has a summary of the properties of the current TPF-I observatory concept. The prime mission lasts five years with approximately three years budgeted for star system surveys and two years budgeted for detailed, follow-up studies of targets found by the surveys. Enough expendable resources are carried to permit extending the mission another five years if consumption of these resources is as predicted and the observatory remains healthy.

Observations consist of aligning the observatory's viewing axis to a target star, adjusting the formation baseline length to an optimum value (tuning), and then rotating about that axis for multiple hours until a sufficient signal-to-noise ratio (SNR) is attained. Depending on the length of the observation, data are either downlinked before slewing to the next target system or recorded and played back after completing the observation of a multiple-target set. It is envisioned that the observatory will be capable of completing slews and observations of multiple targets autonomously. However, it is not certain that this capability will be used since the frequency of calibrations requiring ground interaction has not been analyzed yet.

Geometrical thermal constraints will limit the target set to stars within ~± 45° of the ecliptic. This band of stars will be observed multiple times as the Earth/observatory system orbits the Sun. The target set includes many of the stars to be observed by the TPF Coronagraph.

# 1.5 Observatory Description

Two types of spacecraft are used to form the observatory: multiple collector spacecraft and a single combiner spacecraft. Figure 1-5 depicts the current concept for the **collector spacecraft**. The collector spacecraft carry the telescopes that collect the light from the target systems and relay these beams to the combiner spacecraft. Each collector carries a primary mirror that is currently conceived to be monolithic and somewhere between 3.5 m and 4.0 m in diameter. The size of the primary mirror is limited by the launch vehicle fairing diameter. Each collector spacecraft has a 5-layer sunshade that permits the optics to be passively cooled to about 40 K. The sunshade is sized and shaped to permit observation of target stars ~45° above and below the ecliptic plane. The figure shows additional deployable radiators surrounding the primary mirror. Traditional spacecraft electronics and mechanical components are configured to remain on the warm (sunlit) side. The engineering bus features solar power, block-redundant critical electronics, reaction wheels, and small thrusters for formation flight. Larger thrusters might also be required for retargeting of the formation and station keeping. The collector spacecraft include RF systems for spacecraft-to-spacecraft communications, spacecraft-to-Earth communication, and coarse formation flying acquisition. (The formation flying acquisition sensor is the subject of the Formation Sensor Testbed described in a later section.) The spacecraft-to-Earth communication system is a backup since most communications between the ground and observatory are planned to be through the combiner spacecraft. Some architectures demand that some of the collectors also relay optical beams from other collectors. In the top view (Fig. 1-5, left) one can see stray light baffles for these optical relays.

**Table 1-1. Illustrative Properties of a TPF-I Observatory Concept\***

| Parameter | 4-Telescope Dual Chopped Bracewell Design |
|---|---|
| Telescopes | Four 4-m diameter telescopes, diffraction limited at 2 μm operating at 40 K |
| Array size | 60–150 m center-to-center of outer telescope in linear array |
| Baseline range | 40–100 m |
| Wavelength range | 7–13 μm with a goal of 7–17 μm |
| Angular resolution (maximum) | 50–75 milli-arcseconds |
| Field-of-view | 1 arcsec at 12 μm |
| Spectral resolution $\Delta\lambda/\lambda$ | 20 with a goal of 40 |
| Sensitivity | 0.35 μJ at 12 μm |
| Number of core stars | 150 |
| Biomarkers | $H_2O$ and $O_3$ with a goal of also measuring $CO_2$ and $CH_4$ |
| Field of regard | ±45° of anti-Sun direction |
| Orbit | L2 Halo orbit |
| Mission duration | 5 years baseline with a goal of 10 years |
| Mission launch | 2019 with Heavy-class launch vehicle, Delta 4050H |

*Further details are available in Appendix F
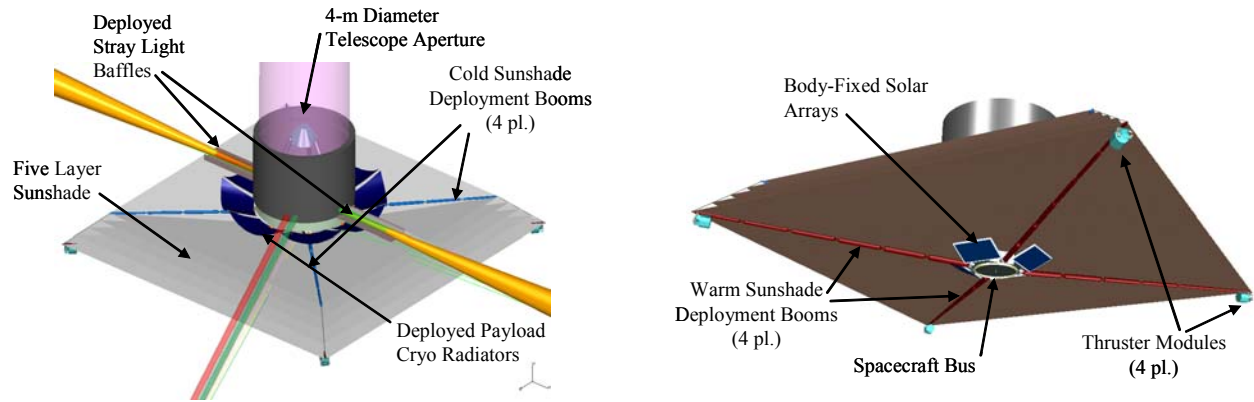
**Figure 1-5.** Collector Spacecraft
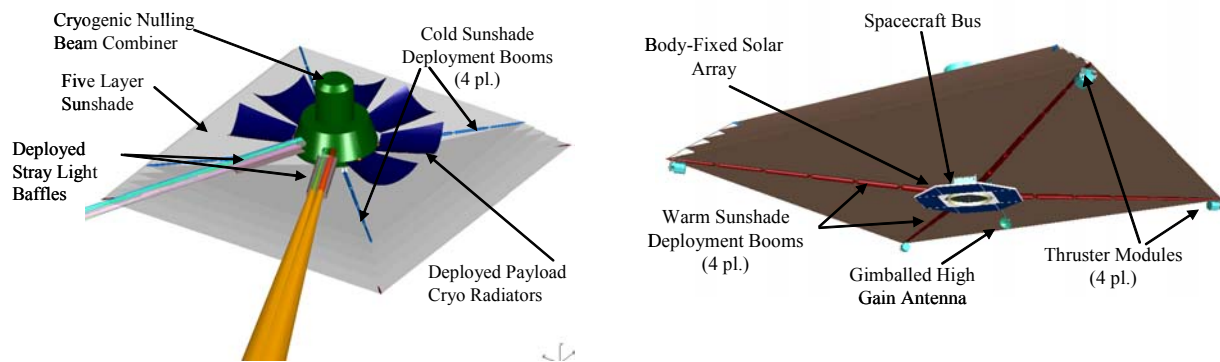


**Figure 1-6.** Combiner Spacecraft

Figure 1-6 depicts a concept for the **combiner spacecraft**. The combiner spacecraft receives the optical beams from the collectors and combines them to produce the interferometric fringes that reveal planet light; consequently, the combiner spacecraft houses the science detectors. The primary detector operates at about 6 K, so the combiner spacecraft carries a cryocooler which was the subject of a technology development effort. The combiner is also the point from which pathlength metrology sources are launched. Like the collectors, the combiner spacecraft has a 5-layer sunshade, deployable cryo radiators, stray light baffles, and traditional spacecraft electronics and mechanical components including reaction wheels, thrusters, and RF systems. Unlike the collectors, the combiner serves as the central hub for formation communication both within the formation and from the formation to the ground. Consequently, it carries more extensive RF systems including a gimbaled high gain antenna for communications with the ground.

The geometric configuration of the deployed array is the subject of ongoing study; however, the two arrangements shown in Fig. 1-7 look the most promising. Both feature four collector spacecraft shown in green and one combiner spacecraft shown in yellow. Beam paths are shown by the colored lines. The **linear Dual Chopped Bracewell** (DCB) design can have its beams combined in either a high resolution
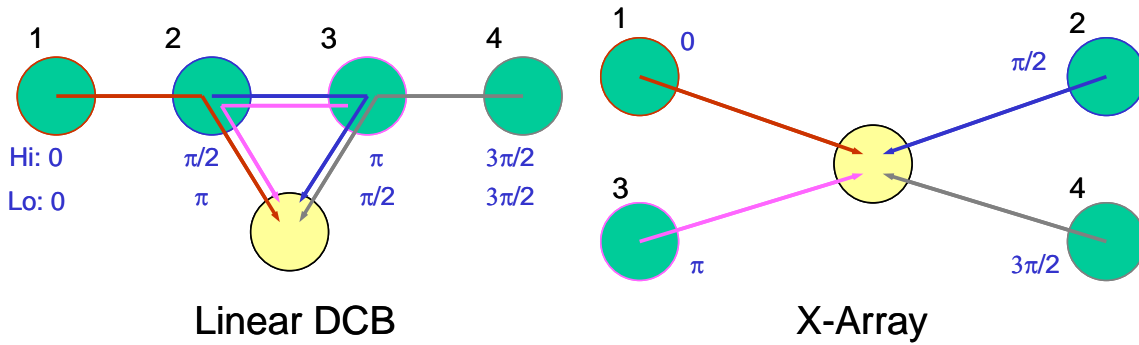
**Figure 1-7.** Leading Formation Architectures

mode (collectors 1+3 & 2+4 combined) or a low resolution mode (collectors 1+2 & 3+4 combined). The linear DCB requires that the inner collector spacecraft carry additional beam relay optics. The **X-array** has one resolution mode but features a nulling baseline (short side of the rectangle), which determines how well light from the target star is rejected. The nulling baseline can be adjusted independently of the imaging or resolution baseline (long side of the rectangle), which determines how well signals from multiple planets can be resolved. To enable this adjustability the combiner of the X-array must have receiving optics that can accommodate beams arriving at different angles from the collectors.

Both architectures demand that the separations between spacecraft be adjustable. The minimum separation distance between spacecraft is limited by concerns of collision. In the current designs, the sunshields are square and measure 15 m on each side; the current working assumption is that a separation of 5 meters (edge of sunshield to edge of sunshield) is the minimum tolerable. This then translates to the minimum array sizes shown in Fig. 1-8. The maximum separations are limited by stray light concerns. Light from the layers of the sunshields can not be allowed to enter the science beam or the light will swamp the planet signals. The current concept for the stray light baffles permit maximum separations of about 35 meters edge-to-edge, which implies the maximum array sizes shown in the right hand side of the figure.
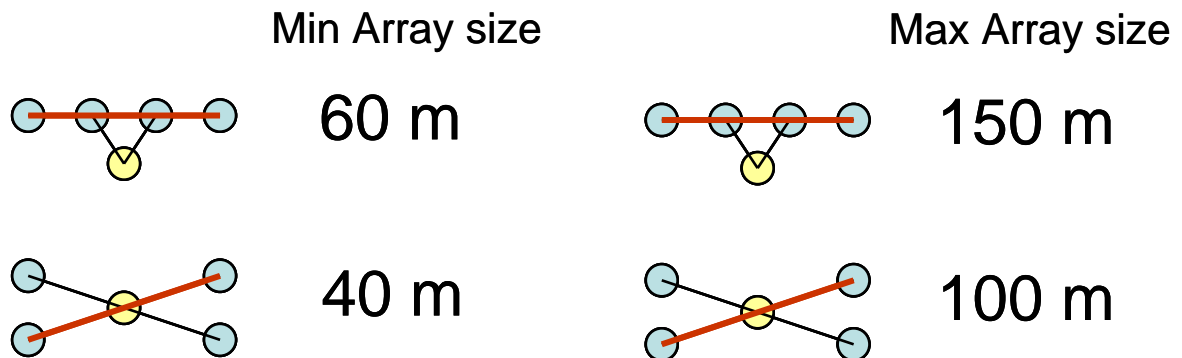


**Figure 1-8.** Limits of Array Sizes
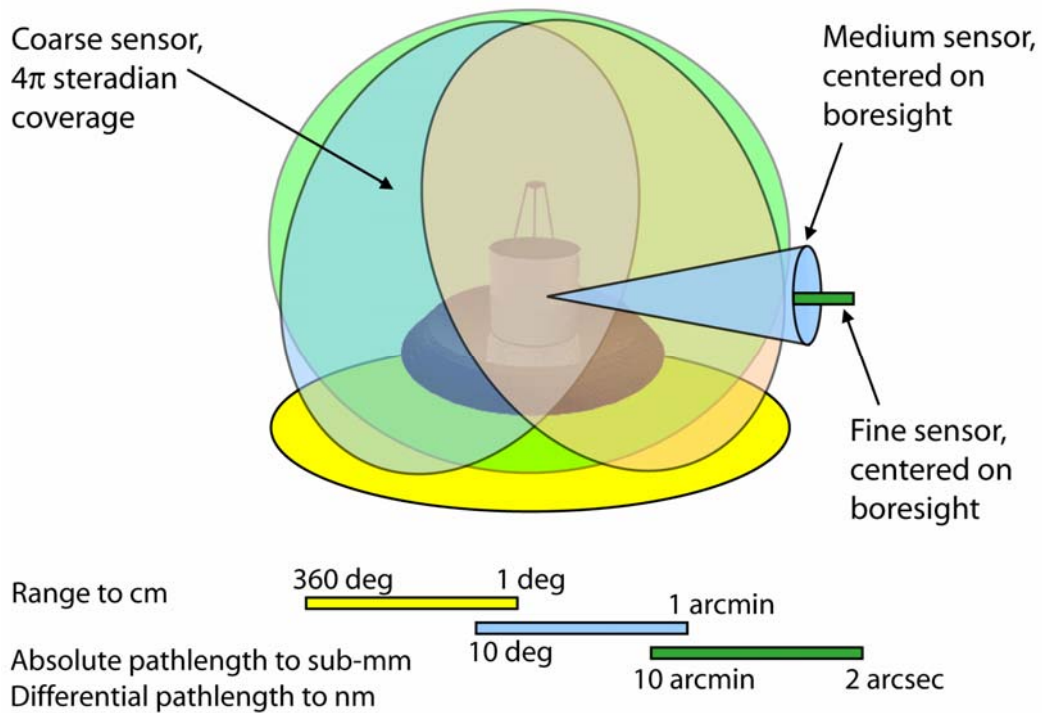
**Figure 1-9.** Formation Sensor Envelopes

One of the things needed for establishing the formation is a suite of sensors that provide measurements of the relative orientation, range, and bearing angle between spacecraft. Figure 1-9 shows the concept for this suite. First applied is a set of coarse sensors that together can sense in every direction. (This coarse sensor is the subject of the Formation Sensor Testbed described in a later section.) A concept for the medium sensor has not been explored in detail yet, as there is promise that the coarse sensor may perform well enough that it could hand off directly to the fine sensor. The fine sensor is comprised of the metrology systems of the instrument itself and will likely include an extension of the metrology system, which began during the development of the StarLight mission, or related technologies being used on the Space Interferometry Mission that require picometer-level knowledge.

Figure 1-10 is a simplified block diagram of the **instrument** for a linear DCB architecture. The diagram shows the science beams, but excludes elements and beam paths used for metrology and control loops. Light is collected on spacecraft #1, conditioned for beam transport, and relayed to spacecraft #2. Spacecraft #2 relays the light to the beam combiner spacecraft where it is compressed. The beams are then fed to the delay lines, which are the subject of a technology development effort described in a later section. After some pointing and shear corrections the beams encounter the adaptive nuller, which is also the subject of a technology development effort. After some additional corrections the beams enter the nullers, which are another technology development item. The output of one of the nullers goes through a chopping mechanism. Chopping is used to shift the instrument's response on the sky by $\pi$, thereby allowing planet signals to be distinguished from the much brighter, but predominantly symmetric, zodiacal dust clouds (local and exo-) through which the planets are observed. The beamtrains then enter the cross combiner, spatial filters, dispersive elements and finally the science detector. Spatial filters are expected to be important in relaxing the fabrication tolerances of upstream optical elements and consequently are the focus of a technology development effort.
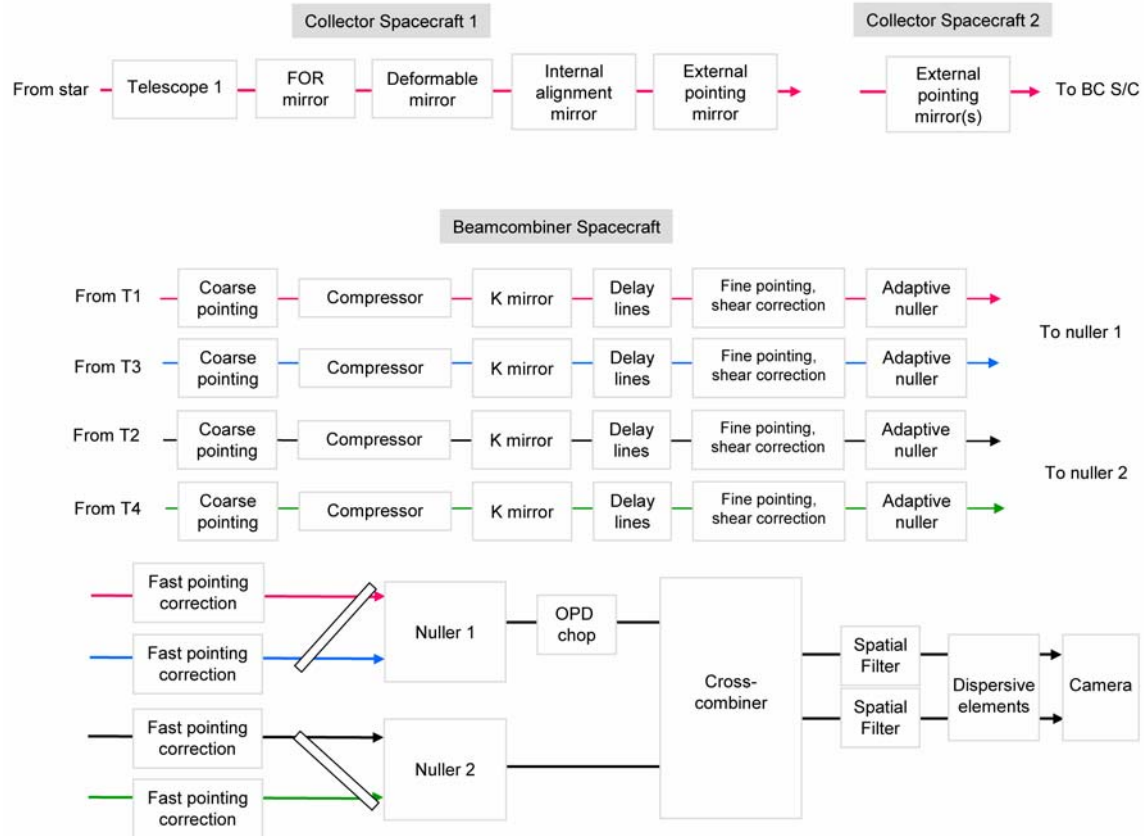
**Figure 1-10.** Schematic Overview of the Design Concept for the TPF Interferometer

# 1.6 TPF-I Technology Plan Overview

The material contained in this technology plan is divided into several themes: (1) starlight suppression; (2) formation flying; (3) cryogenic technology; and (4) integrated modeling and model validation. This division into themes is followed in the description of requirements and the technology roadmaps, as well as in the divisions of chapters in the latter part of the document. Overall, the plan places the most emphasis on the development of starlight suppression and formation flying technology.

Chapter 2, *Preliminary Requirements and Error Budgets*, describes the requirements that set the foundation for technology development described in subsequent chapters. This chapter describes the technology needs of starlight suppression, formation flying, cryogenic technology, and integrated modeling for the most part in terms of error budgets and preliminary error budget allocations. In cases where error budgets have not been fully developed, the reasoning behind the current technology goals is described with the acknowledgement that more detailed justification is needed prior to the next revision of this plan.

Chapter 3, *Technology Development Strategy*, describes the philosophy and roadmap of technology development that will be followed in Pre-Phase A. The requirements described in the previous chapter are organized in terms of inter-related testbed tasks. The Pre-Phase A goals are presented in the context of a long-term plan towards the development of a TPF-I flight system. Included here are the technology

roadmaps and high-level gates and milestones for the different themes, as well as the current and predicted heritage from related NASA missions. The objectives in the chapter are described in terms of high-level gates and milestones, with the milestones noted as being major advances along the path to a technology gate. The gates define the final accomplishment of a technology task or testbed. The gates in this technology plan are listed below, and appear along with their related milestones at the end of Chapter 3.

## Optics and Starlight Suppression Gates

**Starlight Suppression (Depth & Bandwidth at Temperature):** Using the Achromatic Nulling Testbed, demonstrate that infrared light over a spectral bandwidth of $\geq 25\%$ can be suppressed by $\geq 10^6$ at $\leq 40$ K. Accompany these results with an optical model of the Achromatic Nulling Testbed, validated by test data, to be included in the model of the flight-instrument concept. This demonstrates the approach to the broadband starlight suppression needed to characterize terrestrial planets for habitability at a flight-like temperature. *Gate TRL 5.* **Date: Q1/FY2007.**

**Planet Extraction:** Using the Planet Detection Testbed (PDT), demonstrate extraction of a simulated (laser) planet signal at a star/planet contrast ratio of $\geq 10^6$ for a rotation of the flight formation lasting $\geq 5000$ s. Accompany these results with a control system model of the Planet Detection Testbed, validated by test data, to be included in the control system model of the flight-instrument concept. Success shows flight-like planet sensing at representative stability levels within a factor of 20 of the contrast at 1/10 the flight observation duration. *Gate TRL 5.* **Date: Q3/FY2007.**

**Dispersion Control at Temperature:** Using the Adaptive Nuller**,** demonstrate that optical beam amplitude can be controlled with a precision of $\leq 0.2\%$ and phase with a precision of $\leq 5$ nm over a spectral bandwidth of $> 3$ µm in the mid IR for two polarizations at $\leq 40$ K. Accompany these results with a model of the Adaptive Nuller, validated by test data, to be included in the model of the flight-instrument concept. This demonstrates the approach for compensating for optical imperfections that create instrument noise that can mask planet signals at the temperature required for flight operations. *Gate TRL 5.* **Date: Q3/FY2009.**

## Formation Flying Gates

**Formation Flying (5-Spacecraft Simulation With Fault Recovery):** Using the Formation Algorithms & Simulation Testbed, simulate the safing and recovery of a five-spacecraft formation subjected to a set of typical spacecraft faults that could lead to mission failures unique to formation flying such as collisions, sensor faults, communication drop-outs, or failed thrusters in on or off states. Simulations can be limited to single-fault scenarios. This demonstrates the robustness of formation control architecture, as well as fault-tolerance of the on-board formation guidance, estimation, and control algorithms to protect against faults that have a reasonable probability of occurring sometime during the TPF-I prime mission and that are unique to TPF-I's unprecedented use of close formation flying. *Gate TRL 5.* **Date: Q4/FY2007.**

**Formation Flying (Multiple Robot Demonstration With Fault Recovery):** Using the Formation Control Testbed, demonstrate that a formation of multiple robots can be safed following the injections of a set of typical spacecraft faults that have a reasonable probability of occurring during flight.

Demonstrations can be limited to single-fault scenarios. This validates the software simulation of fault recovery for formation flight. *Gate TRL 5.* **Date: Q4/FY2008.**

## Cryogenic Technology Gate

**Cryocooler Development:** With the Advanced Cryocooler Technology Development Program, demonstrate that the development model coolers meet or exceed their performance requirements to provide ~30 mW of cooling at 6 K and ~150 mW at 18 K. This demonstrates the approach to cooling the science detector to a temperature low enough to reveal the weak planet signals. *Gate TRL 5.* **Date: Q4/FY2006 (Completed Q2 2005).**

## Integrated Modeling Gate

**Observatory Simulation:** Demonstrate a simulation of the flight observatory concept that models the observatory subjected to dynamic disturbances (e.g., from reaction wheels). Validate this model with experimental results from at least the Planet Detection Testbed at discrete wavelengths. Use this simulation to show that the depth and stability of the starlight null can be controlled over the entire waveband to within an order of magnitude of the limits required in flight to detect Earth-like planets, characterize their properties, and assess their habitability. *Gate TRL 5.* **Date: Q4/FY2009.**

The remaining chapters of the technology plan are then devoted to a more detailed description of technology and testbed activities, separated into the individual themes. Chapter 4 describes *Optics and Starlight Suppression Technology*, divided into component, subsystem, and system testbeds. Chapter 5 describes *Formation Flying Technology*, divided into formation knowledge, control, and propulsion systems. Chapter 6 describes *Cryogenic Technology* in terms of cryogenic structures, and materials, as well as cryocooler technology. Chapter 7 describes tasks related to integrated modeling and the development of a comprehensive observatory simulation.

The document concludes with a list of appendices that provide further background information. Appendix A provides the organization charts that describe the management of the work described here. Apppendix B contains a summary table of activities. Appendix C shows detailed schedules. The member of the TPF-I Science Working Group and the TPF Technology Advisory Committee are listed in Appendix D and Appendix E, respectively. The current flight-system configuration is given in tables in Appendix F. The NASA Technology Readiness Levels, quoted extensively as part of the testbed descriptions, are listed and defined in Appendix G. Optical materials and properties to suit an adaptive nuller are listed in Appendix H. Finally, a list of acronyms and suggestions for further background reading are given in Appendix I and Appendix J.
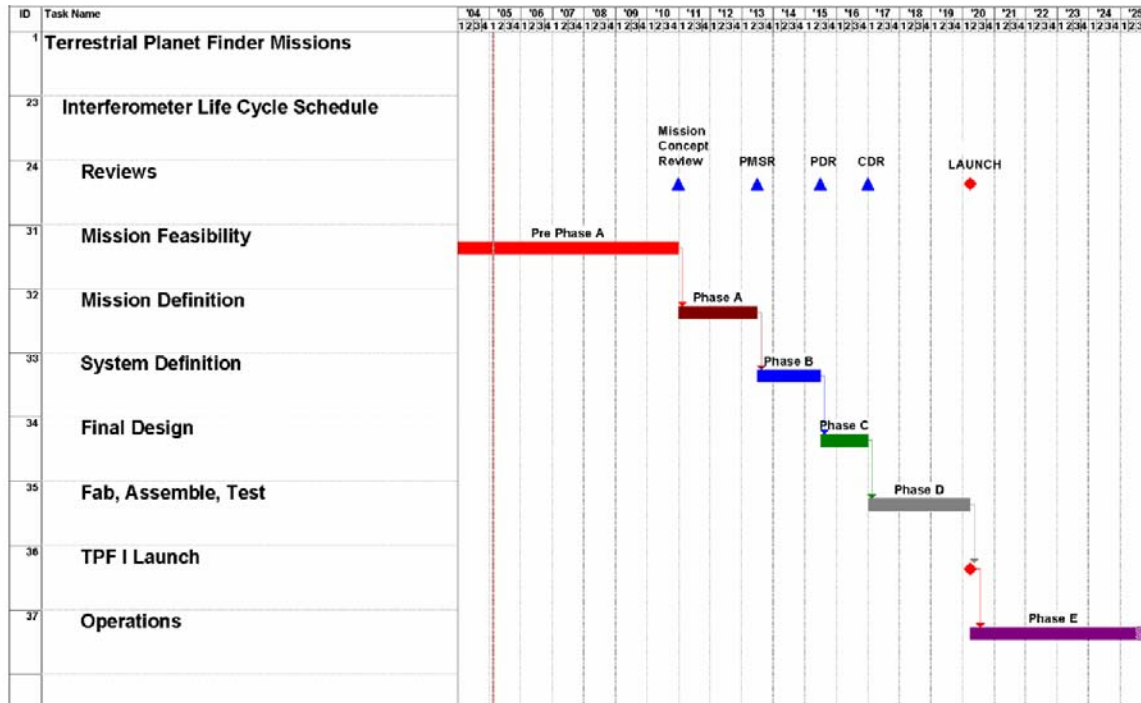
**Figure 1-11.** TPF Life Cycle Schedule

# 1.7 TPF-I Project Schedule

The TPF-I Project is in the first (or Pre-Phase A stage) of the NASA Project Life Cycle. In this phase a wide range of missions and technology concepts are explored, and the emphasis is on establishing top-level goals, science requirements, and the technological feasibility of the mission. Figure 1-11 shows a top-level TPF-I schedule. Launch is planned to be near the end of calendar 2019 (first quarter of fiscal 2020). The boundaries between the phases are notional as detailed analysis has not been performed of the durations of major development-phase tasks such as the fabrication of primary mirrors. The details of the schedule for the ongoing technology development activities are included in the appendices.

**Bibliography**

C. Henry, O.P. Lay, M. Aung, S.M. Gunter, S. Dubovitsky, G.H. Blackwood, "Terrestrial Planet Finder: architecture, mission design, and technology development," in *New Frontiers in Stellar Interferometry*, edited by Wesley A. Traub, Proceedings of SPIE Vol. 5491 (SPIE, Bellingham, WA 2004) 265–274.

G.H. Blackwood, E. Serabyn, S. Dubovitsky, M. Aung, S.M. Gunter, C. Henry, "System design and technology development for the Terrestrial Planet Finder infrared interferometer," in *Techniques and Instrumentation for the Detection of Exoplanets*, edited by Daniel R. Coulter, Proceedings of SPIE Vol. 5170 (SPIE, Bellingham, WA 2003) 129–143.

E. Serabyn and M.M. Colavita, "Fully symmetric nulling beam combiners," *Applied Optics* 40, 1668–1671 (2001).

# 2   Preliminary Requirements and Error Budgets

## 2.1 Starlight Suppression Requirements

### Planet Detection and the Suppression of Starlight

An earth-like planet is approximately $10^7$ times fainter than its Sun-like parent star at a wavelength of 10 μm. Viewed from a distance of 15 pc, the angular offset is no more than 67 milliarcseconds. The technique of interferometric nulling is employed to cancel out the signal from the star while isolating the photons from the planet, and has been discussed extensively in the literature. We show in the following section that a null depth of about $10^{-6}$ is required for the detection of such a planet, that degree of suppression being sufficient to reduce the level of photon noise and systematic noise in the measurement.

Consider the light arriving from the star. Each collector samples a patch of the incoming wavefront, which is then routed to the combiner spacecraft, phase-shifted, added to the contributions from the other collectors and coupled into a single-mode spatial filter prior to detection. The amplitudes and phases of the electric fields in the spatial filter can be represented schematically as shown in Fig. 2-1. Figure 2-1a depicts the ideal case for a Dual Bracewell configuration, in which the fields have been phased exactly to sum to zero and no stellar photons appear at the detector.
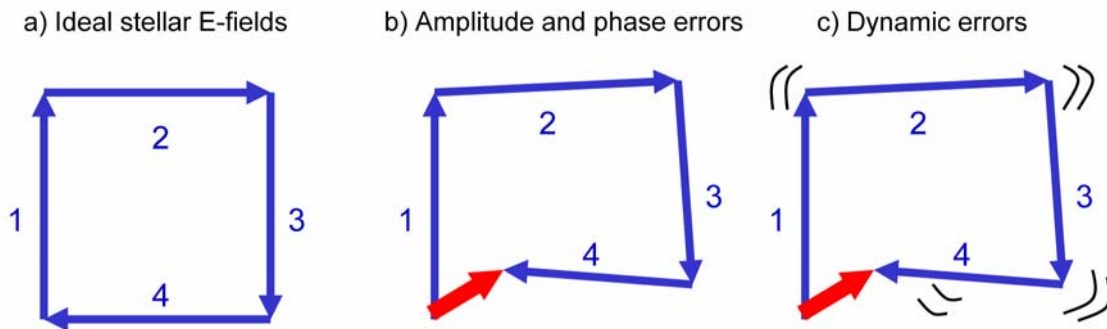


**Figure 2-1.** a) Summation of electric fields in the spatial filter for an ideal dual-chopped Bracewell nulling configuration. b) Amplitude and phase errors in the contributions from the different collectors lead to a residual leakage of photons. c) As the amplitude and phase errors vary with time, the residual photon leakage rate fluctuates and can mimic the presence of a planet.
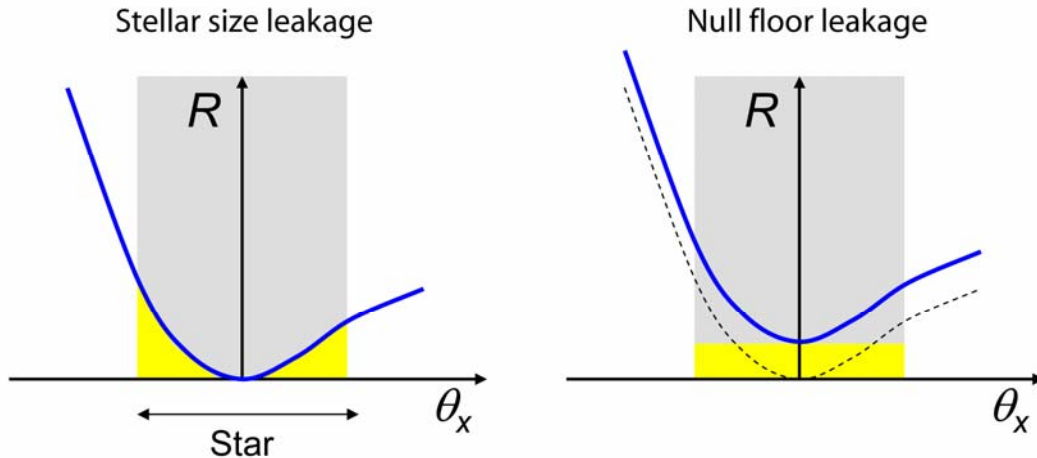
**Figure 2-2.** Schematic illustration to depict the distinction between size leakage and null floor leakage. The horizontal axis represents angular offset on the sky relative to the center of the star; the vertical axis represents the response of the interferometer. The grey rectangle represents the angular diameter of the star that leaks around the null, even in the case of an ideal instrument with zero on-axis response. Null floor leakage is caused by imperfections in the instrument that degrade the on-axis response.

The wavefront for planet photons is tilted with respect to the stellar wavefront, introducing additional phase shifts that can result in constructive summation of the planet light at the same time as the starlight is cancelled. The relative phasing of the planet E-fields varies as the array is rotated, leading to characteristic temporal variation in the detected planet photon rate.

The ideal stellar null is only obtained for a point-like source of light, however. Stars emit from an extended disk, and a number of the photons 'leak around' the ideal null, as shown in Fig. 2-2. To this 'stellar size leakage' must be added the leakage arising from both exozodiacal and local zodiacal dust emission. Together, these leakage photons are a source of random photon noise for even an ideal instrument. Imperfections in the instrument generate additional sources of random photon noise: stray light, thermal emission from the optics, and errors in the relative amplitudes and phases of the collector electric fields. The latter — termed 'null floor leakage' — results from mismatches in the optical beam trains, and is illustrated in Figs. 2-1b and 2-1c.

The random errors just described arise from shot noise — the statistical fluctuation in photon arrival rates. Systematic errors are fundamentally different in nature: if the instrument amplitude and phase errors vary with time (Fig. 2-1c), then the leakage electric field will also fluctuate and can mimic a planet signal. It is the systematic errors, not the random photon noise, that drive the requirements on the TPF-I instrument. A detailed description of this analysis can be found in Lay (2004).

To provide a stable null, the instrument must continually maintain the location of the null on the position of the star. This is done by controlling the optical pathlengths throughout the instrument. Monitoring of the nulled photon rate itself does not provide sufficient accuracy at the bandwidths needed, since other sources of emission (e.g., local zodi, exo-zodi) provide an additional background of photons. Instead, we plan to use a combination of laser metrology, fringe tracking and regular calibrations to maintain the null

position. The laser metrology measures variations in the pathlengths internal to the instrument at high bandwidth. Fringe tracking uses light from the star at shorter wavelengths (~3–5 μm) to provide the path offset that needs to be corrected by the delay line. It can be shown that because the fringe tracker does not operate in the nulled state, the presence of a planet does not produce a significant bias in the tracking point (e.g., for a planet-star contrast ratio of $10^8$ at 4 μm, the bias introduced by the planet to the delay tracking point will be ~$10^{-8}$ fringes or ~$10^{-9}$ arcseconds). There will, however, be segments of optical pathlength that are not common between the fringe tracker and the nulling science back-end. Drifts in these uncommon paths will lead to phase errors. To combat this, calibration measurements are performed several times per rotation of the array to measure the relative amplitudes and phases of the electric fields from each collector at the science back-end. The amplitudes are measured by blocking all but one beam-train and measuring the photon rate. The phases can be determined by blocking pairs of collectors and measuring the photon rate. It is this calibration, and the associated correction of amplitude and phase offsets, that removes the low frequency component of systematic errors, and enables the SNR to be continually improved through multiple rotations of the array.

## Models and Simulation of TPF-I Sensitivity

A number of models are being developed to characterize the system-level performance of TPF-I. The relationships between four of them are illustrated in Fig. 2-3. The Interferometer Performance Model (IPM) is a semi-analytical model of the TPF-I performance. It is the source of requirements, and is discussed in more detail below. The output of the IPM is a prediction of the SNR obtained after a specified length of time, which depends on the target system parameters and the array architecture.

The Star Count model uses this information as the basis for calculating the number of stars that could be observed by TPF-I in a mission of specified duration. The input set of stars is taken from the Hipparcos catalog, and a series of 'science culls' are applied to remove stars that are unlikely to have planets of interest (e.g., close binaries). Stars with high ecliptic latitudes (> 45°) are also removed, since they violate the Sun shading constraints of the mission. The remaining stars are plotted in Fig. 2-4, as a function of distance and angle subtended by the Inner Habitable Zone (IHZ). A given spectral type of star lies on a "$1/x$" locus in the plot, with M stars to the lower left and F stars to the upper right. The Inner Working Angle of the array determines how far to the left we can go in the plot and still separate the planet from the star. The integration time needed to detect an Earth-like planet is calculated for each of the stars. The smallest values (the 'easiest' targets) are obtained in the lower left of the plot, where the stars are nearby and stellar leakage is small. The integration times increase as we move up (increased distance) and to the right (increased stellar leakage). The Star Count model accumulates the integration time, starting with the easiest stars, until the available mission time allocated for planet detection is exhausted. The total number of stars observed depends on the array architecture. A similar approach is used to determine the number of detected planets that can be characterized by spectroscopy. These two numbers can then be compared to the science requirements. Further details can be found in Dubovitsky and Lay (2004).
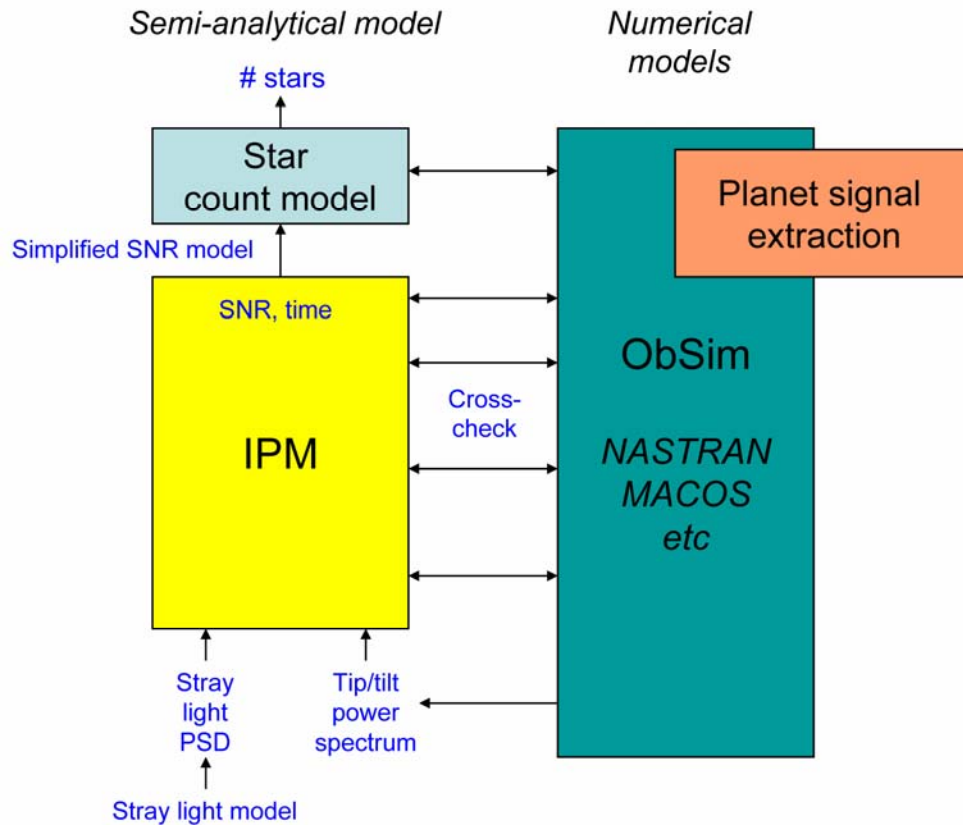
**Figure 2-3.** Relationship between modeling efforts on TPF-I. The Interferometer Performance Model and the Observatory Simulation are shown. The stray light PSD is an example of numerical data supplied by an external model; the tip/tilt power spectrum is an example of data supplied to the IPM from ObSim.

The Observatory Simulation (ObSim) is a numerical time-domain simulation of the TPF-I performance. It is intended both as a high fidelity cross-check of the Interferometer Performance Model and as a source of some of the low-level data needed by the IPM (e.g., the power spectrum of closed-loop tip/tilt fluctuations). It is further described in Chapter 7.

The TPF IPM is maintained as a series of Excel spreadsheets, and is used both to estimate the performance of different architectures and to derive the requirements for the baseline design. Based predominantly on analytical calculations, the IPM is intended to be complementary to the numerical calculations of the Observatory Simulation; cross-checks will be performed between the two approaches. The spreadsheet performance model is run as a bottom-up calculation, meaning that the overall performance is calculated based on the specified low-level inputs (as opposed to a top-down sub-allocation approach). The inputs can be adjusted and balanced until the desired output performance is obtained, at which point the input values assumed become the requirements on the instrument.
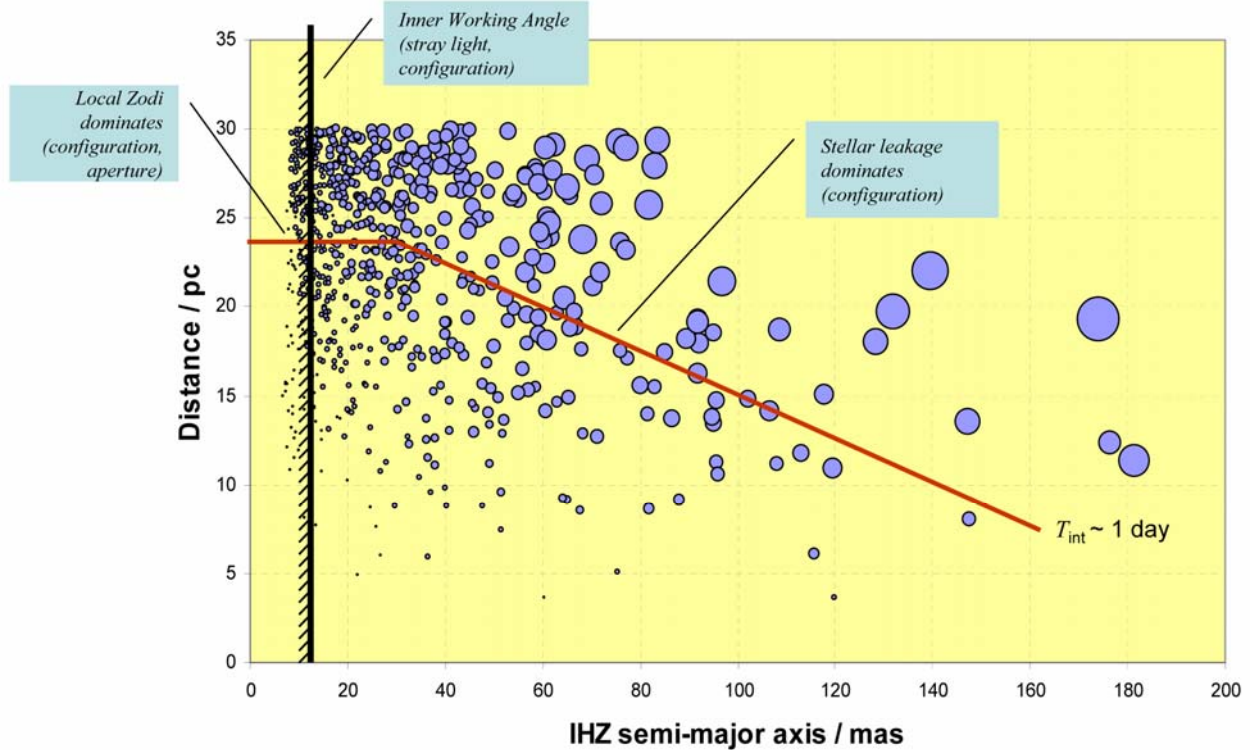
**Figure 2-4.** TPF-I stars and observing constraints. Each circular symbol represents a star from the Hipparcos catalog. The diameter of the circle is proportional to the intrinsic diameter of the star (i.e., physical diameter, in meters, not arcsecs). The red line shows an approximation to a contour of constant integration time (~1 day) to detect an Earth-like planet. The integration time increases to the upper right of the plot, as the stars become larger (more stellar leakage) and more distant (lower planet flux).

## Starlight Suppression Error Budget

Figure 2-5 shows a simplified version of the TPF-I error budget. The values shown result in an SNR of 10 for an ozone spectral channel spanning 9.5–10.0 μm, which currently represents the driving requirement on the integration time. The earth-like planet orbits a G2 Sun-like star with an angular separation of 50 mas at 15 pc distance. In this example the plane of the planetary system is inclined with respect to the line of sight. The ecliptic latitude is 30° (this determines the contribution from Local Zodiacal dust). The array has a linear Dual Chopped Bracewell configuration, comprising four 4-m diameter collectors spaced at 30 m intervals with phases of 0, π, π/2 and 3π/2, for a total array size of 90 m.

The overall SNR is built up from 53 rotations of the array, each with a period of 50,000 s. The total observing time is 31 days (which does not currently include any overhead for calibration). This is consistent with the science requirement to observe approximately half the terrestrial planets found, assuming that the frequency of Earth-like planets is approximately 10%. Should there be more terrestrial planets detected, a greater fraction of the mission time would be devoted to spectroscopy. The SNR for a single rotation is broken out into the root-mean-square (rms) of the planet signal variations and the
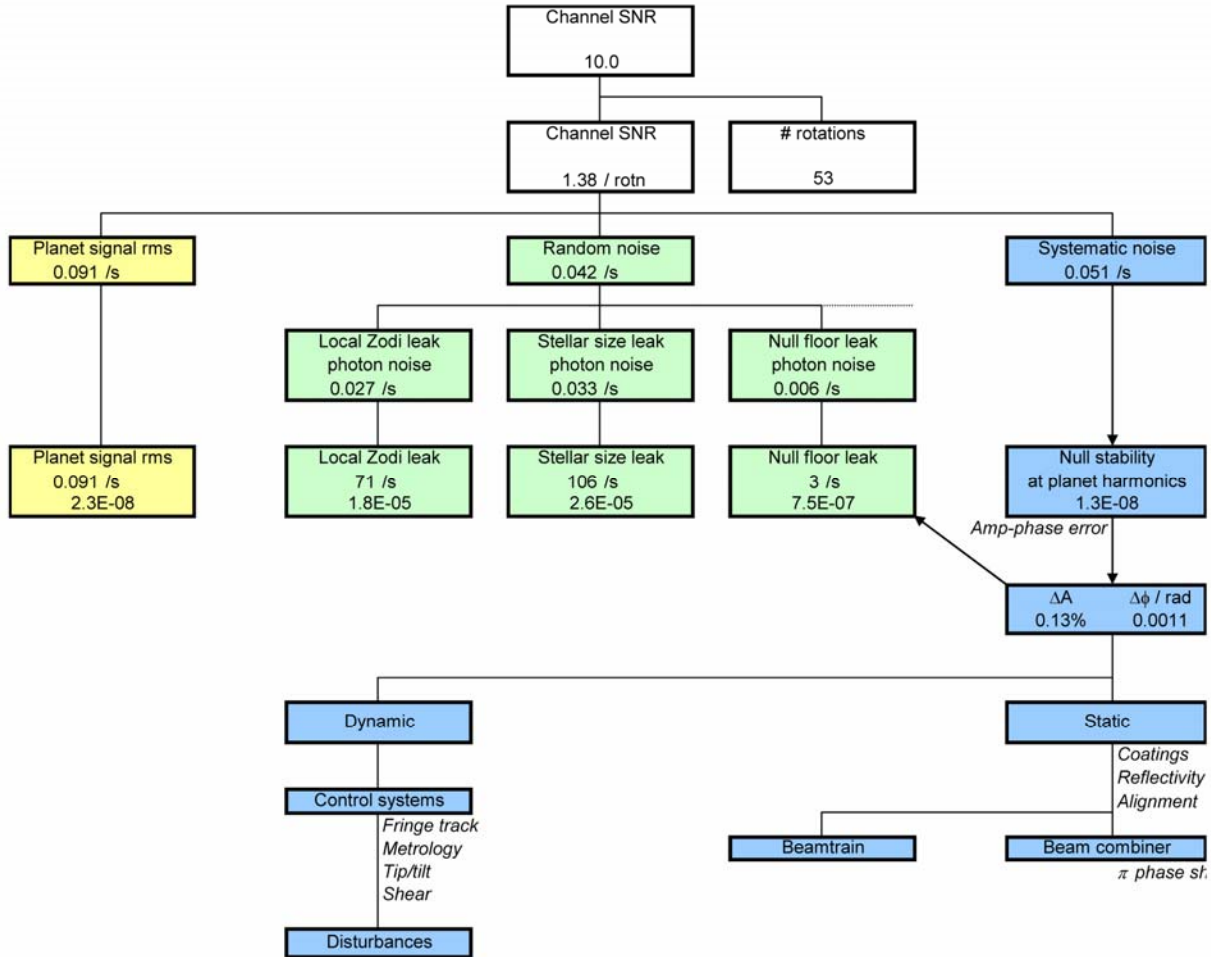
**Figure 2-5.** Simplified TPF-I Error Budget for the Signal-to-Noise Ratio Required for Ozone Detection at 10-μm Wavelength

contributions from random and systematic noise. The root-mean-square (rms) modulation of the planet signal in this spectral band is less than 0.1 photons/s, corresponding to a fraction $2.3 \times 10^{-8}$ of the stellar signal in the same channel—the modulated output being less than the total flux of the planet. In this example, the random noise has approximately equal contributions from the stellar size leakage and Local Zodiacal dust. Other contributions, including Exo-Zodiacal dust emission, instrument thermal emission, and stray light, have been omitted for clarity. The conversion from leakage photon rate to leakage photon noise is based on shot noise for a rotation of 50,000 s. The null floor leak term represents the photon noise arising from mismatches in the instrument beamtrains (Fig. 2-1b). The null floor makes a much lower contribution to the random noise budget than the Local Zodi and stellar leakage, since it is driven by need to minimize the systematic error.

The systematic error contribution to the error budget is indicated by the blue boxes, and is chosen to be similar in magnitude to the random error. The contribution of 0.051 photons/s corresponds to a null fluctuation of order $10^{-8}$ at frequencies similar to the planet signal. These null fluctuations result primarily

from non-linear combinations of amplitude ($\Delta A$) and phase ($\Delta\phi$) errors of the electric fields from the collectors. Analysis shows that the electric fields delivered by each collector must be matched in amplitude to within an rms error of less than 0.13% (equivalent to 0.26% intensity error), and matched in phase to within 1 milliradian at $\lambda = 10$ μm (equivalent to 1.5 nm of path). These conditions must be met simultaneously for all wavelengths in the science band for both polarization states, and over all timescales (including DC offsets and vibrations in the kHz frequency range). The null depth resulting from this level of control is $7.5 \times 10^{-7}$. Meeting these amplitude and phase requirements is the primary technical challenge for the TPF-I system, and they drive almost all aspects of the instrument design. Performance reserve is currently held in three locations in the budget; there is a factor of 2 for the instrument throughput, a factor of 2 on the variance of systematic phase fluctuations and a factor of 2 on the variance of systematic amplitude fluctuations. These do not appear explicitly in Fig. 2-5. In the future, these three suballocations will be rolled up to give an overall signal-to-noise performance reserve for a standard observing scenario.

In Fig. 2-5 the amplitude and phase errors have been further categorized into static and dynamic terms. Static errors arise from mismatches in the coatings, reflective and transmissive optics, and the static alignment of the system, including both dispersive and birefringent effects. Introducing an achromatic $\pi$ phase shift in the nulling beam combiner has been a focus of research, but matching the transmission of the different beamtrains — each of which contains of order 30 optical elements — across the full range of wavelengths and polarization is also a formidable challenge. The dynamic terms include all time-variable effects. The formation-flying system is continually in motion, and a series of control systems must be used to stabilize the optical path at the 1 nm level and to manage the tilt and shear of the wavefront that couples into the single-mode spatial filter. It is clearly important to validate the static terms over an optical bandwidth that is representative of the flight system. On the other hand, if the instrument can be demonstrated to be stable at one wavelength then we can argue that it will be stable at all wavelengths (with the exception of time-varying dispersive terms, which should be small). This reasoning forms the basis for the choice of nulling testbeds.
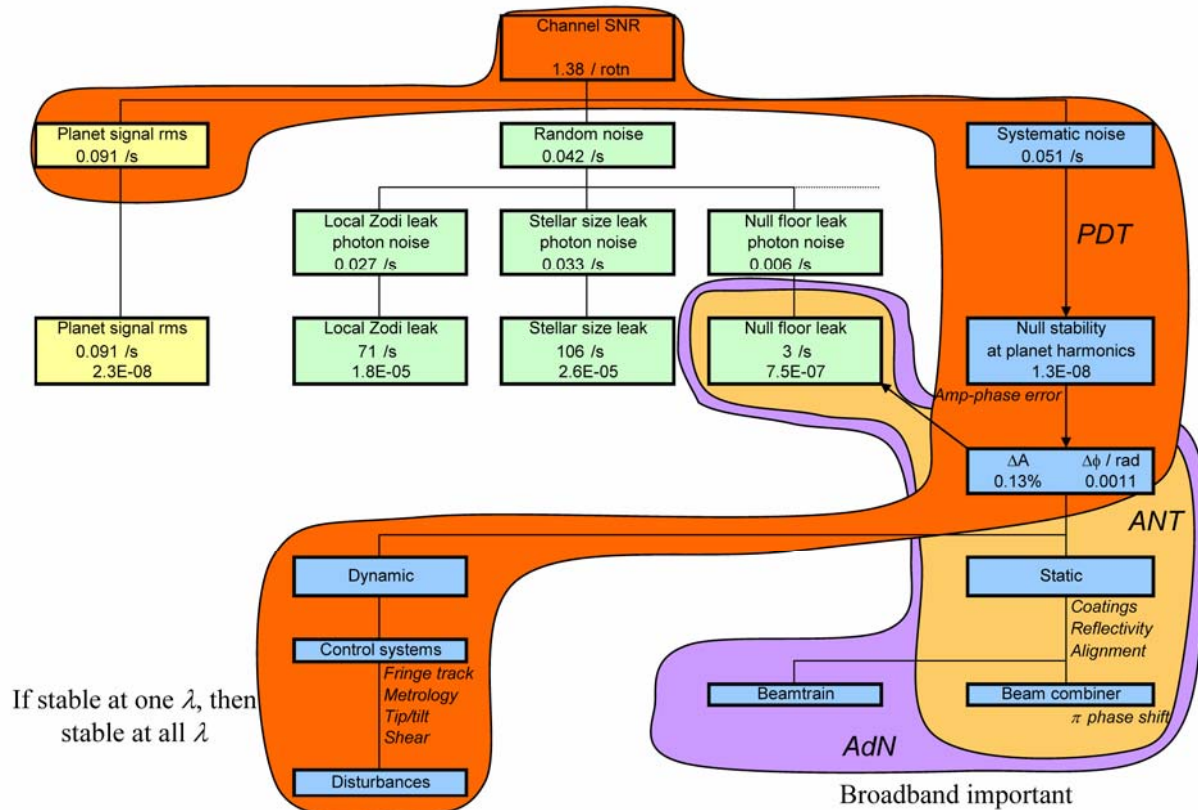
**Figure 2-6.** Relationship Between the Achromatic Nulling Testbed (ANT), Adaptive Nuller (AdN), and Planet Detection Testbed (PDT) with the Simplified TPF-I Error Budget

## Flight Requirements and Requirements of Pre-Phase A Testbeds

The three nulling testbeds address different segments of the error budget, as shown in Fig. 2-6. The Achromatic Nulling Testbed (ANT) validates the ability to manufacture a nulling beam combiner and to obtain a deep null for two input beams over a broad bandwidth in the absence of flight-like disturbances and controls. While the ANT employs real-time control to stabilize the environment, there is no attempt to make this flight-like in functionality, and therefore no validation of the dynamic terms in the error budget. The Adaptive Nuller (AdN) demonstrates the ability to correct for amplitude and phase variations as a function of both wavelength and polarization. This correction compensates for quasi-static mismatches between the beamtrains and combiner and enables a considerable relaxation on the optical tolerances of the instrument. The Planet Detection Testbed (PDT) demonstrates that a stable null can be obtained from 4 monochromatic input beams in the presence of disturbances, and shows that a simulated planet signal can be extracted from the data. A full four-beam system is necessary to validate the predictions for systematic error. The three testbeds form a complementary set that span the instrumental terms in the error budget.

**Table 2-1.  Comparison of Current Flight Requirements with Pre-Phase A Nulling Testbed Requirements**

| Parameter | Flight Performance | Achromatic Nuller | Planet Detection Testbed | Adaptive Nuller |
|---|---|---|---|---|
| Null depth | $7.5 \times 10^{-7}$ | $1 \times 10^{-6}$ | $1 \times 10^{-6}$ | $1 \times 10^{-5}$ |
| Amplitude control | 0.13% | Derived | 0.12% | 0.1% (static) |
| Phase control | 1.5 nm | Derived | 2 nm | 1 nm (static) |
| Stability timescale | 50,000 s + | 100 s | 5,000 s | 100 s |
| Bandwidth | 7–17 μm | 25% | $\lambda = 10.6$ μm | 6–12 μm |

Table 2-1 compares the current flight requirements to the requirements on the three nulling testbeds. In the Pre-Phase A period of the mission planning, the testbeds are intended to establish the feasibility of the flight design, and are not required to demonstrate the full level of performance needed.  Therefore the testbed requirements come close to, but do not meet, the flight requirements.  The degree to which the testbeds reduce risk will be re-assessed with each revision of the technology plan.  As the testbed work advances and the starlight-suppression error budget matures, the requirements will be re-examined.

## Bibliography

S. Dubovitsky and O.P. Lay, "Architecture selection and optimization for planet-finding interferometers," in *New Frontiers in Stellar Interferometry*, edited by Wesley A. Traub, Proceedings of SPIE Vol. 5491 (SPIE, Bellingham, WA 2004) 284–295.

O.P. Lay, "Systematic errors in nulling interferometers," *Applied Optics* 43, 6100–6123 (2004).

# 2.2 Formation Flying Requirements

The high-level requirements for formation flying are summarized in Table 2-2. Requirements are listed separately for *knowledge* and *control* of range, bearing, attitude, and the first-derivative with respect to time (rates) of these quantities. The requirements depend on the operating mode of the array.

## Operating Modes and Sensor Envelopes

There are four modes defined: safe stand-off, reconfiguration, hand-off, and observation. The precise boundary between the different operating modes is to some extent arbitrary, since it depends on the capability of the sensors that are chosen. The *acquisition* sensor has the poorest resolution but the widest coverage in range and bearing angle. The acquisition sensor will be used primarily to establish the array configuration, reconfigure it, and recover from faults that would cause elements of the array to lose their station. The *fine* sensor has the most restricted coverage in bearing angle and is used to maintain the formation during science observations. The medium sensor has a capability allowing hand-off between the acquisition sensor and the fine sensor. It is the delay and delay-rate limitations of the interferometer during the science observations that drive the formation flying requirements.

## Knowledge and Control of Range and Bearing

The requirements on formation-flying are decoupled as much as possible from the requirements on nulling. The formation-flying system is envisioned as the 'coarse stage' of a multi-layer control system that maintains the optical pathlengths. Centimeter-level variations in the relative positions of the spacecraft are sensed by the instrument's fringe tracking system and compensated by the optical delay lines in each beamtrain, each of which is required to provide a control range of $\pm 10$ cm of optical delay. The small changes in the relative bearing angles between the spacecraft are compensated by the articulation of steering mirrors on the collector and combiner spacecraft. The thrusters and reaction wheels will be important disturbance sources for the interferometer, but opto-mechanical modeling will be needed to establish the appropriate requirements.

The range and bearing control requirements during science observations are imposed by the limitations of the fringe sensor and delay line of the interferometer. If the fringes are allowed to move beyond the throw of the delay line, they will be lost. Similarly, if the fringes move too quickly for the fringe tracker to sense them, they will also be lost, even if they are within range of the delay line. The limitations of the delay line therefore impose requirements on range and bearing angle, and limitations of the fringe tracker impose requirements on range rate and bearing rate.

**Table 2-2.  Summary of  Flight Requirements for Formation Flying**

| Ref | Parameter | Units | TPF-I Formation Flying Requirements per Operating Mode | | | |
|---|---|---|---|---|---|---|
| | | | Safe-Standoff | Reconfiguration | Hand-off | Observation |
| 1 | **Operating Envelope** | | | | | |
| 2 | Formation Sensor | | Acquis. Sensor | Acquis. Sensor | Med Sensor | Fine Sensor |
| 3 | Inter-S/C Range | m | 20–200 | 20–10,000 | 20–80 | 20–80 |
| 4 | Inter-S/C Bearing | – | $4\pi$ steradians | $4\pi$ steradians | 10° cone | 10 arcmin cone |
| 5 | Inter-S/C Range Rate | < cm/s | 200 | 200 | 5 | 0.2 |
| 6 | Inter-S/C Bearing Rate | < arcmin/s | 60 | 60 | 10 | 2.5 |
| 7 | **Acquisition Time** | < s | 5 | 30 | 10 | 10 |
| 8 | **Range** | | | | | |
| 9 | Knowledge | cm | 100 | 50 | 1 | 0.1 |
| 10 | Control | cm | 200 | 200 | 5 | 2 |
| 11 | **Range Rate** | | | | | |
| 12 | Knowledge | cm/s | 1 | 0.1 | 0.1 | 0.001 |
| 13 | Control | cm/s | 5 | 0.5 | 0.5 | 0.050 |
| 14 | **Bearing** | | | | | |
| 15 | Knowledge | arcmin | 1800 | 60 | 1 | 0.067 |
| 16 | Control | arcmin | – | 300 | 5 | 0.333 |
| 17 | **Bearing Rate** | | | | | |
| 18 | Knowledge | arcmin/s | – | 1 | 0.167 | 0.0007 |
| 19 | Control | arcmin/s | – | 5 | 1.000 | 0.0100 |
| 20 | **Attitude (Abs. Sensor)** | | | | | |
| 21 | Knowledge | arcmin | 1 | 1 | 0.1 | 0.1 |
| 22 | Control | arcmin | 60 | 60 | 3.0 | 1.0 |
| 23 | **Attitude Rate (Abs. Sensor)** | | | | | |
| 24 | Knowledge | arcsec/s | 1 | 1 | 1 | 1 |
| 25 | Control | arcsec/s | 5 | 5 | 5 | 5 |

| Operating margin | Design reserve |
|---|---|
| (OPD +/-) | (OPD +/-) |
| 0.50 cm | 4.56 cm |
| 5 % | 55 % |
| **5** % | 46 % |

*sum*

Link 1
Link 2

Unused delay
(OPD +/-)
5.06 cm

*A-B*

*A*

*B*

Total available delay
(OPD +/-)
**10** cm

Delay range used
(OPD +/-)
4.94 cm

*\*0.5*

*sum*

Mech. delay range +/-
5 cm

Fringe search
(OPD +/-)
**1.00** cm

Link 1 contribution
(OPD +/-)
1.97 cm

Link 2 contribution
(OPD +/-)
1.97 cm
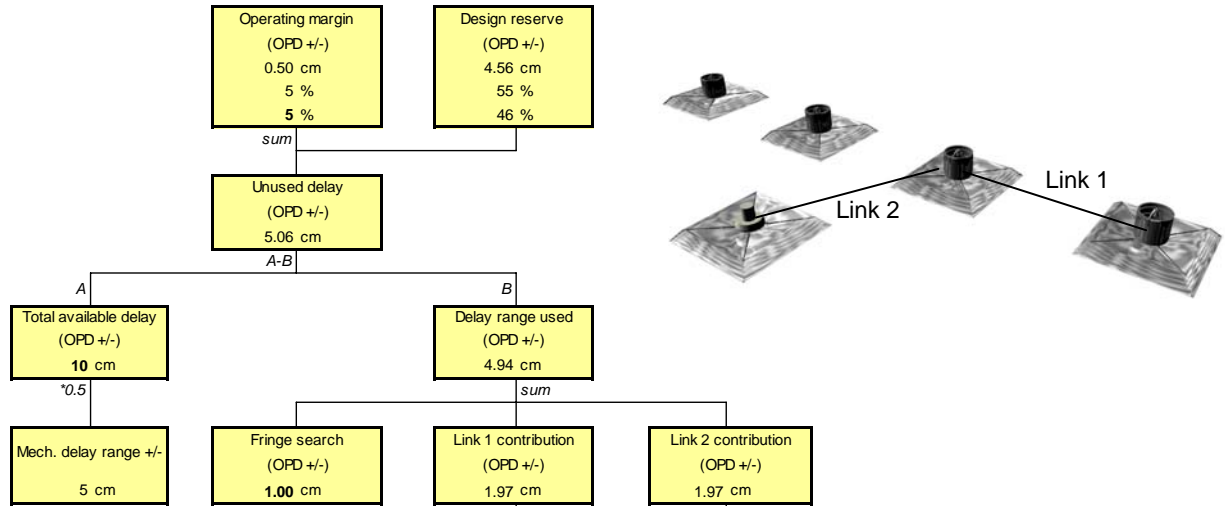
**Figure 2-7.** Formation Flying Range/Bearing Control Error Budget Flow-Down (IPM), 1 of 2



Link 1 contribution
(OPD +/-)
1.97 cm

*sum*

Range control
+/-
**1.0** cm

Bearing contribution
(OPD +/-)
0.97 cm

*sum*

Out-of-plane

Bearing control +/-
in-plane
0.00 cm

Bearing control +/-
out-of-plane
0.97 cm

In-plane

*2nd order dependence*

$\theta R$

Bearing control +/-
in-plane
**-** arcsec
**-** arcsec

100m
20m

Bearing control +/-
out-of-plane
**20** arcsec
**100** arcsec
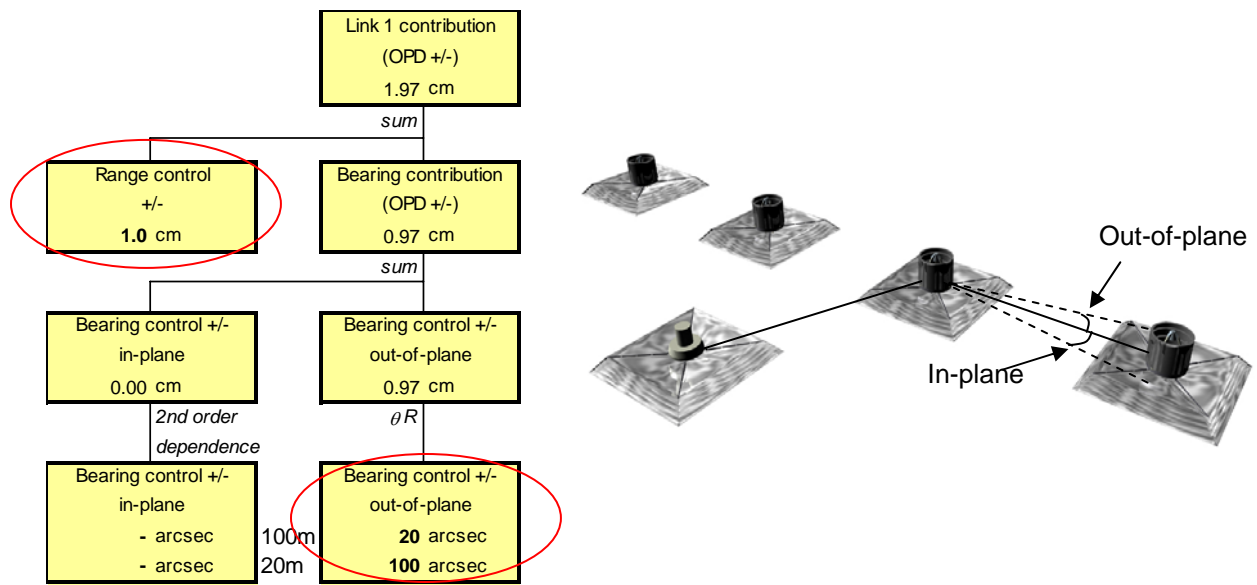
**Figure 2-8.** Formation Range/Bearing Control Error Budget Flow Down (IPM), 2 of 2. In-plane contributions in bearing control (lower left) are set to zero in this error budget flow-down.

The optical path-difference is required to be controlled to ±1 cm along the beam path, for both in-plane and out-of-plane directions. This ±1 cm control requirement is shown in Table 2-2, row 10 under the 'Observation' operating mode. A bearing requirement of ±0.33 arcmin is equivalent to ±1 cm spacecraft position control at the shortest baseline with the collector spacecraft center-to-center separation of 100 m. The error budget for the optical path-difference based formation control is shown in Fig. 2-7 and Fig. 2-8.

**Formation Flying Error Budget Tool**

As the technology developments and the interferometer requirements are refined, the formation performance requirements will also evolve. In anticipation of periodic updates of the formation flying requirements, and also to allow for trade-offs and performance assessments, a detailed formation error budget tool has been developed. This tool allows for sensor knowledge errors and control actuator errors to be included, taking into account random noise (e.g., sensor noise) and systematic noise (bias, frame mis-alignments, etc.).

As an initial test case, this formation error budget tool was used to predict the performance of the Formation Control Testbed (FCT). This is illustrated in Fig. 2-9. (The propulsion numbers as shown in Figure 2.9 under the RCS Control are relevant only to the ground testbed hardware using on-off impulsive cold gas system.) Also, a preliminary simulation-based capability assessment of the FCT Robot system was also performed, based on component specifications and verified performance through calibration and test results where available. Items shaded in gray color are error budget allocations, where items shown in yellow are the preliminary assessment of the capabilities of the FCT based on existing design and the known performance based on tests where available. Items highlighted in red signify un-met requirements at present. The specific requirements in question are the quiescent time in-between consecutive thruster firing to limit the self-induced disturbances while in the science mode. Using conventional on-off impulsive thrusters, this requirement is known to be tight. For the TPF Flight design the selection of proportional thruster using Ion-propulsion is expected to meet this requirement. Items crossed-out with red lines are additional parameters built into the tool for enhanced fidelity but not used for this test-case analysis. Green tags signify verification of the performance of the specific item through simulation.

# Propulsion Systems

The TPF-I science observations require precision formation flying maneuvers and thus a fine level of propulsion capability. TPF-I formation flying control requirements are based on the inter-spacecraft starlight beam-path range/bearing control requirements of ±1 cm, and ±1 arcmin. Precision propulsion is critical to realize this level of fine control (given the fine metrology sensors). Based on the currently estimated spacecraft mass (~1500 kg), representative observation rotation period (~50,000 seconds) and a collector array length (~150 m), the total continuous inward force needed to track a circular path is on the order of 3–4 mN. This is well within the capability range of Ion propulsion technology.

Aside from a fine impulse-bit to enable precision motion for formation control, a number of additional attributes are needed in the propulsion system, including: (i) minimal self-induced mechanical disturbance, (ii) low self-contamination risk of the cryogenic optical surfaces, (iii) wide thrust range capable of addressing both the precision formation motion during science mode and rapid reconfiguration of formation to a new science observation configuration, maximizing mission science, and (iv) fuel efficiency. The number, location, and orientation of thrusters, their thrust, and their levels must take into account spacecraft system design, configuration, and accommodation issues. This includes the force lever arm for rotation authority, the packaging for stow-ability for launch, the manner of deployment, considerations of plume direction and impingement, and IR contamination signatures.
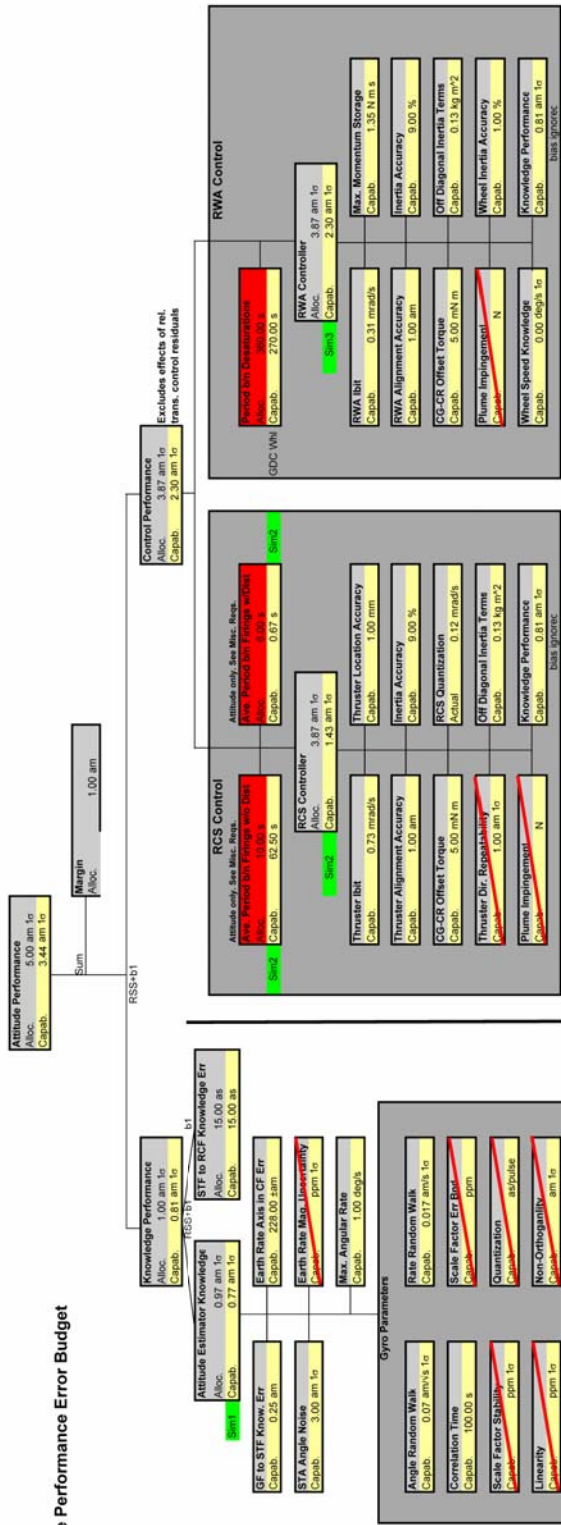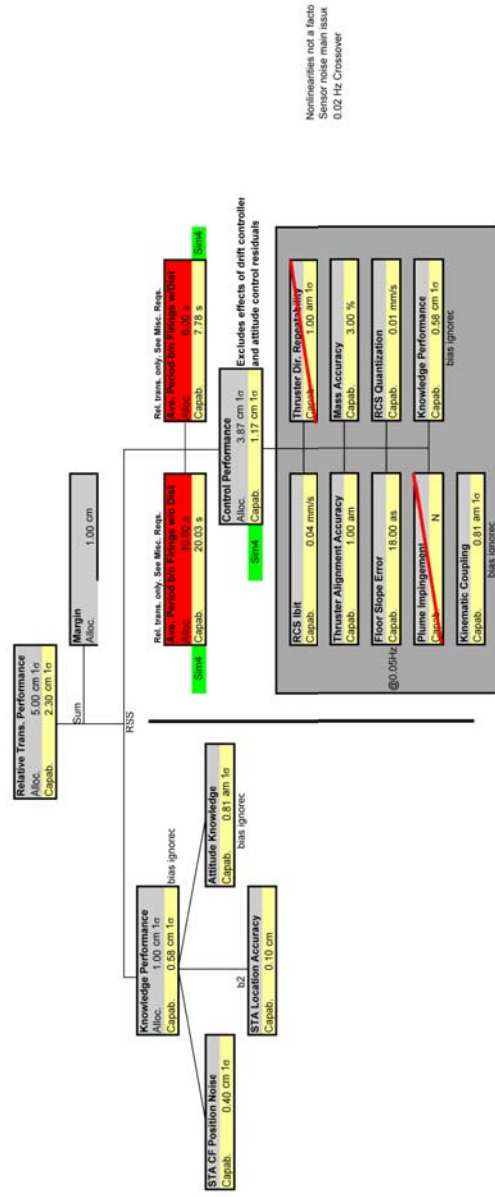
**Figure 2-9.** Formation Error Budget Tool

The choice of thruster technology should limit the vibrations that would be induced in the spacecraft structure. Unlike on-off impulsive propulsion, continuous low-level thrusting, as would be possible with ion thrusters, significantly reduces the broadband disturbances injected into the system and spreads the total impulse, thus reducing the peak thrust force level.

The structural dynamics of the spacecraft will also directly influence the formation-flying control bandwidth and performance. Even though some preliminary control performance has been assessed through simulations, detailed analysis for the spacecraft system (sunshade, optical beam train, etc.) as well as testing to characterize the damping, will be needed during Phase A/B to refine the formation flying control design.

Thruster sizing for retargeting and re-baselining maneuvers where precision control of beam path is not required is driven by the need to minimize the duration of non-science mission operations, given a fixed cryogenic life of the mission.

The current baseline thruster configuration consists of 16 thrusters arranged in non-radial direction (from the center of the spacecraft) to avoid plume impingement to the nearby spacecraft. All thrusters are mounted on the warm side.

## Flight Requirements and Requirements of Pre-Phase A Testbeds

The flight requirements and testbed requirements for formation flying are listed in this section. The requirements for the Formation Algorithms & Simulation Testbed are identical to the flight requirements listed in Table 2-2. The requirements for the Formation Sensor Testbed are given in Table 2-3. The requirements for the Formation Control Testbed are given in Table 2-4.

In addition to requirements to enable TPF-I science, there are a number of enabling requirements unique to a formation flight system beyond those of traditional single-spacecraft missions. An overview of these requirements is given below in Fig. 2-10, within the context of the technology development effort under TPF-I.

### Relative and Absolute Formation Sensing

Acquisition of relative position knowledge of each of the spacecraft with respect to all other spacecraft is critical in establishing and safely maintaining a formation. The acquisition sensors must quickly acquire the knowledge of the location of all other spacecraft, with a minimum of delay and thus with minimum risk of drift-induced collision between the spacecraft.

*Coarse Sensor:* The focus of the Formation Sensor Testbed (FST) is thus to develop the needed technology for a $4\pi$ coverage range and bearing sensor, giving instantaneous position of all other spacecraft within its range. This capability would be implemented on each of the collector spacecraft as well as on the combiner spacecraft. The FST Technology development effort is shown in the yellow shaded area in Fig. 2-10. FST formation acquisition sensor, with its $4\pi$ coverage, though with limited accuracy, is complemented by a fine metrology sensor in a parallel development under the Modulation Sideband Technology for Absolute Ranging (MSTAR) effort.

*Medium Sensor:* To bridge the gap between the performances of the Formation Acquisition Sensor and the Fine (metrology) Sensor, a Medium (accuracy) Sensor is required to provide a seamless handoff. Performance requirements of the Medium Sensor are chosen to allow for the knowledge and control to be refined in order to enable Fine (metrology) Sensor acquisition, lock and tracking. Operationally, data from all available sensors will be used by the on-board formation state estimator to seamlessly provide the best available estimate of the spacecraft-to-spacecraft range and bearing knowledge.

*Fine Sensor:* With its high resolution and accuracy, though with limited field-of-view coverage, the MSTAR metrology sensor is suitable for the Observation mode, which involve inter-spacecraft path-length control, fringe acquisition, and tracking. The MSTAR technology development effort is shown in the blue shaded area in Fig. 2-10. Note that the fine sensor knowledge requirement is chosen to meet the required control performance. In the case of the MSTAR fine metrology sensor the expected sensing capability is much better than needed. Similarly, the attitude knowledge and control capability is better than the stated requirements; however, the stated requirements minimize the use of propellant.

## Fault Tolerance

The evaluation of robust performance of precision tracking with coordinated spacecraft in the presence of a fault can only realistically be done well in a testbed environment. Since the spacecraft are distributed,
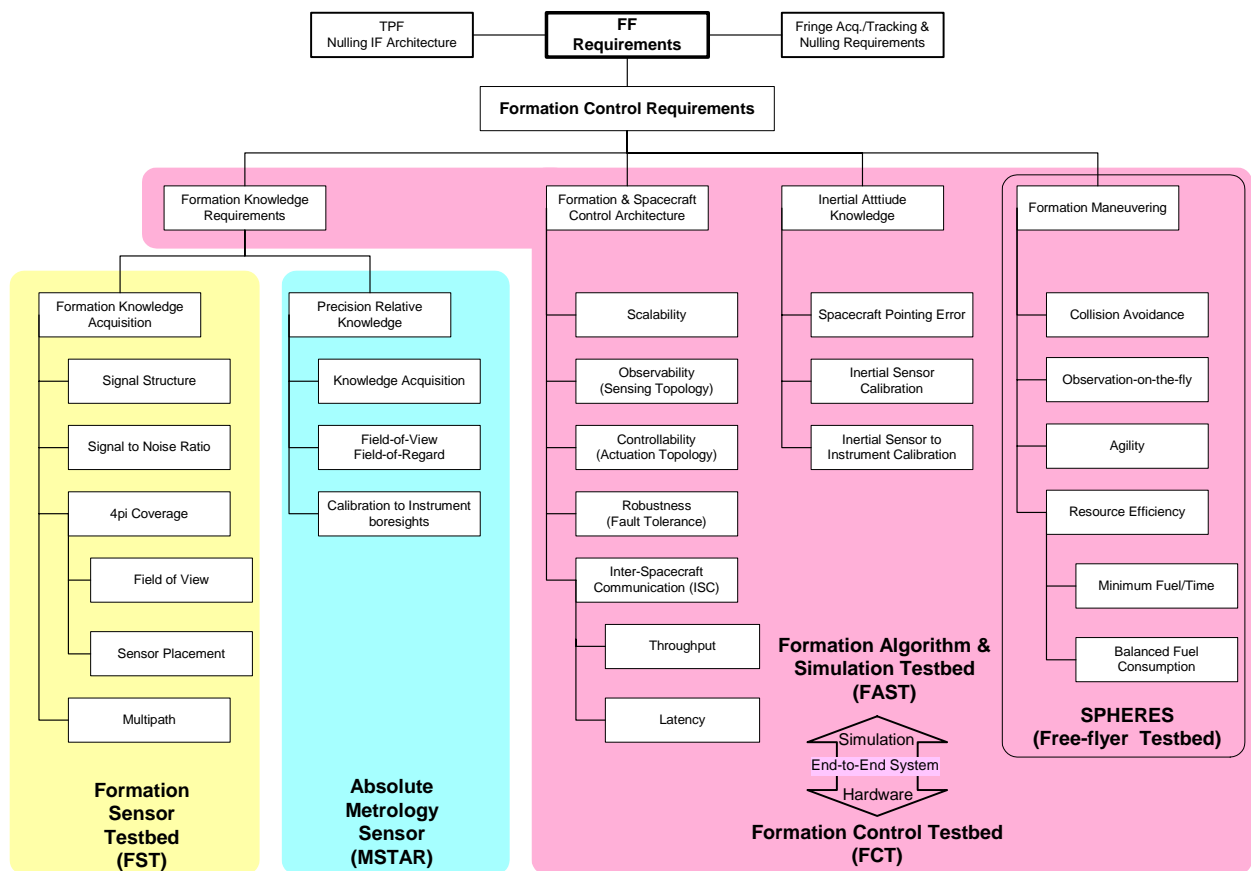


**Figure 2-10.** Formation Flying Requirements Overview

precision formation flight guidance requires a common relative inertial frame and a common clock time. The effect of errors in inertial alignment, biases, scale factor, jitter, etc. in the star tracker and gyros, communication latency, clock bias, bearing errors in the laser pointing, system delays, thruster uncertainties, and environmental perturbations all require a testbed to guide the development of a high fidelity simulation.

It may be possible to evaluate these conditions with two spacecraft, although the effect of uncertainties on the precise coordination of three spacecraft is not the same. Furthermore, three spacecraft form a network inducing more realistic communication latencies. However, detection and identification of faults in the sensors and actuators becomes substantially different from two spacecraft to three. For example, with three spacecraft the metrology system between spacecraft forms a triangle (i.e., a known plane) in the common inertial space measured by each spacecraft, whereas only a line in this three dimensional space is obtained with two spacecraft. Suppose a star tracker fails, then this failure can not only be detected but

**Table 2-3.  Requirements of the Formation Sensor Testbed vs Flight Requirements**

| Parameter | Flight Performance | Formation Sensor Testbed | Comments |
|---|---|---|---|
| **Cooperative mode** | | | |
| **Operating  Volume** | | | |
| Angle | $4\pi$ | $4\pi$ | |
| Range | 10 km | 16 m – 1 km | 10 km for evaporation |
| **Range accuracy** | 0.5 m | 0.5 m | |
| **Bearing accuracy** | 1° | 1° | |
| **Update rate** | 1 Hz | 1 Hz | |
| **Sweet-spot operations** | | | |
| **Operating  Volume** | | | |
| Angle | 10° | 10° | Full cone angle |
| Range | 16–100 m | 20–100 m | Center-to-center with 15-m shade |
| **Range accuracy** | 0.5 m | 0.5 m | |
| **Bearing accuracy** | 1° | 1° | |
| **Update rate** | 1 Hz | 1 Hz | |
| **Non-cooperative mode** | | | |
| **Operating  Volume** | | | |
| Angle | $4\pi$ | $4\pi$ | |
| Range | 16–200 m | 16–50 m | Center-to-center with 15-m shade |
| **Range accuracy** | 1 m | 4 m | |
| **Bearing accuracy** | 30° | No requirement | FST goal is 70° |
| **Update rate** | 1 Hz | 1 Hz | |
| **S/C Accommodation** | | | |
| **Thermal shield geometry** | 5–20 m | 5–20 m | diameter |

identified by the coordinated measurements of all three spacecraft. With two spacecraft the failure can only be detected, although through the gyros, it might also be identified. Essentially, to identify a sensor fault, three measurements are required and can be integrated, if dissimilar, analytically. However, the detection and identification process will be different for two and three spacecraft, leading to differences in the time to identify and thereby changing the system response to a failure and its effect on the precision of formation flying as the performance of the guidance system gracefully degrades. Since analytical redundancy should play a significant role in the development of a fault-tolerant guidance system for distributed spacecraft, it appears that three spacecraft are essential for the evaluation of the robust performance of formation flight guidance in the presence of both system uncertainty and system faults.

## Collision Avoidance

Collision-free formation knowledge acquisition requirement serves as the key formation system requirement (see operating modes of Safe-Standoff and Reconfiguration in Table 2-2). Both the Safe-Standoff and formation Reconfiguration operating modes are supported by the Formation Acquisition Sensor being developed by the FST, and as such the requirements in these two columns are supported by the Formation Acquisition Sensor performance. Note that Safe-Standoff is a degraded mode of the Formation Acquisition Sensor, and as such is only required to safe-guard against spacecraft collisions or drifting out of sensor range.

## Attitude and Relative Position Knowledge

In addition to the use of relative position knowledge, the formation control system requires the inertial orientation of each of the spacecraft to effectively point each of the collector telescope boresights to the science target star and to direct the starlight beams from one spacecraft to another. This capability is readily achievable with the star tracker sensor used for the traditional single spacecraft attitude control. A combination of formation sensor and star tracker provides a full 6 degrees-of-freedom of position inertial attitude, and relative position knowledge of each of the spacecraft. Traditional single spacecraft missions only control their inertial attitude and the position of the spacecraft is typically controlled from the ground through trajectory design and periodic maintenance through Trajectory Correction Maneuvers. Due to the relative close proximity of spacecraft within the formation and the round trip transmission delays of telemetry/commanding, ground-in-the-loop spacecraft position control is deemed unacceptably risky. Consequently, attitude as well as spacecraft position within a formation is required to be controlled on-board. Planning and execution of all formation maneuvers, with the desired 6 degrees-of-freedom motion trajectories, is required to be performed on-board by the formation guidance function. Formation guidance also ensures maximum possible resource efficiency (time, fuel), while avoiding collisions between spacecraft and protecting sensitive instrument boresights from undesirable noise sources (Sun, glint, relative thermal, etc.).

## Distributed Sensing, Communications, and Control

Coordination and interaction within all the elements and functions of a formation require an overall formation control architecture. Formation control architecture encompasses the distributed sensing, communication, and control across all spacecraft in formation. The Formation Algorithm and Simulation Testbed (FAST) and Formation Control Testbed (FCT) develop, demonstrate and validate an end-to-end formation control system, with a focus to meet specific enabling functional and performance requirements

for TPF-I. With detailed modeling and development of key formation estimation, guidance and control algorithms, FAST demonstrates the feasibility of five spacecraft TPF-I formation flight performances in simulation. Additionally, FAST models and simulates to predict FCT multi-robot based hardware-in-the-loop formation flying performance. In turn, FCT test results are used to refine and validate the FAST simulation based predictions. With the FAST implemented formation control architecture and algorithms validated by FCT test results, the FAST simulation can predict the TPF-I five spacecraft flight performance with higher confidence.

## Propulsion Systems

Station-keeping may pose a significant technology challenge. The array will have many degrees of freedom that must be controlled. The requirements for propulsion systems are not dealt with in any detail in this technology plan, under the assumption that the required technology will be developed independently of TPF-I. The need for a more detailed investigation is acknowledged, because of the requirements that are unique to TPF-I. Such a study would flow down the propulsion system requirements from the candidate architectures, with the aim of optimizing the number and location of thrusters, the average thrust levels, the minimum impulse bit, and the total impulse per thruster. Additionally, the requirements could be broken down by the operational mode of the array, such as array re-configuration versus science observation modes.

## Interactions Between Spacecraft

Because TPF-I will work in an environment that cannot be entirely duplicated on Earth, especially where our understanding of effects of propulsion between spacecraft is concerned, great care in modeling spacecraft interactions will be needed. The spacecraft are likely to be highly sensitive to perturbations. Corrections in station keeping of one telescope may influence the position of neighboring telescopes and potentially induce vibrations on the large sunshades. Although this concern is deemed to be less of a concern than others described in this plan, it will be considered in future enhancements to the formation flying algorithms and modeling.

**Table 2-4.  Requirements of the Formation Control Testbed vs Flight Requirements**

| Parameter | Flight Performance | Formation Control Testbed | Comments |
|---|---|---|---|
| **Number of spacecraft** | 5 | 3 | |
| **Operational capability** | | | |
| Standalone operations | 5 yrs | 36 min | Total floatation time |
| Mission duration | 5 yrs | 5+ yrs | |
| Observational duration | ~20 hrs | ~15 min | For an "observation on the fly" |
| Availability | Continuous | 8 hrs/day | Ground testbed facility |
| **Motion DOFs** | 6 | 5+1 | FCT:+articulated DOF |
| **Operating envelope** | 3D space | 2D plane | FCT: with limited out-of-plane |
| **Control** | 2 cm / 20 arcsec | 5 cm / 60 arcmin | |
| **Fault recovery** | Active and passive | None | |
| **Flight capability** | | | |
| **Sensor** | | | |
| Inertial | Gyro/accel | Gyro/accel | |
| Celestial | Star tracker | Psuedo-star tracker | |
| Relative | Coarse, Med., Fine | Medium | |
| **Actuator** | Thruster, RWA | Thruster, RWA | |
| **Control Architecture** | Distributed | Distributed | |
| **Control Algorithms** | Flight | Flight | Developed by FAST |
| **Dynamic DOFs** | 6 | 5 | FCT: +1 articulated DOF |
| **Range of motion** | | | |
| Angular-in-plane | $2\pi$ | $2\pi$ | |
| Angular-out-of-plane | $\pm 45°$ | $\pm 45°$ | |
| Linear-in-plane | Limited by sensor range | Limited by lab space | |
| Linear-out-of-plane | Limited by sensor range | $\pm 25$ cm | Emulate deadband during observations |
| **Maneuvers** | | | |
| Acquisition | 3D space | 2D space | |
| Array rotation in-plane | Yes | Yes | |
| Array re-sizing | Yes | Yes | |
| Array re-targeting | Yes | Yes | |
| **Collision Avoidance** | 3D space | 2D space | |
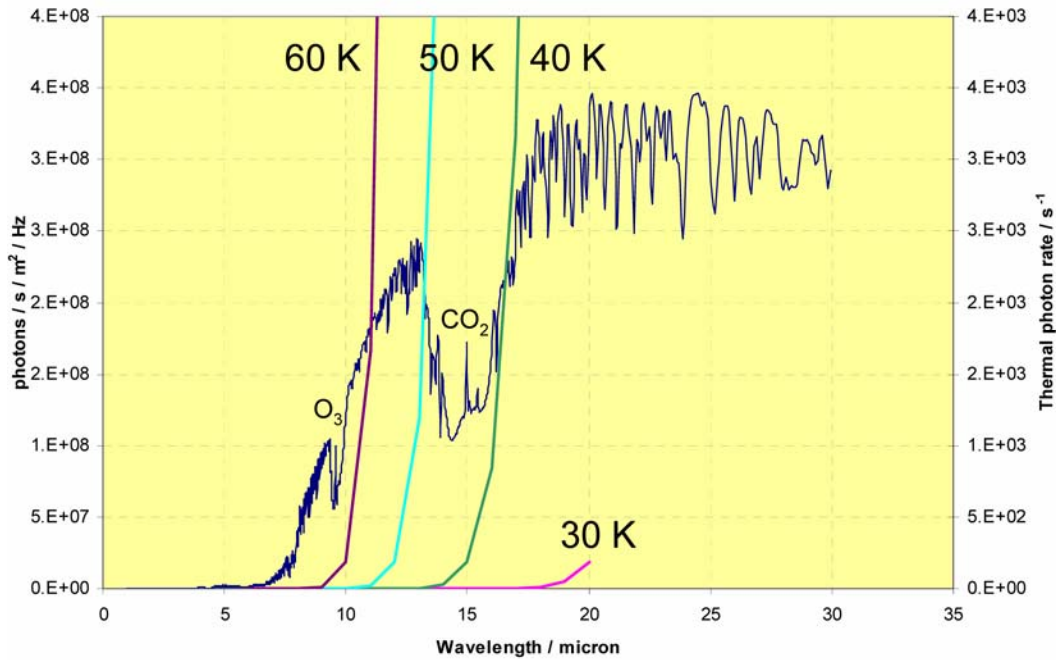
**Figure 2-11.** Impact of optics temperature on thermal photon rate. The spectrum is for an Earth-like planet at 15 pc (scale on left axis), with clear absorption features from Ozone and Carbon Dioxide. The thermal photon rate for a spectral channel width of 1 μm (scale on the right axis) is shown for temperatures ranging from 30 K to 60 K. The thermal photons become the dominant source of random noise at a wavelength of 17 μm beyond ~1000 photons s$^{-1}$ (but the integration time needed is determined by the SNR required at shorter wavelengths where the thermal photon rate is substantially reduced).

# 2.3 Cryogenic Technology Requirements

## Thermal Noise

Operation in the mid-infrared band dictates the need for cooling of the optics. While the thermal noise contribution is small at 10 μm and is omitted from Fig. 2-5, the contribution rises exponentially at longer wavelengths, as illustrated in Fig. 2-11. The current requirement is for cooling to 40 K in order to preserve the performance at 17 μm.

TPF-I is being designed to operate at $L_2$. During part of its orbit, the Moon and/or Earth will be above the horizon defined by the sunshade. Both are very bright, and their light might glint off spacecraft structures and onto optical elements. Any such glints could change the null depths, and would be a function of the array orientation. The baffling, cleanliness, and surface finish requirements will need to be studied to exclude both direct and diffracted light from the optical train. Whereas this topic is not treated in detail in this plan, it is a known concern that will be examined in revisions to this plan in Pre Phase A of the project. The only specific sources of straylight considered so far have been reflections or glints from the

sunshields of neighboring spacecraft. Other solar system sources of straylight, such as the Earth and Moon as seen from L2, have not yet been considered.

## Structural and Thermal Stability

The cryogenic technology development described in this plan is focused on the requirement of determining, with the high degree of precision necessary, the material and sub-component characteristics necessary for accurate modeling of the thermal and dynamic stability of the TPF-I telescope performance at cryogenic temperatures. Most importantly, the thermo-mechanical linear and non-linear characteristics and their scatter need to be tested and identified to levels consistent with a detailed error budget.

How well one needs to know the damping characteristics at 40 K for candidate materials depends on the expected nano-mechanics of the large, precision, and complex cryogenic structures that will be implemented for TPF-I. Future cryogenic testbeds and flight hardware will undoubtedly have many joints and adjustments, and these may be significantly exercised in the course of the alignment and subsequent cooling to the 40 K operating temperature. This cycling will likely affect the alignment tolerances associated with the cryogenic nano-structural behavior of the interferometer. To the maximum extent possible, joints should be avoided by employing an integrally machined structure making use of isotropic material. In this regard, work related to the James Webb Space Telescope (JWST) will provide a wealth of information for TPF-I. The JWST structure uses orthotropic materials and has more joints per unit volume than any other cryogenic structure previously flown in space. A more accurate mechanical model of TPF-I is needed from which to base the requirements. An error budget then needs to be developed to provide more detail guidelines for the cryo-structure development effort. These guidelines will assure that material properties and critical sub-components are characterized and modeled at cryogenic temperatures to levels of precision commensurate with the mission requirements, which in many cases may be at or beyond the current state-of-the-art. The area of cryogenic technology development is currently being addressed by a suite of testbeds and modeling tools development activities.

Current allocations for phase control and stability suggest that the mechanical systems may need to control end-to-end optical path differences and wavefront errors down to nm levels of stability over periods of observations exceeding several hours. This implies that the TPF Interferometer needs to maintain extreme structural and thermal stability to achieve its performance goals, which at cryogenic temperatures poses even greater technological challenges for achieving the required optical performance. In comparison, JWST has optical path differences and wavefront error allocations in the hundreds of nm, making the TPF-I optical performance goals perhaps two orders of magnitude more challenging. Of particular concern is the technology development required for design, modeling, test validation and performance prediction of lightweight, stable, precision-composite structures for cryogenic applications.

# Cryocooler Technology

The TPF Interferometer will require that its detector be cooled to minimize the noise in the science measurements. The detector cooling would be possible with either an active cooler or using stored cryogens, but the projected mission lifetime of 5 years, with a goal of 10 years, seemed sufficiently long that active coolers were deemed necessary. The TPF Project therefore sought early on to define its cooler requirements and to invest in advancing the performance of active coolers.

 The first step in the Advanced Cryocooler Technology Development Program (ACTDP), which began in 2002, was to develop a specification for cooler concepts. This led to a list of flight requirements, of which several key parameters are listed in Table 2-5. The requirements that were then imposed on the development-model coolers were the same as the flight requirements. This specification was based on two types of information. The first type of information came from the specifications of cryocoolers for missions that were in flight or in the midst of flight development. Examples of these missions are the Atmospheric Infrared Sounder (AIRS) instrument, Hubble Space Telescope's Near Infrared Camera and Multi-Object Spectrometer (NICMOS) instrument, and the Ramaty High-Energy Solar Spectroscopic Imager (RHESSI) instrument. Experience from these missions and others provided many of the requirements about form, fit, and function in the ACTDP specification. The second type of information came from the needs for three future NASA missions: James Webb Space Telescope, TPF-I, and Constellation-X. The ACTDP was initiated as a joint effort to serve the needs of these missions, and so concepts for these missions were used to derive the key performance requirements for the coolers. In fact the requirements became stricter over the course of the program. The cooling requirements for all coolers were initially identical, and during the early phase of the program they were revised to all be 20 mW at 6 K and 150 mW at 18 K. However, the requirements became stricter for the vendors that built JWST-specific coolers, as shown in Figure 2-12. These coolers now required a cooling capability of 30 mW at 6 K.

The JWST concept was the most mature at that time and so had the biggest influence on the specifications. In particular, the 30 mW at 6 K and 150 mW at 18 K cooling capacity of the coolers was based on a detailed budget for the mid-infrared instrument on JWST. The budget for the 6 K load included nine contributors to the thermal load with five of them being conductive, three radiative, and the ninth a focal plane dissipating 3 mW of power. The budget for the 18 K stage had twelve contributors. A performance margin of about 100% was included in the requirement for the cooler. It was felt then and still is that TPF-I requirements for cooling capacity will be less demanding than those of JWST.

Table 2-5. Cooler Requirements for the Advanced Cryocooler Technology Development Program

| Parameter | Flight Requirements |
|---|---|
| Cooling capacity at 6 K | 30 mW (JWST-specific coolers; deployment and remote cooling), 20 mW otherwise |
| Cooling capacity at 18 K | 150 mW |
| Vibratory force at cold head | < 0.005 N zero-to-peak in any axis |
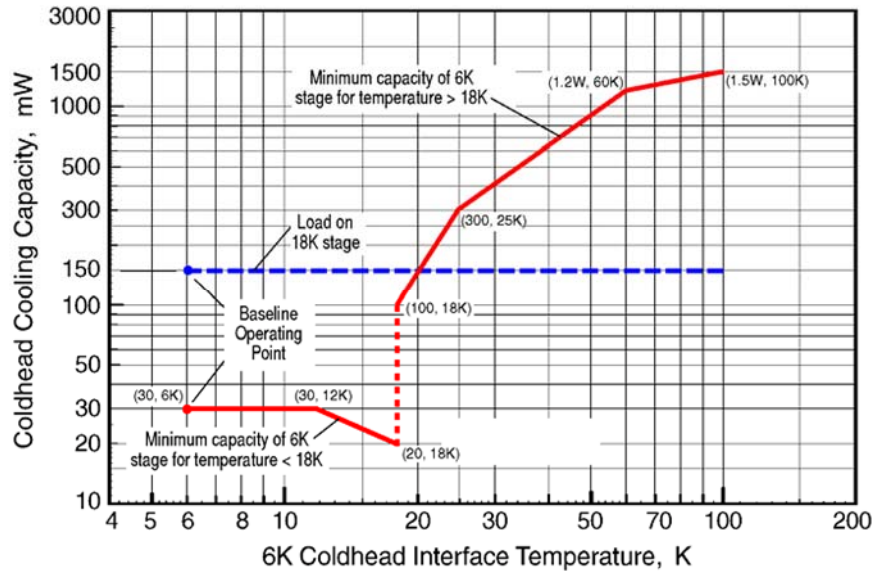
**Figure 2-12.** Required Cooling Capability versus Temperature for the 6 K Coldhead of JWST-Specific Cryocoolers in  The Advanced Cryocooler Technology Development Program

From the beginning the specification included requirements that limited the dynamic disturbances the cooler would generate.  Some of these requirements limit the disturbances introduced on the warm side of the spacecraft by the compressors and drive motors.  Another requirement limits the vibrations introduced on the cold side of the spacecraft:  the cryocooler 6 K and 18 K coldhead subassemblies, when rigidly mounted, are not to impart into their supports a vibratory force greater than 0.005 N zero-to-peak in any axis.  At the time the requirements were drafted for the program, this was in fact the state of the art in cryocooler vibration characteristics, it seemed unlikely that cryocoolers could be made quieter, and so the requirements did not push the state of the art in that direction.  This remains a subject to be explored in further detail.  Should the actual vibration requirements of TPF-specific coolers be far stricter than the current state of the art or the requirements imposed on the JWST coolers, it may have significant consequences for schedule and cost within the current technology plan.

## Bibliography

C. Noecker, Z. Wei, and J. Decino, "Stray light estimates for the TPF formation flying interferometer," in *Optical Systems Degradation, Contamination, and Stray Light: Effects, Measurement, and Control*, edited by Philip T. Chen, John C. Fleming, and Michael G. Dittman, Proceedings of SPIE Vol. 5526 (SPIE, Bellingham, WA 2004) 249–256.

D.R. Coulter , R.G. Ross, Jr., R.F. Boyle, and R.W. Key,  "NASA advanced cryocooler  technology development program," in *IR Space Telescopes and Instruments*, edited by John  C. Mather, Proceedings of SPIE Vol. 4850 (SPIE, Bellingham, WA 2003) 1020–1028.

*Cryocoolers 13*, edited by Ronald G. Ross, Jr., ISBN: 0-387-23901-4 (Springer, New York, 2005).

# 2.4 Integrated Modeling and Model Validation Requirements

Because of the size and complexity of the TPF-I design concept, the end-to-end system will never be tested on the ground. The project will have to rely heavily on the use of engineering and science simulations to predict on-orbit performance requirements from the lowest level of assembly on up. The requirements of TPF-I impose on the models a level of predictive accuracy heretofore never achieved, especially in the area of microgravity effects, material property accuracy, thermal solution convergence, and all other second order physics typically ignored. This further imposes extreme challenges on the approach to experimental validation of models, since ground testing conditions and sensor accuracy will often be worse than the performance levels expected on orbit.

## Modeling Uncertainty Factors

TPI-I will need to develop and validate on testbeds, a modeling methodology which authenticates the processes and models that will eventually be implemented for predicting the TPF-I flight performance. This will involve modeling the testbeds to the best of our ability by comparing measured and predicted performances, quantifying Modeling Uncertainty Factors (MUFs) to reflect where the agreement between the model predictions and measurements breakdown, incorporating the MUFs within the testbed requirements to validate the error budget allocation process, then incrementally implementing the same procedure to build up the flight system models starting with the flight materials characterization through to model validation of progressively higher levels of flight hardware assembly.

The design Team will identify the required margin and levels of MUFs to achieve the mission. A future version of the Technology Plan will then be able to expand on how the required MUF levels will be validated.

## Model Validation and Testbeds

TPF-I is planning a suite of ground testbeds through which various aspects of the models and simulations will be verified and validated. Technology developed on these testbeds will then be carried later into the ground testing activity of the actual flight system, as required by the Verification and Validation (V&V) process in Phase B and beyond.

Model validation needs will not push the performance levels of the testbeds beyond what is required from the flow down of the error budget. However, model validation will influence the design of the testbeds in that they will need a sufficient level of adjustability, modularity and testing flexibility to investigate the existence of the individual physics contributing to the analytical predictions, to their sensitivities, and to their scalability. It is expected that these testbeds will be instrumental in uncovering "unknown unknowns" not initially anticipated in the models, and to that effect, there will be a continuous process within the model validation activity to re-evaluate what critical physics or assumptions have not yet been incorporated into the analyses.

The exact details of the testing approach and performance levels required for model validation will be defined through an ongoing process of flowing down, through analysis, the flight system requirements to the system testbed performance. Some requirements are understood, and some are less clearly defined, e.g., larger testbeds planned for Phase A-B. The requirements for all the testbeds will be firmed up as soon as the flight design and flight performance requirements are formally established.

By the end of the project, the primary questions asked to the analysts will be "why do you believe the prediction?" To help achieve this challenge, a novel modeling strategy will be implemented on TPF-I, as it is on TPF-C. It is standard practice to include hardware fabrication tolerances as margins within the error budget. For TPF-I, models will be treated as "software fabrication" by including additional margin in the error budget to account for modeling tolerances, *a.k.a.* modeling uncertainties. This implies that the accuracy of the prediction will be quantified by tracking contributions to the modeling errors during the project lifecycle.

The concern that arises from this new modeling paradigm is the issue of "over-designing" the system by imposing tighter nominal performance requirements to make up for larger margin allocations in modeling uncertainties. This unfortunately is inevitable when analysis is the only means to validate on-orbit system performance, as it will be for an increasing number of flight systems in the future. The best that can be done to alleviate this concern is to address the problem up front, and to devise means by which modeling uncertainties can be evaluated, tracked, and reduced to minimize its overall contribution to the margin. It is recognized that modeling uncertainties will be naturally reduced through the course of the project as testbeds and design mature. Nonetheless, there will still be residual uncertainties in the prediction of those flight performances that can only be validated through analysis, and those need to be accounted for in the V&V process.

## Requirements of Pre-Phase A Models

Because the TPF-I requirements are in a realm where there exists no past experience to develop engineering judgment from, the Project will devise a more rigorous approach to defining and reducing uncertainties. This paradigm is fairly new to NASA missions, with JWST and Space Interferometry Mission using engineering judgment to define empirical uncertainty bounds through the mission lifecycle. The plan is to:

1. Develop analytical techniques to propagate and evaluate uncertainties,

2. Develop models and error budgets for each of the testbeds from which uncertainties are evaluated by comparing predicted results to experimental data – this implies that some testbeds will have to perform to flight levels if not better, or that scaling laws will have been defined,

3. And most importantly, to develop methods of reducing uncertainties by improving modeling tool accuracy and by proposing design options which minimize uncertainties.

One such means of reducing modeling uncertainty is to allow on-orbit adjustments through control strategies, either active or passive. The control errors will therefore define the performance uncertainties. TPF-I will continue exploring, when necessary, other mitigating design solutions which implement control strategies for on-orbit adjustments.

In effect, the TPF-I modeling challenge is now turned into validation of analysis bounds, whereby the uncertainty needs to be quantified and managed in the error budget by propagating error contributions from the lowest level of assembly on up. Another implication of this new modeling paradigm is that modeling margin allocations will be used to derive levels of accuracy required from the model validation, as well as the measurement accuracy of the test facility itself. Questions regarding what constitutes a validated model have plagued projects in the past. Through the use of the modeling error margins, we will now be able to derive rational and consistent acceptance criteria for the validation and delivery of models.

# 3   Technology Development Strategy

## 3.1  Technology Development Philosophy

The following paragraphs expand on the guiding philosophical principles behind this technology plan. The principles appear in italics and are described in the text that follows.

*Identify technical needs through the development of requirements, operational scenarios, error budgets, design concepts, and analyses.*  With the help of the Science Working Group a set of mission objectives, fundamental requirements and operational scenarios are established for the design.  The planet detection and characterization objectives described above drive the core of the TPF-I technology efforts since planet detection and characterization are the principal objectives of the mission.  As secondary objectives, comparative planetology and general astrophysics are not permitted to impose more stringent design requirements, although modest design changes that would expand TPF-I's capabilities may be considered. Using these starting points and ideas from earlier industry studies, additional requirements are derived and an extensive error budget is formulated.  These products are used as the basis for preliminary design concepts and as the basis for decisions regarding what technology developments are required.

Figures 3-1 and 3-2 show the philosophical relationships between requirements, testbeds, design concepts, and modeling as represented by this plan.  Figure 3-1 shows the relationships in the early phases of development (Pre-Phase A through Phase B) and Fig. 3-2 shows the relationships for later phases (C through E).  The lines connecting text represent the flow of information to and from the elements. Broader lines represent more frequent changes.

The flow of ideas begins with the mission objectives.  These are translated into detailed requirements and error budgets.  In the early phases of development the requirements and error budgets influence flight design concepts and associated technology testbeds.  In particular, the error budgets help to reveal what new technologies are required by showing what aspects of performance are unprecedented.  The error budgets also define the measures of success for the testbeds.  Flight design concepts either confirm that the right technologies are being developed or can have the occasional direct impact on testbeds when revolutionary approaches eliminate the need for a particular technology or when an overlooked need is identified that causes the addition of a technology development.  The lower half of the loops highlights the critical role modeling plays in the overall technology plan.  Testbed results provide evidence for the validation of models and are instructive in the limits of precision of models and of direct testing techniques.  Flight design concepts identify what is to be modeled to prove that there is a design solution that satisfies the requirements and error budgets.  Modeling is the critical juncture that determines whether technology and design concepts have matured to the point that a proof of concept has been achieved or whether another trip through the loops is required.  There is no path from the mission objectives to the statement "we think this will work" without modeling.

Mission Objectives

Requirements & Error Budgets

Never been done before,
Measures of success

Add/delete

Error budget element achieved

Revolutionary approach

What needs to be done

Tech Testbeds

Try again

Flight Design Concepts

Data for modeling techniques,
limits of precision, & validation

What to model

Modeling

We think this will work
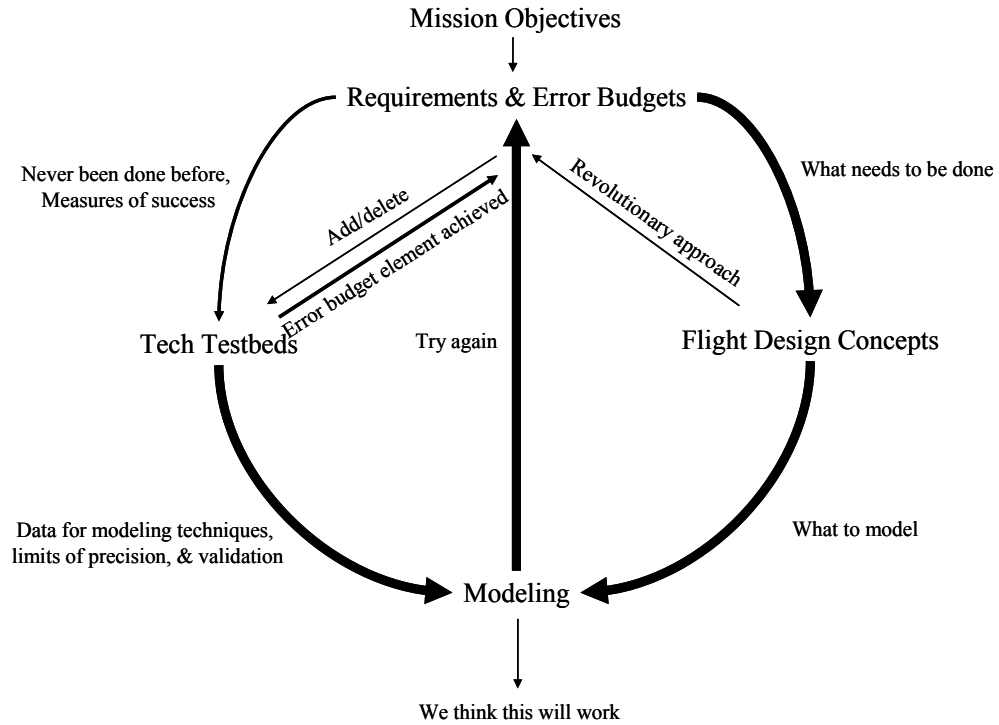
**Figure 3-1.** Relationships of Products of Early Design Phases

It is important to stress that the modeling should be performed in parallel with the testbed work, not in serial. The modelers must be able to coordinate the suite of measurements that are needed to validate the models. Exactly what measurements are needed may be impossible to predict in advance, as the shortcomings of the models may only be evident when confronted with new results, as each new milestone draws near. Moreover, such measurements, deemed necessary in hindsight, may prove extremely difficult or expensive to recreate after the fact. Only through concurrent development of models and testbeds can the necessary models be validated in a suitable manner.

The flow changes somewhat in the later stages of development. The technology testbeds evolve to become flight hardware and software testbeds and flight assemblies. By this time the number of iterations from requirements through modeling should drop as the expense of doing so greatly increases. Modeling continues to serve as a critical link towards the ultimate statement of flight readiness, "This will work." This is especially true for TPF-I since by its sheer size it will be impractical to perform end-to-end testing of the complete observatory within a flight-like environment. Finally, it is recognized that testbeds and models continue to be important in Phase E as they are critical tools for troubleshooting flight anomalies.

As the frontiers of modeling scope and precision are expanded it also becomes correct to call certain modeling efforts technology development tasks themselves. This is the case on TPF-I for the Observatory Simulation task and more focused efforts about modeling uncertainties and cryo structures modeling. These efforts are described in greater detail in Chapters 6 and 7.

Mission Objectives

Requirements & Error Budgets

What needs to be done

Try again

Flight Design Concepts

Flight Development Testbeds &
Flight H/W & S/W Testing

What to model
Data for modeling techniques,
limits of precision, & validation

Modeling

This will work
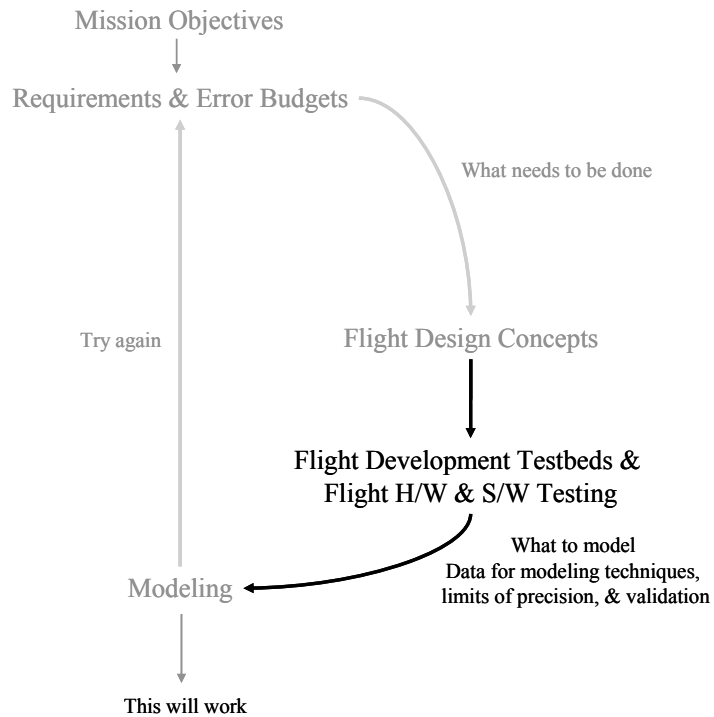
**Figure 3-2.** Relationship of Products of Later Design Phases

*Seek expert advice to supplement the project team's identification of technical needs.* The TPF-I Project identifies technology needs as expressed in this plan. New ideas, however, come from various sources. Direct input is available from TPF-I engineers and scientists, whose connections in the broader community include members from many organizations. The design team has included members of multiple NASA centers and industry partners. University contracts are funded through JPL to nurture studies that explore new technology. The technology teams have included members of other government institutions, industry, and universities. The TPF-I Project regularly convenes formal reviews of its technology plan by panels of experts to comment and identify gaps in technology development. The advisory groups include the TPF-I Science Working Group, the TPF Technology Advisory Committee, and the Navigator Program's External Independent Readiness Board (EIRB). Internationally, the Project is seeking to develop a closer collaboration with the European Space Agency's (ESA's) Darwin mission team. The Darwin mission, like TPF-I, is planned to be a formation flying interferometer that is intended to search for terrestrial planets. It should be noted that the field of ground- and space-based interferometry continues to expand, and interactions with this community at conferences and workshops continues to provide new ideas for advanced technology.

*If a flight-proven solution to a TPF-I requirement already exists — use it.* Many TPF-I requirements do not exceed the scope of what has already been done. Examples of this are the power and uplink/downlink telecommunications requirements which fall well within the ranges of previous space missions. Consequently, the design concepts use industry-standard solar arrays and RF equipment rather than demanding new technologies. This does not mean TPF-I will not incorporate advances in these

technologies as they become available. As improvements become commonplace, TPF-I will take advantage of them, but only after they are considered low risk.

*Avoid development efforts that duplicate those of other NASA projects preceding TPF-I.* If NASA is already sponsoring technology development for another mission that is planned to launch before TPF-I and that satisfies a TPF-I technical need, then the plan is to inherit the results of that development rather than fund a parallel development. Some vigilance is required to mitigate the risk of depending on another effort to serve TPF-I. Missions get cancelled or postponed. Technology development efforts fail. Critical lessons about how to apply the new technology are learned during the course of development and flight operations. So the TPF-I development plan will have to follow such developments closely and carry budget reserves, schedule reserves, and design options that can compensate for adverse events associated with the new technologies. An important point is that TPF-I is not depending on the technology developments sponsored by ESA for its Darwin mission or by other U.S. organizations such as the Department of Defense. While not precluding collaborations in the future that might include the delivery of hardware and software, the approach now is to develop all the unique technology that TPF-I needs using NASA funding. Should a collaboration with ESA continue into Phase A of TPF-I, the technology plan will be revisited and reassessed. A description of the specific technology development efforts upon which TPF-I is depending is provided in the roadmaps of Section 3.2.

*Make a plan.* This document provides the strategy. It emphasizes the fundamental physics demonstration of stable nulling interferometry and the fundamental engineering challenge of formation flying. Tactics are specified by detailed budgets, schedules, work agreements, and such that are modeled after the management products used during flight project development. It is recognized that making a plan is not enough. The plan must be maintained to adapt to changing conditions. For example, the previous TPF Technology Development Plan was developed in 2002–2003 to support the expected architecture downselect from either a TPF-C or TPF-I in 2006. It has now been decided to proceed with both observatories. TPF-C will launch first, so the pace of TPF-I technology efforts has been reconsidered and is reflected in this revision. The goal of this plan is to prepare the project for transition to Phase A no later than ~2010 with the eventual goal of approval for a ~2019 launch. The TPF-I technology plan will be reviewed each year and revised to reflect changes in technology maturity as well as programmatic projects.

*Execute the plan.* The Project is fully staffed for the current budget. Most of the contracts required to implement this plan are already in place. Lab space has been found. Progress against the plan is monitored through established metrics and milestones described in the plan itself. The team files short written reports distributed by email each week. Internal project management reviews are held monthly wherein schedules, budgets, workforce, technical results, and concerns are discussed. Management reviews with NASA HQ are conducted quarterly. Technical interchange meetings are held several times each year with the Science Working Group and Technical Advisory Committee. Action items from these meetings are assigned, statused, dispositioned, and documented.

*Investigate multiple potential solutions where affordable.* Technology development occasionally fails; consequently, for some needs, the TPF-I plan includes multiple approaches. One example of this is spatial filters where three approaches are currently being pursued: chalcogenide fibers, silver halide fibers, and metal waveguides. Another example is the Achromatic Nulling Testbed where three approaches to field inversion are being investigated: through focus, periscope, and phase plates.

*Leave a legacy*. TPF-I will not be launching for many years. Many of the people working on the project today will not be involved in the flight development effort, so care is being taken to record what is being learned along the way. First and foremost is that key experimental results from the testbeds be reproducible and consistent with the integrated modeling. This is done by documenting the configuration of the testbed and the procedural steps used to achieve the results in lab notebooks and engineering drawings. It also involves achieving the results consistently and repeatably to a high degree of confidence in understanding the physics and modeling of the results. As the high-level technology goals specified in this plan are achieved, closeout reports are produced to record the results. These reports are refereed by the Project Technologist who serves as a check against the testbed cognizant engineers. The reports are reviewed and concurred upon by the TPF Technology Advisory Committee, Navigator Independent Review Team, and NASA Headquarters. Finally, the cognizant engineers are encouraged to publish their achievements in journals and conference papers. A second dimension of the legacy is that the testbed results can be explained with validated models. It is insufficient to achieve a technology goal without a model that explains the fundamental physics behind the empirical results. Consequently, data from major testbeds like the Achromatic Nulling Testbed and the Planet Detection Testbed are used to validate modeling efforts.

The TPF-I Project is committed to maintaining strong industry and university involvement and will solicit, award, and manage a set of industry and university contracts to develop and demonstrate the needed technologies for TPF-I. The development of TPF-I will take advantage of the rich technology inheritance from many outside sources of key technologies and the many NASA missions currently under development.

# 3.2 Technology Roadmaps

This section presents the roadmaps for TPF-I technology development. Separate maps are provided for optics and starlight suppression, formation flying, cryogenic, and modeling technologies. In the maps, shaded boxes are options that are receiving or have recently received TPF funding and are described in detail in following sections. Clear boxes are other options being considered in the trade studies to select approaches for flight that have not been funded by TPF. The small shaded triangles attached to some of the boxes indicate which options are currently considered to be the most likely outcomes of the trade studies and in some cases explain why certain TPF-sponsored options are not funded. Several of these results anticipate heritage from other missions or technology development efforts. These dependencies are described in Section 3.3, "Technology Heritage." At the end of Pre-Phase A at least one of the candidate options for flight must show promise for each technology. Later development phases can be used to make final flight selections if more than one option proves viable in time.

## Optics and Starlight Suppression

Figure 3-3 is the roadmap for optics and starlight suppression technology development. The deep nulling of starlight needed for TPF-I will demand very exact matching of multiple optical beams. The phases, amplitudes, and polarizations of these beams must be matched over a relatively broad waveband in a stable way for long periods of time. There is much here that is unprecedented; consequently, there are several technology efforts planned.

**Beamsplitters** are a key component of the TPF-I instrument nuller. The challenge for beamsplitters is operation over the relatively broad waveband of interest. Four options are under consideration.
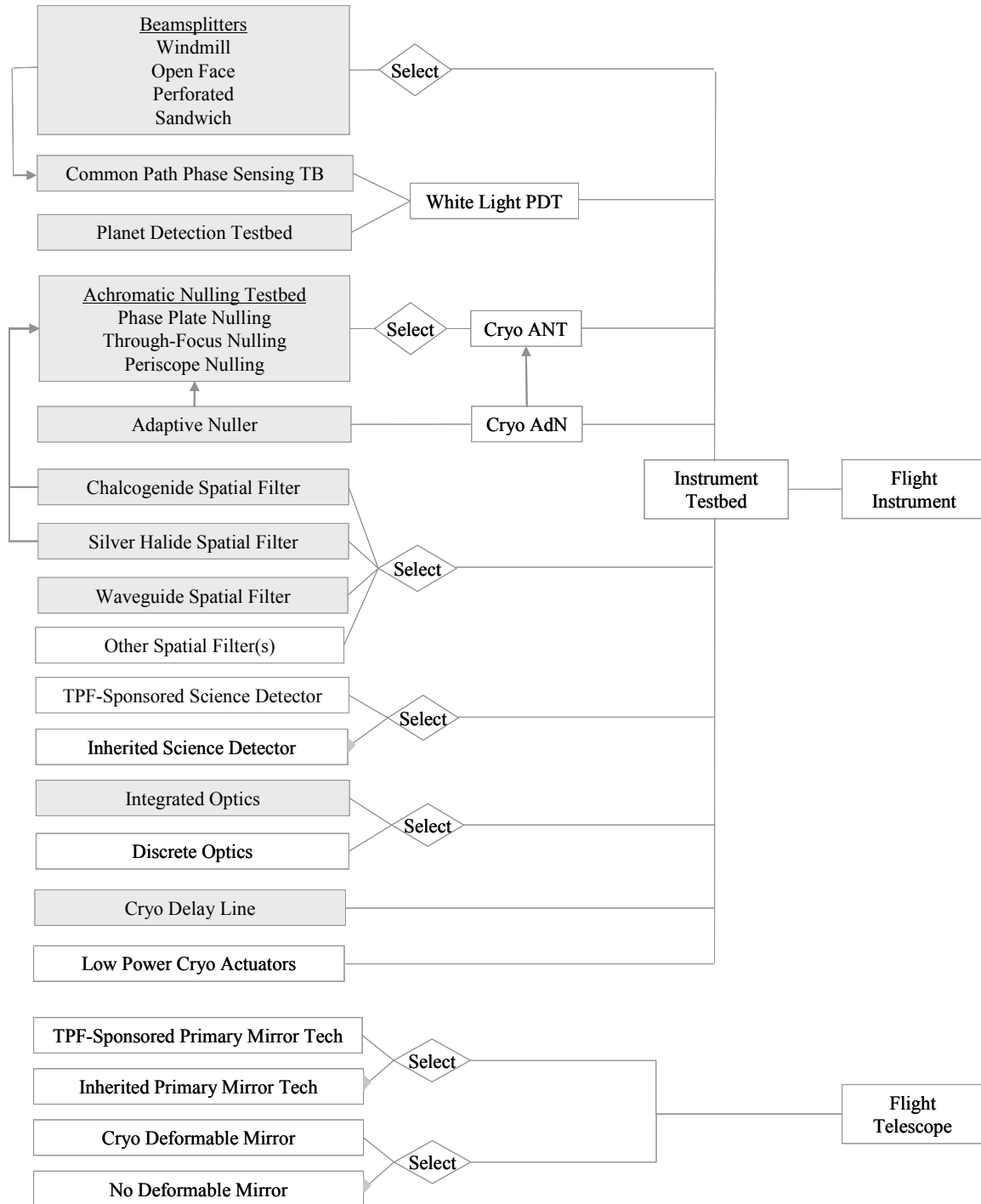


**Figure 3-3.** Roadmap of Optics and Starlight Suppression Technologies

Examples of the windmill, open face, and perforated designs will be fabricated and tested in the Common Path Phase Sensing Testbed. A specification of the sandwich beamsplitter design will be produced so that the feasibility of its fabrication can be assessed by industry. If judged to be feasible, then funding might be provided in later years to fabricate an example of the sandwich beamsplitter for test and evaluation.

The principal purpose of the **Common Path Phase Sensing Testbed** is to evaluate a new way to control phasing for the nuller. The convention is to split light somewhere within the beam train. Shorter wavelength light is sent to a fringe tracker, longer wavelength light to the science detector. This testbed keeps the fringe tracker light and science light together on a common path farther along the beam train so as to reduce systematic errors by making a more accurate measurement of the science light beam path. Lessons learned in this testbed will be applied to the white light version of the Planet Detection Testbed (PDT) and/or the instrument testbed.

The **Planet Detection Testbed** is one of two flagship efforts of starlight suppression technology development. Both explore multiple dimensions of the beam matching challenge. The PDT explores the dynamics of keeping nulls stable by testing control algorithms applied to a 4-beam nuller operating on a laser light sources simulating a star and planet. A later version of the PDT will attempt to replicate deep nulling results on broadband (white) light.

The **Achromatic Nulling Testbed** (ANT) is the second flagship effort of starlight suppression technology. The ANT is the principal effort exploring the effects of chromaticity and cryogenic temperatures on null depths. The ANT is used to investigate the promise of three different nulling architectures: phase plate, through-focus, and periscope. After selecting one of the nulling architectures, the ANT will be tested at cryogenic temperatures.

The **Adaptive Nuller** is an invention aimed at compensating for quasi-static errors in the beam train that affect either phase or amplitude. After testing the Adaptive Nuller by itself it will be integrated into the room temperature version of the ANT. Later a cryogenic version of the Adaptive Nuller will be developed and tested with the ANT at cryogenic temperatures.

**Spatial filters** are another key component. These filters are the last optical element affecting the beams before they strike the detectors. It is hoped these filters will remove higher order optical aberrations from the wavefronts, thereby enabling deeper nulls. While such filters are common in other spectral bands they are new to the IR band that TPF-I uses.

The current expectation is that **science detector technology** can be inherited from either the Spitzer or James Webb Space Telescope missions. Detailed analysis has not yet been performed that can verify this assumption so the roadmap includes an option for a TPF-sponsored development of a detector.

**Integrated Optics** is an investigation into fabrication of monolithic optical components that serve the function of multiple discrete parts, thereby reducing the overall system complexity. The initial focus is on waveguides for the nuller, but the technology is generic enough that it might be applicable to other elements of the instrument. Presently, integrated optics represents an alternative approach to the use of discrete optics in the ANT and PDT. It is expected that integrated optics will not be required to achieve the null depths desired, but if the discrete optics fail to deliver then the infusion of integrated optics might

be critical to success. Even if the need for integrated optics in Pre-Phase A is not critical, the work will still be valuable since it shows great promise for simplifying the design for the flight instrument.

An effort to develop a **Cryogenic Delay Line** achieved early success and consequently was suspended for a few years, but will be restarted in the future to continue the push for TPF levels of performance.

A key requirement for TPF-I flight is that the optics be kept at or below 40 K during observations. The current concept is that this is achieved through passive cooling. This approach might demand cryogenic actuators that consume less power than those now available since a number of the optics in the interferometer must be adjustable. Consequently, a placeholder exists in the map for the development of **Low Power Cryogenic Actuators**. Detailed analysis to be performed in later years will determine whether or not a specific TPF-sponsored development is required.

The roadmap for the starlight suppression and optics leads to an **Instrument Testbed**. This testbed is notional. The purpose of this testbed is to bring together the many instrument technology development efforts in a single place to test their compatibility at a subsystem/instrument system level before committing to a design for the flight instrument. Key characteristics of this testbed are that it would cover the entire waveband and would be capable of cryogenic operation. This testbed would provide a good test of the Observatory Simulation.

The bottom portion of Fig. 3-3 shows the roadmap for potential telescope technologies. Two types have been identified so far: **Primary Mirror and Cryo Deformable Mirror Technology**. The planets to be observed are dim, so sensitivity is a challenge for the interferometer. The current concept has a primary mirror of diameter between 3.5–4.0 meters. The plan is for them to be monolithic structures rather than segmented, though a more detailed trade of this in the future might change this assumption. There is a lot of ongoing research into the construction of large mirrors for both ground and space applications. The TPF-I plan right now is to wait and follow the progress of these efforts, so the Inherited Primary Mirror Technology option is shown as the most likely outcome. Future events may dictate that a dedicated TPF-I effort in this area is required, so a placeholder for a TPF-sponsored Primary Mirror Technology task is also shown in the roadmap.

Current thinking is that a cryogenic, deformable mirror for wavefront control near the front of the beam train will not be required if development of the spatial filters is successful. More detailed modeling of the system is required to be certain, so an option to develop a deformable mirror is shown in the roadmap. This mirror would be larger than the deformable mirror that is required within the Adaptive Nuller, so a separate development might be necessary.

## Formation Flying

Figure 3-4 is the roadmap for formation flying technology development. The TPF-I challenge is to fly multiple spacecraft in formation over separations measured in tens of meters to relative ranges that are measured in centimeters for observations that last for days.
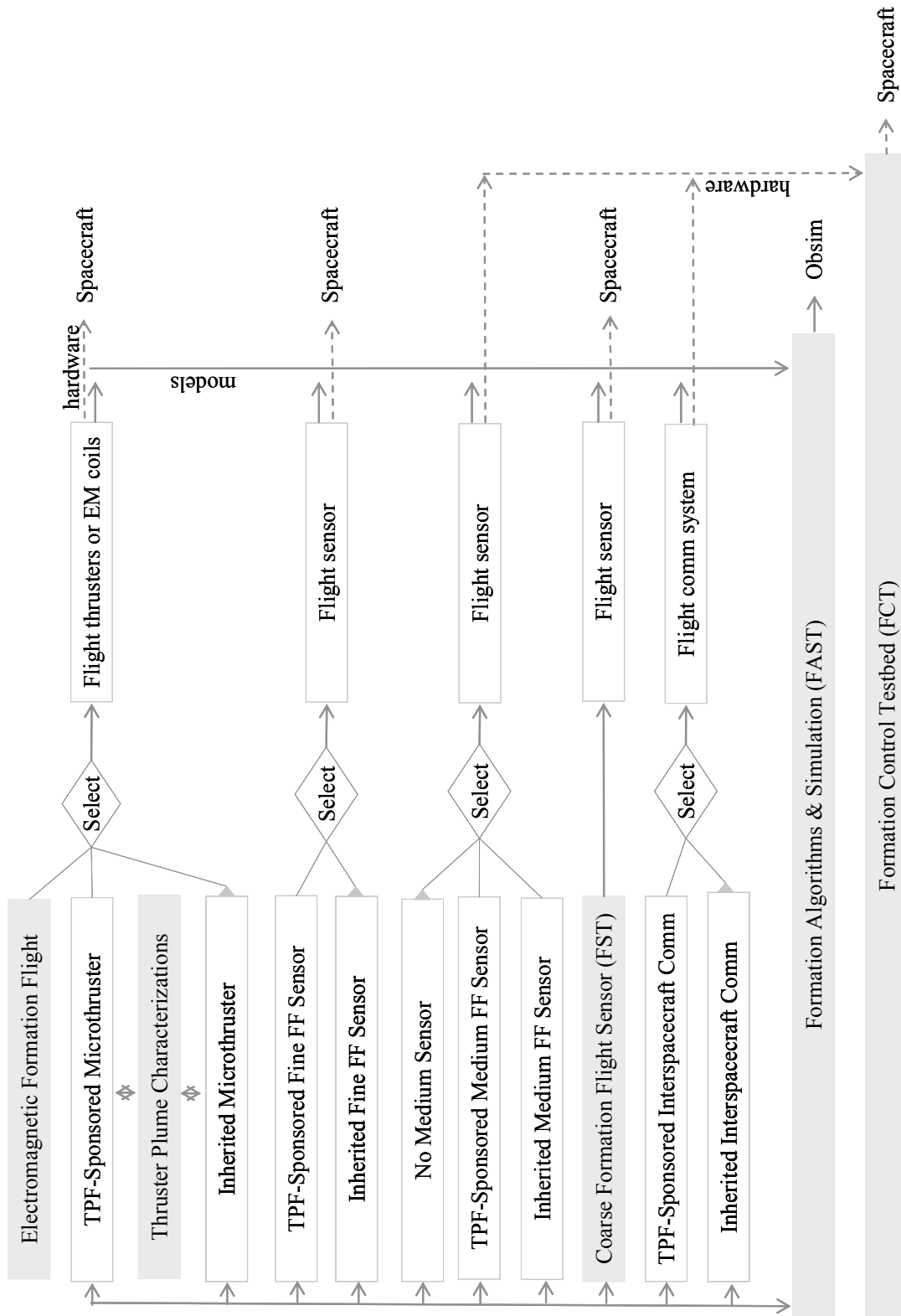
**Figure 3-4.** Roadmap of Formation Flying Technologies

The **Electromagnetic Formation Flight** task is an approach to controlling the formation. Superconducting coils are used instead of small thrusters to control the relative positions of spacecraft within the formation. This task includes a hardware testbed.

The **Thruster Plume Characterizations** task is a tool used for trade studies. This effort takes candidate thruster technologies and tests them for characteristics of specific interest to TPF-I, namely, the thruster plume emission in the mid-IR and the potential for contamination of cryogenic surfaces. Analytical models of the plumes are also constructed and validated using test data.

The Coarse Formation Flight Sensor (**Formation Sensor Testbed**) task is intended to produce a sensor technology for formation acquisition. It is expected to lead directly to the development of a flight sensor.

Many of the options are simulated by the **Formation Algorithms and Simulation** (FAST) task to assess whether flight requirements can be satisfied. As such, the FAST is another tool used to conduct trade studies and to inform the project of performance levels needed from the testbeds. The FAST is also used following selections between options to predict the potential performance of the flight concept (solid lines on the right). Validated simulations from FAST feed the larger Observatory Simulation task which attempts to model the performance of TPF-I from photons in to science data out.

The **Formation Control Testbed** (FCT) is a hardware testbed used to validate FAST simulations that might in the future host tests of some flight hardware (dashed lines on the right).

## Integrated Modeling

Figure 3-5 is the roadmap for integrated modeling development. Text shown outside of boxes refers to other technology development tasks. These tasks contribute information to the modeling task that appears to their right. So for example, the Advanced Cryocooler Technology Development Program (ACTDP) contributes information for the development of a performance model of the cooler and information about the dynamic disturbances from the coolers.

The core of the TPF-I modeling effort is the **Observatory Simulation** task. In the roadmap a string of boxes near the bottom show the different stages of the Observatory Simulation development. The first stage of the effort is the invention of techniques and tools to perform the modeling to an unprecedented degree of precision. The **Cryogenic Structures, Model Uncertainty Evaluation,** and **Integrated Modeling of Optical Systems** tasks all contribute new rules, procedures, or computer codes for integration into the Observatory Simulation effort.

Moving to the upper left of the map one finds Component Performance Models. The component models are the traditional, stand-alone models of flight design concepts. Each of these models is based on experimental data from TPF-I development efforts or test data from inherited items. These models are delivered by the technology development leads.
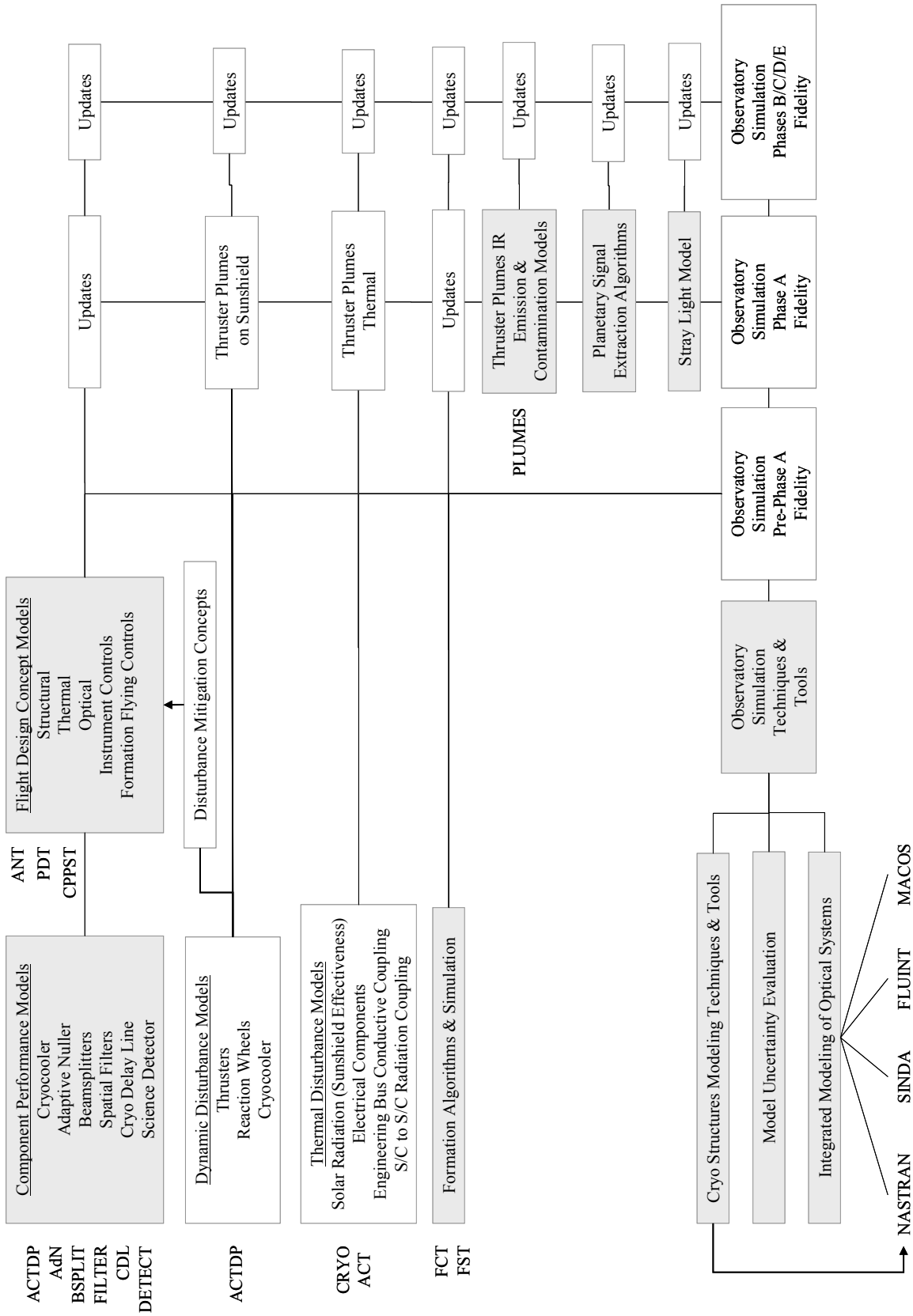
**Figure 3-5.** Roadmap for Integrated Modeling

Dynamic disturbance models also come from component developers. The reaction wheels will likely be catalog items. The large thrusters needed to retarget the formation will also likely be catalog items. The small thrusters for formation control during observations and the cryocooler are developments. These developments will have to include tests to characterize the mechanical disturbances produced so that they can be modeled. It is already anticipated that systems to isolate the optics from the mechanical disturbance generators will be required. Though there is no concept specifically for TPF-I yet for these isolators, industry already has several approaches that may suffice when tailored. Future study by TPF-I design team will produce concepts for these which will then be incorporated into the Flight Design Concept Models.

The Flight Design Concept Models are the traditional, stand-alone models of the design. These models are starting points used to conduct high-level trade studies. After these first-order trades the stand-alone models are integrated to help form a Pre-Phase A version of the complete Observatory Simulation. Another piece of this integration is the inclusion of disturbances simulated by the Formation Algorithms and Simulation task.

Phase A will see updates to the Observatory Simulation that include the contribution of thruster plumes to IR noise, planetary signal extraction algorithms, and stray light effects. These efforts are already under study. Other updates like the dynamic effects of thruster plumes striking the sunshields and the thermal effects of these plumes await Phase A staffing and funding.

# 3.3 Technology Heritage

TPF-I is pioneering the fields of space-based nulling interferometry and formation flying for NASA. ESA's technology program for the Darwin mission is advancing these same fields since Darwin's science objectives parallel TPF's. Several NASA missions will provide technology advances that benefit TPF-I, including:

  a) Spitzer Space Telescope: operational in 2003

  b) Keck Nulling Interferometer: planned for 2005

  c) Large Binocular Telescope Interferometer: planned for operation in 2007

  d) Space Interferometry Mission (SIM): planned for launch in 2010

  e) James Webb Space Telescope (JWST): planned launch in 2011

  f) Laser Interferometer Space Antenna (LISA): launch around 2011

  g) Terrestrial Planet Finder Coronagraph (TPF-C): planned launch in 2014

  h) StarLight: in development until 2002

  i) Formation flying demonstrations by various organizations

TPF-I will benefit from cryogenic and mid-infrared detector technology developed for the Spitzer Space Telescope and the James Webb Space Telescope. The heritage from JWST is most relevant for cryogenic technology, in particular the large deployable sunshields, passive cooling technology, and the Berylium mirror technology. Also of specific interest are JWST's development of cryogenic actuators, including cryogenic opto-mechanical devices and wavefront sensing and control techniques. The experience of JWST with the integration and test of a large cryogenic observatory and observatory modeling are also of direct interest. Heritage from the Herschel Space Telescope is also possible through its development of silicon carbide mirror technology.

The Keck Interferometer and the Large Binocular Telescope Interferometer have both developed technology for ground-based interferometry that has direct application in TPF-I. These projects are the closest ground-based analogs to TPF-I, since their primary objectives are the study of extrasolar planetary systems at mid-infrared wavelengths. They will provide heritage in methods of mid-infrared starlight suppression, pathlength control, beam transport, fringe tracking, tip/tilt correction, cryogenic actuators, and integration and test of interferometer systems.

For the development of techniques of interferometric sensing and control of optical surfaces, vibration suppression, and integrated modeling of space interferometers, there will be heritage from the Space Interferometry Mission as well as LISA. SIM has developed space-qualified laser metrology systems for nanometer control and picometer sensing of its optical surfaces. Precision laser metrology, stabilized lasers, corner-cubes, active control, vibration isolation and suppression, and precision optics are all areas where technology inheritance is possible from SIM and LISA. TPF-I will also benefit from parallel technology development for TPF-C, whose metrology requirements are similar. Other potential contributions from TPF-C include primary mirror technology, space-qualified deformable mirrors, and modeling techniques.

TPF-I has directly benefited from technology developed for the StarLight mission. In particular, the current efforts in formation flying at JPL were focused prior to 2002 on developing the formation flying capability of StarLight. Simulations of formation flying control showed at the time that the formation control algorithms could meet the StarLight requirements of 10-cm ranging and 1-mrad control, and also served as the basis for FAST, now implemented in a real-time distributed-system architecture. The Formation Interferometry Testbed (FIT) demonstrated fringe acquisition with greater than 40 μm/s relative motion in the lab, with fringe lock for relative rates up to 30 μm/s, which were deemed to be typical of interspacecraft motions while in formation. Precision metrology sensors, as well as ranging and angle sensors were also developed for StarLight and provide direct heritage to the development of TPF-I sensors.

TPF-I is benefiting from the Code R Distributed Spacecraft Technologies (DST) program. One development task in this program is a candidate for the TPF-I medium precision formation flying sensor. The DST sensor uses a near-infrared directly modulated laser diode modulated with a pseudo-random signal for ranging; a Multiple-Quantum-Well Modulated Retroreflector array for ranging signal return, identification, and data modulation; and a high bandwidth/large area photodiode for ranging signal return and data detection. It is intended to provide submillimeter range and arcminute bearing inter-spacecraft positional information and also supports non-interfering bidirectional communications at megabit/sec rates. A second development task is the Modulation Sideband Technology for Absolute Ranging (MSTAR). MSTAR is a candidate for the TPF-I formation flying fine precision sensor. It is a laser-

based ranging system.  A third development task is the Miniature Xenon Ion Thruster (MiXI) which is a candidate for use as the control actuator for fine precision formation flying.  MiXI is a significantly scaled-down ion thruster using xenon propellant that is able to produce thrust levels in the range of 0.5–3 mN at 3000-s specific impulse with greater than 50% efficiency using less than 100 W of power.

Finally, TPF-I formation flying might benefit from future NASA missions under study like the Space Technology 9 mission, which has formation flying as one of five candidate technologies being competed for selection, or lunar and Mars exploration missions that demand autonomous rendezvous and docking.

# 3.4  Technology Gates and Milestones

Technology gates are the most important steps in the development efforts and represent fundamental, novel achievements in mitigating major technical risks about the TPF-I mission.  The technical criteria of a technology gate will be satisfied before the project enters a new phase of development (e.g., from Pre-Phase A to Phase A).    The technology gates are specified in this section.

Technology **milestones** are more modest achievements than gates.  Some milestones show incremental progress of a technology testbed towards achieving a gate.  Technology milestones are specified for each technology task described in Chapters 4 through 7.  Descriptions of selected milestones that are closely related to the technology gates are included in this section.

For Pre-Phase A, a series of technology **gates** will culminate in achievements of TRL 5 to at least within an order of magnitude of flight requirements for selected error budget terms for *critical* new technologies.  A development path towards achieving flight levels will also be identified.  Testbed results will validate testbed models consistent with measured performance and the error budget allocations.  In cases where the testbed descriptions currently lack quantitative criteria, these criteria will be developed as part of the initial testbed effort.

## Pre-Phase A Gates and High-level Milestones

### Optics and Starlight Suppression Technology

1. **Dispersion Control:** Using the Adaptive Nuller**,** demonstrate that optical beam amplitude can be controlled with a precision of $\leq$ 0.2% and phase with a precision of $\leq$ 5 nm over a spectral bandwidth of > 3 $\mu$m in the mid IR for two polarizations.  This demonstrates the approach for compensating for optical imperfections that create instrument noise that can mask planet signals. *Milestone TRL 4.* **Date: Q2/FY2006.**

2. **Dispersion Control at Temperature:** Using the Adaptive Nuller**,** demonstrate that optical beam amplitude can be controlled with a precision of $\leq$ 0.2% and phase with a precision of $\leq$ 5 nm over a spectral bandwidth of > 3 $\mu$m in the mid IR for two polarizations at $\leq$ 40 K.  Accompany these results with a model of the Adaptive Nuller, validated by test data, to be included in the model of the flight-instrument concept.  This demonstrates the approach for compensating for optical imperfections that create instrument noise that can mask planet signals at the temperature required for flight operations. *Gate TRL 5.* **Date: Q3/FY2009.**

3. **Starlight Suppression (Depth):** Using the Achromatic Nulling Testbed, demonstrate that infrared light of a single wavelength (laser) can be suppressed by $\geq 10^6$. This demonstrates the physics of suppressing the light from stars so that light from terrestrial planets can be observed. Flight-like null depths are achieved at room (non-flight) temperature. *Milestone TRL 3.* **Date: Q1/FY2004 (completed).**

4. **Starlight Suppression (Depth & Bandwidth):** Using the Achromatic Nulling Testbed, demonstrate that infrared light over a waveband of $\geq 25\%$ can be suppressed by $\geq 10^6$. This demonstrates the approach to the broadband starlight suppression (dimming of a range of wavelengths) needed to characterize terrestrial planets for habitability. Flight-like null depths are achieved at room (non-flight) temperature. *Milestone TRL 5.* **Date: Q1/FY2006.**

5. **Starlight Suppression (Depth & Bandwidth at Temperature):** Using the Achromatic Nulling Testbed, demonstrate that infrared light over a spectral bandwidth of $\geq 25\%$ can be suppressed by $\geq 10^6$ at $\leq 40$ K. Accompany these results with an optical model of the Achromatic Nulling Testbed, validated by test data, to be included in the model of the flight-instrument concept. This demonstrates the approach to the broadband starlight suppression needed to characterize terrestrial planets for habitability at a flight-like temperature. *Gate TRL 5.* **Date: Q1/FY2007.**

6. **Planet Detection (Contrast Ratio of $10^5$):** Using the Planet Detection Testbed, demonstrate detection of a simulated (laser) planet signal at a star/planet contrast ratio of $\geq 10^5$. This demonstrates that several opto-mechanical control loops can be integrated and operated in a testbed configuration that includes the principal functional blocks of the flight instrument. These functional blocks include fringe tracking, pathlength metrology, beam shear and pointing correction, 4-beam combination, and phase chopping. Success shows that an instrument can be operated with a stability representative of flight requirements and within a factor of 200 of the contrast that permits the suppression of the background noise from local and exo-zodiacal dust clouds. *Milestone TRL 4.* **Date: Q4/FY2005.**

7. **Planet Detection (Contrast Ratio of $10^6$):** Using the Planet Detection Testbed, demonstrate detection of a simulated (laser) planet signal at a star/planet contrast ratio of $\geq 10^6$. This demonstrates that several opto-mechanical control loops can be integrated and operated in a testbed configuration that includes the principal functional blocks of the flight instrument. Success shows that an instrument can be operated with a stability representative of flight requirements and within a factor of 20 of the contrast that permits the suppression of the background noise from local and exo-zodiacal dust clouds. *Milestone TRL 4.* **Date: Q1/FY2007.**

8. **Planet Extraction:** Using the Planet Detection Testbed, demonstrate extraction of a simulated (laser) planet signal at a star/planet contrast ratio of $\geq 10^6$ for a rotation of the flight formation lasting $\geq 5000$ s. Accompany these results with a control system model of the Planet Detection Testbed, validated by test data, to be included in the control system model of the flight-instrument concept. Success shows flight-like planet sensing at representative stability levels within a factor of 20 of the contrast at 1/10 the flight observation duration. *Gate TRL 5.* **Date: Q3/FY2007.**

**Formation Flying Technology**

9. **Formation Flying (2-Spacecraft Simulation):**  Using the Formation Algorithms & Simulation Testbed**, s**imulate the control of two spacecraft flying in formation to a relative range of ≤ ±5 cm and a relative bearing of ≤ ±60 arcmin using multiple flight-analogous computers to represent the spacecraft.  This demonstrates formation control architecture and algorithms in a real-time distributed flight-like computational environment needed to control multiple spacecraft flying in close formation to a precision that enables the detection of terrestrial planets. *Milestone TRL 3–4*. **Date: Q4/FY2003 (Completed).**

10. **Formation Flying (5-Spacecraft Simulation):** Using the Formation Algorithms & Simulation Testbed, **s**imulate the control of five spacecraft flying in formation to a relative range of ≤ ±1 cm and a relative bearing of ≤ ±20 arcsec (corresponding to 100-m spacecraft-to-spacecraft separation) using multiple flight-analogous computers to represent the spacecraft.  This demonstrates the formation control architecture and algorithms in a real-time distributed flight-like computational environment needed to control the total number of formation flying spacecraft needed to accomplish TPF-I to a precision that enables the detection of terrestrial planets. Key capabilities to be demonstrated include autonomous on-board formation acquisition and initialization, collision-free formation maneuvering, and precision control of the formation in a TPF-I science configuration. *Milestone TRL 5*. **Date: Q4/FY2006.**

11. **Formation Flying (5-Spacecraft Simulation With Fault Recovery):**  Using the Formation Algorithms & Simulation Testbed, simulate the safing and recovery of a five-spacecraft formation subjected to a set of typical spacecraft faults that could lead to mission failures unique to formation flying such as collisions, sensor faults, communication drop-outs, or failed thrusters in on or off states.  Simulations can be limited to single-fault scenarios.  This demonstrates the robustness of formation control architecture, as well as fault-tolerance of the on-board formation guidance, estimation, and control algorithms to protect against faults that have a reasonable probability of occurring sometime during the TPF-I prime mission and that are unique to TPF-I's unprecedented use of close formation flying. *Gate TRL 5*.  **Date: Q4/FY2007.**

12. **Formation Flying (Multiple Robot Demonstration):** Using the Formation Control Testbed as an end-to-end system-level hardware testbed, demonstrate that a formation of multiple robots can autonomously initialize, maneuver and operate in a collision free manner.  A key maneuver, representative of TPF-I science will be demonstrated by rotating through greater than 90° while maintaining a relative range control of ≤ ±5 cm and a relative bearing control of ≤ ±60 arcmin. This validates the formation control architecture and algorithms and the testbed models developed by the Formation Algorithms & Simulation Testbed while physically demonstrating the approach to achieving the angular resolution required for the detection of terrestrial planets. *Milestone TRL 4*. **Date: Q4/FY2007.**

13. **Formation Flying (Multiple Robot Demonstration With Fault Recovery):**  Using the Formation Control Testbed, demonstrate that a formation of multiple robots can be safed following the injections of a set of typical spacecraft faults that have a reasonable probability of occurring during flight.  Demonstrations can be limited to single-fault scenarios.  This validates the software simulation of fault recovery for formation flight. *Gate TRL 5*.  **Date: Q4/FY2008.**

### Cryogenic Technology

14. **Cryocooler Development:** With the Advanced Cryocooler Technology Development Program, demonstrate that the development model coolers meet or exceed their performance requirements to provide ~30 mW of cooling at 6 K and ~150 mW at 18 K. This demonstrates the approach to cooling the science detector to a temperature low enough to reveal the weak planet signals. *Gate TRL 5.* **Date: Q4/FY2006 (Completed Q2 2005).**

### Integrated Modeling

15. **Observatory Simulation:** Demonstrate a simulation of the flight observatory concept that models the observatory in a static condition (no dynamic disturbances). Validate this model with experimental results from at least the Achromatic Nulling and Planet Detection testbeds at discrete wavelengths. Use this simulation to show that the depth of the starlight null can be controlled over the entire waveband to within an order of magnitude of the limits required in flight to detect Earth-like planets, characterize their properties and assess their habitability. *Milestone TRL 4.* **Date: Q1/FY2008.**

16. **Observatory Simulation:** Demonstrate a simulation of the flight observatory concept that models the observatory subjected to dynamic disturbances (e.g., from reaction wheels). Validate this model with experimental results from at least the Planet Detection Testbed at discrete wavelengths. Use this simulation to show that the depth and stability of the starlight null can be controlled over the entire waveband to within an order of magnitude of the limits required in flight to detect Earth-like planets, characterize their properties, and assess their habitability. *Gate TRL 5.* **Date: Q4/FY2009.**

## Phase A and B Gates

For *Phase A* the technology gates define achievement of TRL 5 to at least within an order of magnitude of flight requirements for *all* new technologies. Phase A gates show that the flight baseline performance requirements in the draft Program Level Requirements Appendix (PLRA) can be met. These gates apply mainly to systems and subsystems. Testbed results will validate preliminary models of the flight system.

For *Phase B* the technology gates define achievement of TRL 5 (for components) and TRL 6 (for systems or subsystems) to *flight requirements* for all new technologies. Furthermore, technologies are benchmarked against the performance goals of the PLRA. Testbed results will demonstrate an "end-to-end" capability to predict flight performance and identify a flight integration and test program that validates this prediction.

Phase A and B gates will be supplied in later revisions of this plan. See the discussion of technology roadmaps for how Pre-Phase A activities are related to later activities.

# 4 Optics and Starlight Suppression Technology

The technology roadmap for an interferometry mission includes heritage of precursor technology and ongoing development efforts from ground-based interferometers, including the Keck Interferometer and the Large Binocular Telescope Interferometer (LBTI), and space missions such as SIRTF, JWST, and SIM. The Keck Interferometer and LBTI will provide experience with cryogenic nulling, cryogenic active optics, metrology, and many system-level concerns. From JWST and SIRTF there will be the legacy of large lightweight mirror technology, passive-cooling shield designs, and advances in detector technology. Ongoing efforts in the development of SIM will provide many of the technologies for precision relative metrology, structure design, vibration sensing and control, and space-qualified interferometry systems.

## 4.1 Core Technology and Testbeds

Although the technology needs for mid-infrared nulling interferometers do not represent major, insurmountable challenges, considerable development at the component and system level is still required. Interferometric nulling of the light from multiple collectors over a band of ~7–17 microns is required, with stable nulls of ~$10^{-6}$. A major driver of system requirements is the depth and stability of the starlight null. Null depth is degraded by a number of factors such as residual wavefront aberrations, beam shear, amplitude mismatch between beams, vibration, errors in telescope pointing, polarization mismatch in the paths for each beam, stray light, and smearing due to the wavelength dependence of the fringe pattern.

End-to-end interferometer system operation is a major technical concern being addressed by the interferometry testbeds. Testing and verification of a robust end-to-end nulling interferometer will be conducted with simulated and realistic flight-like error sources. The success of these laboratory demonstrations would largely preclude the need for technology flight demonstrations and would, in Phase A, allow the initiation of the flight design with a high degree of confidence in the underlying technology.

Technical concerns not retired by inheritance, or design team activities will be addressed by TPF-supported technology development. The planned interferometer testbeds and technology activities are described on the following pages.

# 4.2 Optical Component Technology

## Beam-splitter Development

### Key Technology Addressed

Beam splitter, antireflection coatings

### Objectives

This task pursues a number of novel approaches to the design and fabrication of beam-splitters that could lead to improved system performance and/or simplicity in a nulling interferometer. Related technologies, such as antireflection coatings, are also investigated.

### Approach

Using conventional symmetric beam-splitters in a nulling interferometer places extremely stringent requirements on fabrication tolerances. The Beam-splitter Development task will test a new concept using beam-splitters of relaxed individual tolerances in a configuration that delivers high-performance nulling by virtue of its symmetry (see Fig. 4-1). This "windmill" arrangement for beam combination relaxes the requirement that individual beam-splitters have precisely 50:50 intensity balance, for example, and requires only that the different optical elements mounted in the arms of the windmill device have closely matched properties, a condition that is much easier to fulfill in practice.

Another novel approach being investigated is the "perforated" beam-splitter, in which pupil masks patterned with opaque, reflecting sections are placed over each pupil of the two-element interferometer. Numerical simulations indicate results that should be sufficient to achieve the nulling requirements as shown in Fig. 4-2.

Two approaches that demand symmetry in the beam-splitter rather than the configuration will also be pursued. First, a "sandwich" beam-splitter will be made, consisting of two matched glass substrates in contact with a single layer of beam-splitter coatings. Second, a spatially distributed version of this, the "open-face" variant of the sandwich, will consist of two separated pieces of glass with sophisticated coatings on one and a simple coating on the other. These tasks will
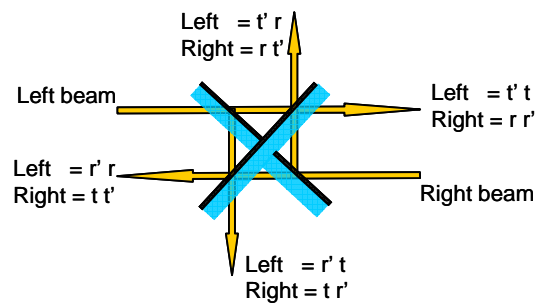


**Figure 4-1.** "Windmill" Beam Combiner
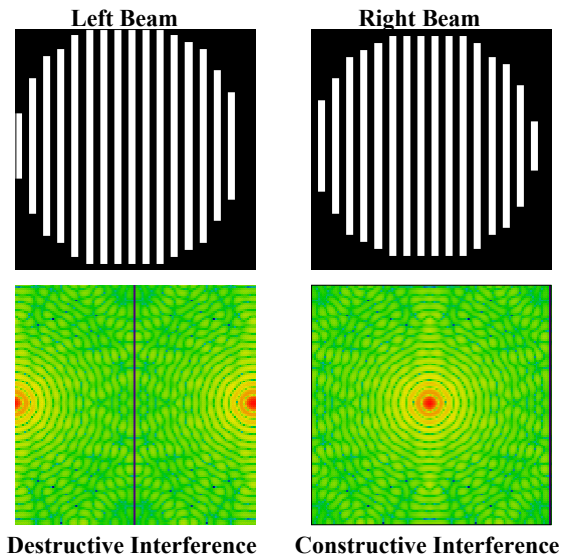


**Figure 4-2.** Pupils of a perforated beamsplitter (top) and the images that result (bottom, logarithmically stretched). In the destructive image, the light level at the position of the source is $6 \times 10^{-5}$.

significantly advance the state of the art in beam-splitter fabrication.

The traditional approach to antireflection coatings, required for the back side of interferometric beam-splitters, is with multilayer thin films. These can be difficult to produce in the extremely broad optical bandwidths required by TPF-I. An alternative to be tested in this task is to create a gradient index at the surface of the optic by selectively removing the material. This approach creates anti-reflection coated optics that are implicitly compatible with a cryogenic environment since no foreign materials need to be applied to the surface of the dielectric to create the anti-reflection effect.

The principal investigator of the beam-splitter development is Dr. Phil Hinz of the University of Arizona.

## Scope

- Design, fabricate, and test windmill nulling beam combiner
- Design, fabricate, and test open-face nulling beam-splitter
- Design sandwich nulling beam-splitter and evaluate its feasibility
- Define quantitative performance targets for the evaluation of each component

## State of the Art                                              TRL 2

Symmetric beam combiner configurations have been used previously in nulling testbeds by employing carefully matched beam-splitter elements. In particular, the Modified Mach-Zehnder design has been used successfully at JPL and elsewhere. However, no symmetric sandwich or "open-face" beam-splitters or windmill designs exists with the performance needed for deep nulling.

## Progress to Date

Revisions to the specifications of the beamsplitters are being completed. The first anti-reflection coating will be implemented by photolithography. Negotiations with the vendors are ongoing and the beamsplitters are on schedule to be fabricated in the fourth quarter of FY2005. The schedule for beam-splitter development is shown in Table 4-1.

**Table 4-1. Beam-splitter Development Schedule**

| Planned Completion Date (FY) | Planned Activities | Performance Targets | TRL |
|---|---|---|---|
| 2004/Q4 | Sandwich beam-splitter specs complete | | 2 |
| 2004/Q4 | Preliminary windmill specs complete | | |
| 2005/Q2 | Open-face beam-splitter specs complete | All specifications established | 2 |
| 2006/Q1 | Sandwich beam-splitter fab feasibility survey complete | | 2 |
| 2006/Q1 | Open-face beam-splitter fab run #1 complete | | 3 |
| 2006/Q2 | Windmill fab run complete | | 3 |
| 2006/Q4 | Windmill evaluation complete | Samples meet specifications | 4 |
| 2007/Q2 | Open-face beam-splitter evaluation complete | Samples meet specifications | 4 |

## Mid-Infrared Spatial Filter Technology

### Key Technology Addressed

Spatial and modal filter technology

### Objectives

Spatial filters are an essential technology for nulling interferometry, significantly reducing the optical aberrations in wavefronts, making extremely deep nulls possible.  The most basic form of a spatial filter, used in infrared nulling up until now, is a simple pinhole.   Even more beneficial is a modal filter, implemented by focusing light into single-mode optical waveguides and later re-collimating the light at the output.  The development of improved techniques for spatial filtering at mid-infrared wavelengths may be crucial to achieving null depths of $10^{-6}$, making planet detection by interferometry possible.   The developed spatial filters must have a single mode throughput of at least 50% and modal suppression of 10 dB  for non-fundamental modes, with a goal of 26 dB.  The wavelength range of 7 to 17 μm will be accommodated using no more than two spatial filters, each with their own separate wavelength coverage.



**Figure 4-3.**  Second Set of Three Long-Fiber Single-Mode Chalcogenide Fibers Delivered by the Naval Research Lab

### Approach

Spatial filters may be implemented in a variety of ways, including single-mode fiber-optics made from chalcogenide glasses, metallized waveguide structures micro-machined in silicon, or through the use of photonic crystal fibers.  By promoting the parallel development of various spatial filter technologies, it is hoped that the 7 to 17 μm spectrum can be accommodated using no more than two technology types.  Spatial filters are being developed under contract for this work: polycrystaline silver halide fibers are



**Figure 4-4.**  Hollow-Metal Waveguide Approach to Single-Mode Filter Design (left); Single-Mode Fiber Characterization Setup at JPL (right)

being developed by Prof. Abraham Katzir at Tel Aviv University (TAU) in Israel; hollow-metal waveguides are being developed by Prof. Christopher Walker at the University of Arizona (UA); and chalcogenide fibers are being developed by Dr. Jas Sanghera at the Naval Research Laboratory (NRL), shown in Fig. 4-3. The performance of their single-mode filter prototypes will be characterized at JPL's recently established in-house optical testing facility.

## Scope

- Technology survey and technology development for broadband mid-IR spatial filters
- Develop a testbed development for the evaluation of spatial filter performance
- Provide TPF-I nuller testbeds with developed spatial filters

## State of the Art                                                         TRL 4

Although fiber optics at near-infrared wavelengths are extensively used by the telecommunications industry, low-loss, mid-IR, single-mode spatial filters are not commercially available. A 4-mm long 10-micron fiber was produced previously for the Observatoire de Paris by Le Verre Fluoré and matched a Gaussian profile to within 2–3% rms. Fibers developed by this task have also shown good single-mode performance, as illustrated in Fig. 4-5.

## Progress to Date

A very small number of prototype spatial filters have been tested at JPL, showing single-mode behavior at 10 microns. The testing facility is shown on the right-hand side of Fig. 4-4. The most promising samples seem to be the chalcogenide fibers developed at the Naval Research Lab. These fibers show good single-mode performance. Two sets of 9-inch (23 cm) fibers have now been delivered. It is expected that the throughput of these fibers will improve by applying an antireflection coating on the fiber ends, and that the fibers will enable the Achromatic Nulling Testbed to achieve its objectives with a 25% bandwidth. The silver halide fibers received so far from Tel Aviv University have not yet yielded the required single-mode behavior. Hollow metal waveguides have not yet been manufactured by the University of Arizona. The schedule for mid-infrared filter technology development is shown in Table 4-2. All work to date has focused on creating spatial filters that function well at wavelengths shorter than 12 µm.
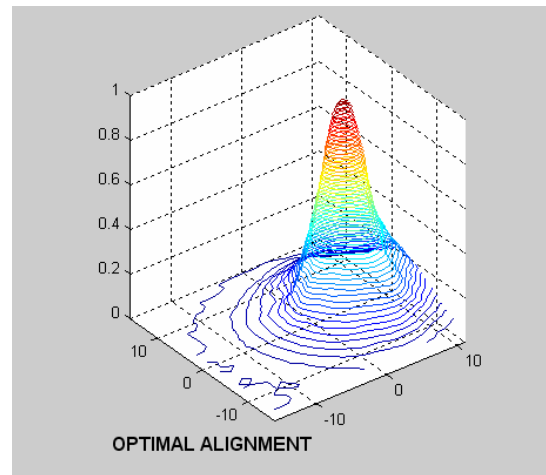


**Figure 4-5.** Test Results of a Beam Output Profile of a Chalcogenide Fiber Produced by the Naval Research Laboratory

**Table 4-2.  Mid-Infrared Spatial Filter Technology Schedule**

| Planned Completion Date (FY) | Planned Activities | Performance Targets | TRL |
|---|---|---|---|
| 2003 | Contractors selected for manufacture of spatial filters | | 2 |
| 2005/Q1 | Deliver phase 1 prototype to JPL (TAU) | Phase 1 prototype: achieves single mode operation with 25% or greater bandwidth | 4 |
| 2005/Q2 | Deliver 6 NRL prototype samples to JPL | | |
| 2005/Q3 | Deliver 10 NRL single-mode samples | | |
| 2006/Q4 | Deliver phase 2 prototype to JPL (NRL) | Phase 2 prototype: achieves single mode operation with 50% or greater throughput. | 4 |
| 2006/Q4 | Deliver phase 1 prototype to JPL (UA) | | |

## Bibliography

Jasbinder S. Sanghera, L. Bradon Shaw, Lynda E. Busse, Vinh Q. Nguyen, Brian J. Cole, Reza Mossadegh, Pablo C. Pureza, Robert E. Miklos, Frederic H. Kung, David B. Talley, Dominik Roselle, and Ishwar D. Aggarwal, "Infrared optical fibers and their application," in *Infrared Optical Fibers and Their Applications*, edited by Mohammed Saad and A. Harrington, Proceedings of SPIE Vol. 3849 (SPIE, Bellingham, WA 1999) 38–39.

Eran Rave, Pinhas Ephrat, Abraham Katzir, "AgClBr photonic crystal fibers for the middle infrared," in *Photonic Crystal Materials and Devices II*, edited by Ali Adibi, Axel Scherer, and Shawn-Yu Lin, Proceedings of SPIE Vol. 5360 (SPIE, Bellingham, WA 2004) 267–274.

Christian Y. Drouet d'Aubigny, Christopher K. Walker, and Dathon R. Golish, "Mid-infrared spatial filter fabrication using laser chemical etching," in *New Frontiers in Stellar Interferometry*, edited by Wesley A. Traub, Proceedings of SPIE Vol. 5491 (SPIE, Bellingham, WA 2004) 655–666.

P. Bordé, G. Perrin, A. Amy-Klein, G. Daussy, and G. Mazé, "Updated results on prototype chacogenide fibers for 10-μm wavefront spatial filtering," Proc. Towards Other Earths: Darwin/TPF and the Search for Extrasola Terrestrial Planets, Heidelberg, Germany, 22–25 April 2003 (ESA SP-539, October 2003), 371–374.

# Integrated Optics

## Key Technology Addressed

Nulling through waveguide techniques

## Objectives

The development of integrated optics for mid-infrared interferometry holds the promise of providing compact and rugged beam combiners that are amenable to inexpensive replication. In principle, with this technology the entire nulling combiner may be fabricated in a thin plate comparable in size to a microscope slide. This technology may potentially reduce the risk inherent in the complexity of the beam-combining subsystem of the interferometer. In contrast, conventional approaches to nulling interferometry involve numerous separate optics and free-space propagation of large (few-cm diameter) collimated beams of light.



**Figure 4-6.** Design of a Dual-Bracewell Nulling Interferometer, having Two Nullers and a Cross-Combiner, to be Fabricated by Precision Laser Micromachining

## Approach

The key technology to building integrated optics for mid-infrared wavelengths is the capability of fabricating waveguide structures whose dimensions are comparable to the 7–17 micron wavelength. The approach being used here is a combination of laser micromachining of silicon in a fluorine atmosphere and standard reactive-ion etching, followed by gold plating. The modeling of waveguide structures is highly advanced and indicates that performance will be high if the manufactured surface roughness is tolerable.



**Figure 4-7.** Scanning Electron Microscope Image of One Side of a Prototype Beam Combiner, Designed for a Wavelength of 60 μm

67

The principal investigator of the Integrated Optics technology is Prof. Christopher Walker at the Steward Observatory of the University of Arizona.

## Scope

- Develop broadband 10-µm beam combiners and nullers using integrated optics technology

## State of the Art                                                    TRL 2

Integrated optics are extensively used by the telecommunications industry and have been successfully adapted for use in ground-based interferometry at H and K band, with the first H-band stellar fringes obtained in 2001.  Up to K-band (2.4 microns) single-mode beam combination has been proven, with success also likely at L' band (3.5 microns).  However, at longer wavelengths coherent (single-mode) optical devices have not been well developed because there has been no obvious application for them in the telecommunications industry.  Even spatial filters, the most basic of integrated optics components, are at a low TRL level at these wavelengths.  Integrated optical devices do not yet exist to cover the 7–17 micron wavelength band of interest to TPF-I.  At present, nulling has only been demonstrated at these wavelengths using conventional discrete optics.

## Progress to Date

Analytic models of integrated optics devices, such as the example shown in Fig. 4-6, have been tested. Very preliminary prototype components have been etched for longer wavelength applications (see for example Fig. 4-7).  The development lab at the University of Arizona is undergoing a comprehensive upgrade in support of this work.  Work has been suspended until further progress is demonstrated with related spatial-filter designs.  The schedule for integrated optics development is shown in Table 4-3.

Table 4-3.  Integrated Optics Schedule

| Planned Completion Date (FY) | Planned Activities | Performance Targets | TRL |
|---|---|---|---|
| 2003/Q3 | Pretest analytical models | Wavelength 60 µm or shorter | 2 |
| 2007/Q2 | Deliver 10 µm beam combiner | Functionality confirmed using interferometer: no performance target | 4 |
| 2007/Q3 | Deliver 10 µm nuller | $10^{-2}$ null depth with 10% throughput | 4 |
|  | Deliver high-performance 10 µm nuller | $1 \times 10^{-5}$ null depth with 10% throughput and 20% bandwidth | 4 |
| 2007/Q4 | Deliver multi-element IO device |  | 4 |

## Bibliography

C.Y. Drouet d'Aubigny, C.K. Walker, D. Golish, M.R. Swain, P.J. Dumont, P.R. Lawson, "Laser micro-machining of waveguide devices for sub-mm and far-IR interferometry and detector arrays," in *Interferometry in Space*, edited by Michael Shao, Proceedings of SPIE Vol. 4852 (SPIE, Bellingham, WA 2003) 568–580.

# 4.3 Interferometer Subsystem Testbeds

## Cryogenic Delay Line

### Key Technology Addressed

End-to-end system testbeds, modeling, and simulation

### Objectives

Delay lines provide the pathlength compensation that makes the measurement of interference fringes possible. When used for nulling interferometry, the delay line must control pathlengths so that the null is stable and controlled throughout the measurement. This activity will develop a low noise, low disturbance, high bandwidth optical delay line capable of meeting the TPF interferometer optical path length control requirements at cryogenic temperatures. A prototype device will demonstrate performance features that give confidence in the ability to satisfy flight performance requirements.

### Approach

Cryogenic testing and characterization will be completed on an optical delay line prototype that was designed and fabricated by JPL under prior funding. The knowledge gained plus new TPF requirements from the interferometer architecture and design teams will be inputs to a redesign for a next generation cryogenic optical delay line. The new design will resolve tradeoffs as to the number of articulation stages, actuator/sensor selection and optical prescription. Magnetostrictive actuators may be used for fine stage control due to their being relatively insensitive to performance losses at cryogenic temperatures. Following redesign and fabrication, the new delay line will be tested and characterized at both room and cryogenic temperatures. Limited design improvements may be implemented based on discoveries from testing and as permitted within funding constraints.

The principal investigator of the cryogenic delay-line development is Robert Smythe at the Jet Propulsion Laboratory.

### Scope

- Develop technology for Interferometer optical path-difference control at cryogenic temperatures
- Implement and test prototype system at 77 K in lab
- Deliver prototype delay line, documentation of performance and design

### State of the Art                                                      TRL 3–4

Interferometer delay lines have been in use in ground-based interferometers since about 1982. Room temperature vacuum delay lines are now relatively common and operate with about 10-nm control of vibration and path fluctuations. However, delay lines of this sort have not been used for cryogenic operation, because observations at visible and near-infrared wavelengths have not required it. Ground-based 10-μm interferometers have not used cryogenic delay lines, because cooling the mirrors of the delay line offers little advantage in sensitivity, given that these interferometers already have typically
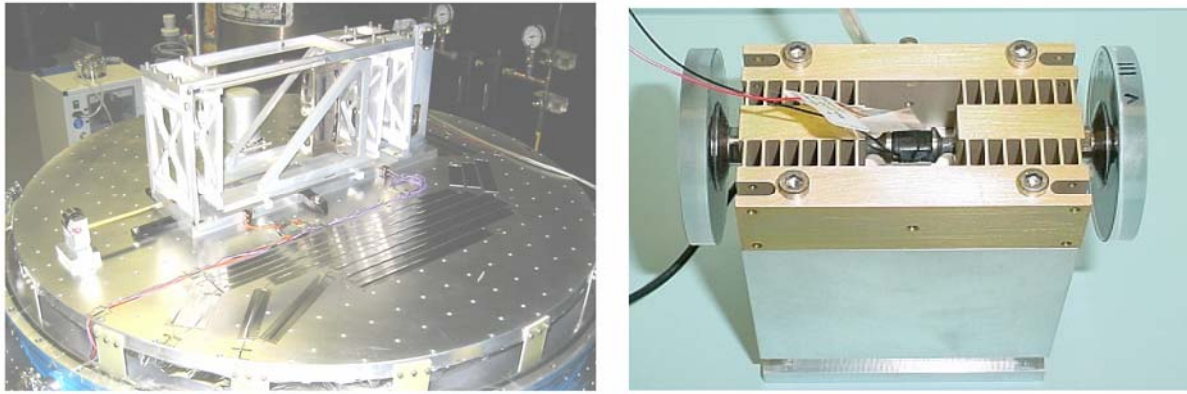
**Figure 4-8.** Prototype of Cryogenic Delay Line (left); Detail of High-Bandwidth Stage (right)

more than 20 warm reflections in each optical path to the detector. The state of the art in cryogenic delay line technology is represented by this task, having achieved a stability of 20 nm rms, operating at 77 K.

**Progress to Date**

In FY2003 the cryogenic delay line, shown in Fig. 4-8 (left), successfully demonstrated pathlength control to 20 nm rms at 77 K. Improved performance will require a redesign of delay line carriage, and this work has been deferred until FY2007. The schedule for the cryogenic delay line development is shown in Table 4-4.

**Table 4-4. Cryogenic Delay Line Schedule**

| Planned Completion Date (FY) | Planned Activities | Performance Targets | TRL |
|---|---|---|---|
| 2003/Q3 | Operate prototype closed-loop at 77 K | 20 nm rms OPD static, 1 cm/sec slew open loop | 3–4 |
| 2007/Q1 | Testing of next-generation design complete (room temperature) | 3–4 nm rms OPD | 5 |
| 2007/Q3 | Demonstrate high performance | 0.5 nm rms OPD | 5 |

**Bibliography**

R.F. Smythe, M.R. Swain, O. Alvarez-Salazar, J.D. Moore, "Terrestrial Planet Finder cryogenic delay line development," in *New Frontiers in Stellar Interferometry*, edited by Wesley A. Traub, Proceedings of SPIE Vol. 5491 (SPIE, Bellingham, WA 2004) 1802–1812.

# Common Path Phase Sensing Testbed

## Key Technology Addressed

Phasing (controlling and stabilizing) a nuller with near-infrared light

## Objectives

The Common-Path Phase Sensing Testbed is being developed to demonstrate a simple and direct "common-path" method of fringe-tracking using the 2 μm light from an artificial star to control the paths within a 10-μm nulling interferometer. The conventional approach, used for example in the Keck Interferometer, is to fringe track using a separate subsystem, thereby inducing possible systematic phase errors, and requiring possible additional system complexity. The planned fringe-tracking scheme should be both simpler and more stable than non-common-path alternatives. Its operation is shown in Figs. 4-9 and 4-10.

**Figure 4-9.** Phase shift as a function of wavelength (in microns) created by use of phase plates: a $\pi$ shift at mid-infrared wavelengths for nulling appears as a 1.5 $\pi$ shift (constructive interference) at near-IR wavelengths for pathlength control.

## Approach

The Common Path Phase Sensing Testbed will direct near-infrared fringe-tracking light along the same optical paths taken by the 10 μm science light. This approach minimizes systematic phase errors and spurious fringe-control commands. Phase plates are used to produce a broad-band half-wave phase shift in the 10 μm nulling wavelength band, and at the same time provide a three-quarter-wave phase shift in the near-infrared fringe-tracking wavelengths. To test the concept, a complete optical breadboard including 10-μm nulling and 2-μm phase sensing is being constructed that will also provide a valuable testbed for the novel beamsplitter designs being developed. Preparations are shown in Fig. 4-11.

The principal investigator of the Common Path Phase Sensing Testbed is Dr. Phil Hinz at the University of Arizona.

**Figure 4-10.** Schematic of the Common Path Phase Sensing Testbed: mid-infrared nulling is controlled by near-infrared fringe tracking, with all the light following the same path through the optics.

71

**Figure 4-11.** Common Path Phase Sensing Testbed at the University of Arizona

## Scope

- Develop a common-path fringe-tracking/nulling architecture
- Demonstrate accurate control of nulling performance with this scheme

## State of the Art                                                        TRL 2–3

Fringe tracking has been used with ground-based optical interferometers since 1979. Fringe tracking by phase-measurement interferometry is now a well-developed technique that is in use at both optical and infrared wavelengths. Space-qualified fringe-tracking systems are at an advanced stage of development for the SIM PlanetQuest mission. However, the proposed scheme is a new approach to fringe tracking, only recently formulated and never before tested, and for this reason is at a low TRL level.

## Progress to Date

Fringes at a wavelength of 2-µm have been acquired. Work is proceeding on schedule. The schedule for the testbed development is shown in Table 4-5. Regular progress reports are available courtesy of the University of Arizona at http://shiloh.as.arizona.edu/~tjm/Testbed_Status.html.

**Table 4-5. Common Path Phase Sensing Testbed Schedule**

| Planned Completion Date (FY) | Planned Activities | Performance Targets | TRL |
|---|---|---|---|
| 2005/Q3 | Testbed assembly complete | Low sensitivity configuration | 2–3 |
| 2005/Q4 | Open-loop characterization | 50 nm pathlength control | 3 |
| 2006/Q3 | Closed-loop control | 5 nm pathlength control | 4 |
| 2007/Q1 | Final report | | 4 |

OPTICS AND STARLIGHT SUPPRESSION TECHNOLOGY

# 4.4 Starlight Suppression Subsystem and System Testbeds

## Adaptive Nuller

### Key Technology Addressed

Full spectral, quasi-static control of intensity and phase of interfering beams for deep, broadband nulls.

### Objectives

The variations in amplitude and phase that may be present across a broad wavelength band make nulling extremely challenging. The Adaptive Nuller is designed to correct these variations, matching the intensity and phase between the two arms of the interferometer, as a function of wavelength, for each linear polarization. This will allow high performance nulling interferometry, while at the same time substantially relaxing the requirements on the nulling interferometer's optical components.

### Approach

A deformable mirror is used to adjust amplitude and phase independently in each of about 12 spectral channels. A schematic of the adaptive nuller is shown in Fig. 4-12, as it would be used to adjust the intensity and phase of one beam in a two-beam nuller. The incident beam is first split into its two linear
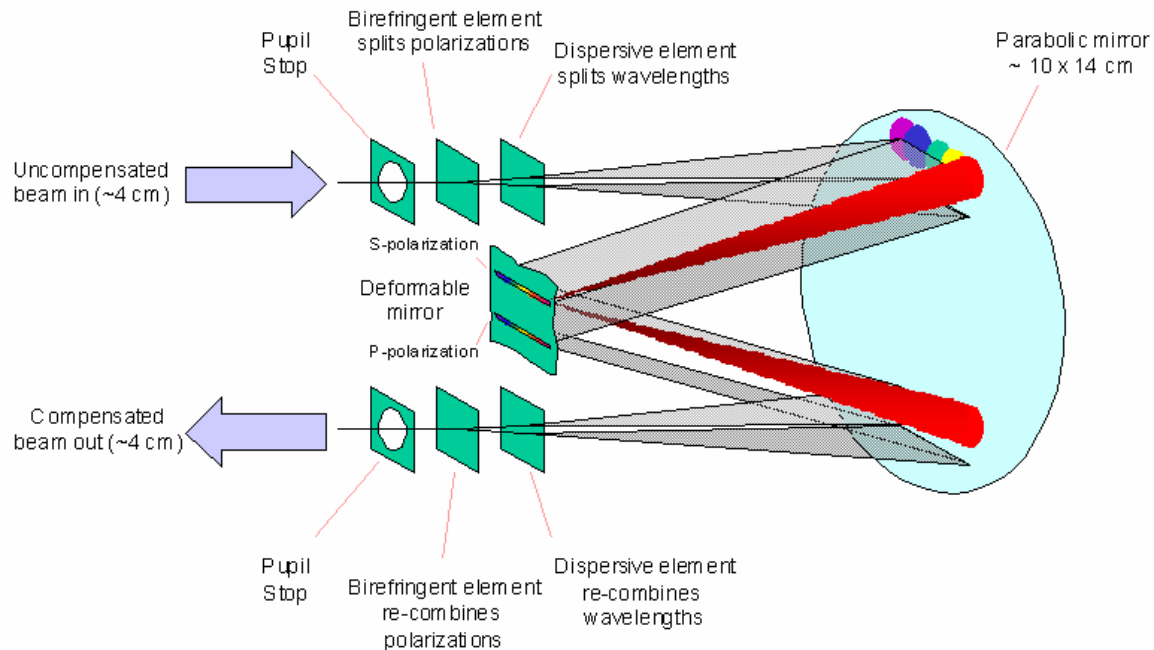


**Figure 4-12.** Schematic of the adaptive nuller. Light in one arm of a nulling interferometer is balanced by splitting it into component polarizations and wavelength channels, then individually adjusting the phases in each channel with a deformable mirror prior to recombining both polarizations. Further details of the design are described by Peters *et al*. (2004).
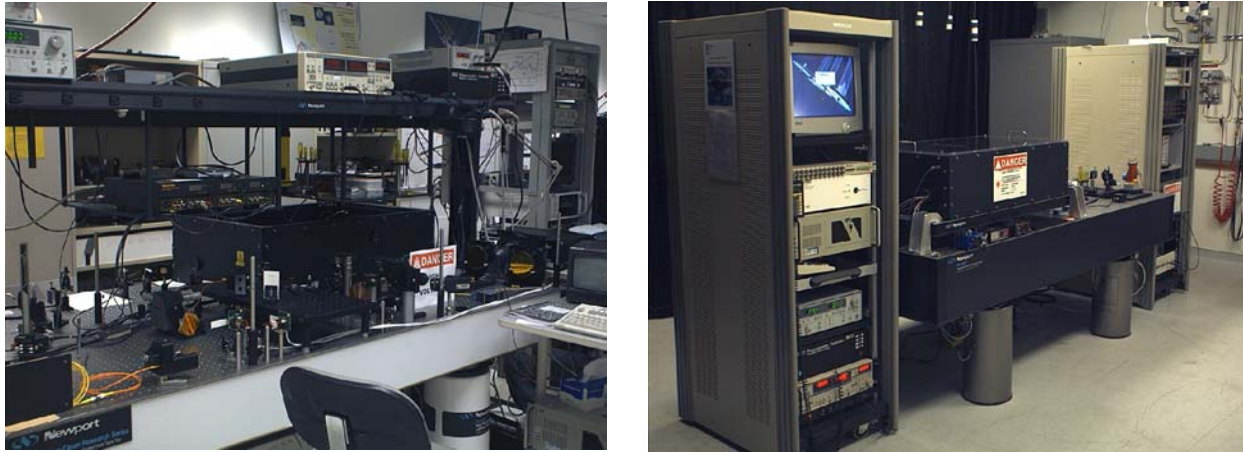
**Figure 4-13.** Optical Layout of a Prototype Adaptive Nuller for Visible/Near-Infrared Wavelengths (left) and Experimental Layout for a Mid-Infrared Adaptive Nuller (right)

polarization components, and also divided into roughly a dozen spectral channels. These beams are then directed onto a deformable mirror, where the piston of each pixel independently adjusts the phase of each channel. Tilt in the orthogonal direction may also be independently adjusted, and, by means of controlled vignetting at a subsequent aperture, provides an independent adjustment of the intensity in each channel. The various component beams are recombined to yield an output beam that has been carefully tuned for intensity and phase in each polarization as a function of wavelength. If the adaptive nuller is used to balance beams entering a nulling interferometer, matching tolerances on optical components in that interferometer are substantially relaxed. Ultimate null depth and stability are now determined by the performance of the adaptive nuller, under active control that can be monitored and readily characterized, and optical components need only be of sufficient quality that the two arms of the interferometer are matched in intensity and phase to within the capture range of the adaptive nuller.

The principal investigator of the Adaptive Nuller is Robert Peters at the Jet Propulsion Laboratory.

### Scope

- Control and match the intensity and phase of two optical beams feeding a nuller
- Achieve individual control of multiple spectral channels and both linear polarizations

### State of the Art                                                      TRL 2

A visible/near-infrared proof-of-concept experiment was completed as the first stage of this development effort, and exceeded its performance target, achieving intensity control to 2% and phase control to 2 nm. This represents the state of the art, as there had been no previous capability demonstrated in this area.

### Progress to Date

The Adaptive Nuller test facilities are shown if Fig. 4-13. The adaptive nuller was first implemented in a testbed for operation at visible and near-infrared wavelengths, with results noted above and illustrated in Fig. 4-14. That testbed has now been dismantled in preparation for the commissioning of a mid-infrared adaptive nuller, to operate over the wavelength range of 8–12 μm. Key components for the mid-infrared testbed have now been received, including a CdCs Wollaston prism, and good progress is being made
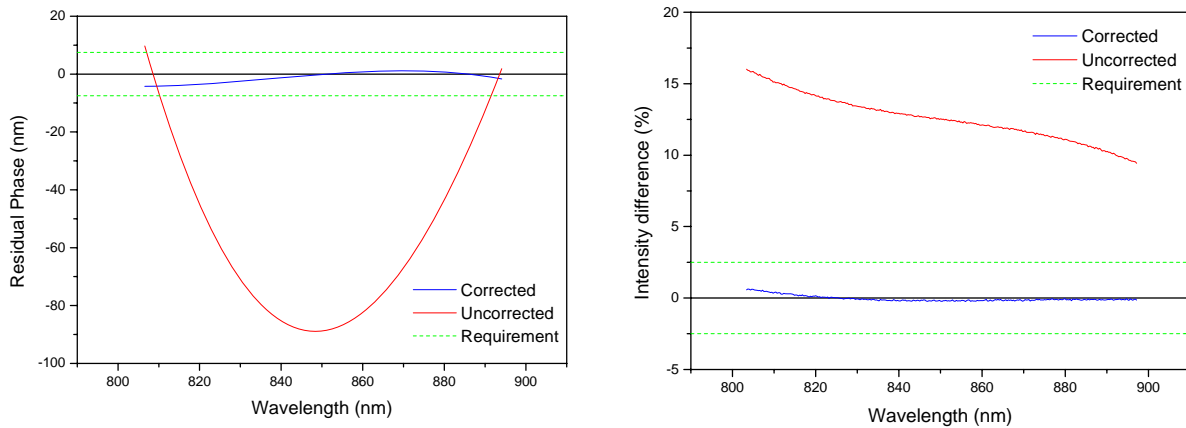
**Figure 4-14.** Correction of phase (left) and intensity (right) demonstrated by the prototype visible/near-infrared adaptive nuller. The achieved correction exceeds the nulling requirements at these wavelengths and suggests excellent nulling control will be possible with a mid-IR adaptive nuller.

with the testbed implementation. The mid-infrared testbed will initially use a deformable mirror that is not designed for cryogenic operation. Options for upgrading the testbed for cryogenic work are being investigated. The schedule for the Adaptive Nuller development is shown in Table 4-6.

## Bibliography

R.D. Peters, A. Hirai, M. Jeganathan, O.P. Lay, "Near-IR demonstration of adaptive nuller based on deformable mirror," in *New Frontiers in Stellar Interferometry*, edited by Wesley A. Traub, Proceedings of SPIE Vol. 5491 (SPIE, Bellingham, WA 2004) 1630–1638.

**Table 4-6. Adaptive Nuller Schedule**

| Planned Completion Date (FY) | Planned Activities | Performance Targets | TRL |
|---|---|---|---|
| **2005/Q1** | Visible/near-infrared adaptive nuller validation | Control intensity to 5%, phase to 15 nm across a bandwidth greater than 100 nm | 2 |
| **2006/Q2 Milestone** | Mid-IR adaptive nuller validation | Control intensity to 0.2%, phase to 5 nm (equivalent to $10^{-5}$ null depth), over a wavelength range of 8–12 μm | 4 |
| **2009/Q3 Gate** | Cryogenic mid-IR adaptive nuller validation | Control intensity to 0.2%, phase to 5 nm (equivalent to $10^{-5}$ null depth) at a temperature of 40 K, over a wavelength range of 8–12 μm | 5 |

# Achromatic Nulling Testbed

## Key Technology Addressed

Broadband Nulling interferometry at mid-infrared wavelengths

## Objectives

The Achromatic Nulling Testbed (ANT) is being developed to address the optical issues related to achieving deep, broadband, dual-polarization, two-beam mid-infrared nulls. The two-beam nuller is the basic building block of all flight architectures that have been considered so far. Several approaches to field inversion and nulling are being investigated at the same time, with the aim of demonstrating, through one of the approaches, two-beam nulling to a level of $10^{-6}$ with a 25% bandwidth. A major goal of this task is the development of a cryogenic nulling interferometer that will meet the above goals while operating at 40 K.
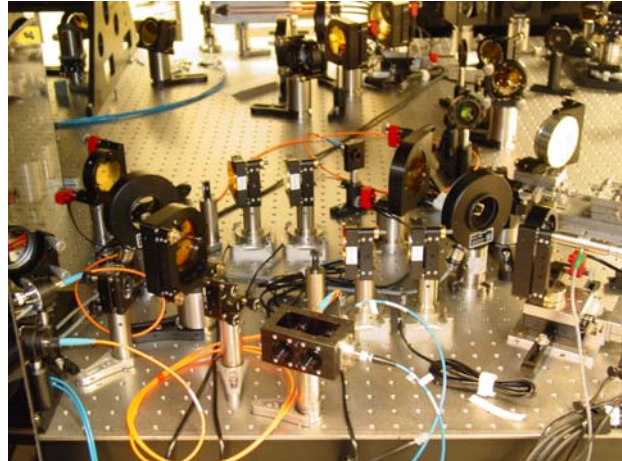


**Figure 4-15.** View of the TPF Mid-Infrared Mach-Zehnder Breadboard Nuller that Achieved $10^{-4}$ Nulls with a 25% Bandwidth

## Approach

The Achromatic Nulling Testbed has as its goal to demonstrate the performance required of the two-beam nulling that would be used in a system of parallel mid-infrared chopping interferometers. The proposed approach is to (1) develop two-beam nulling interferometers that will meet the requirements while
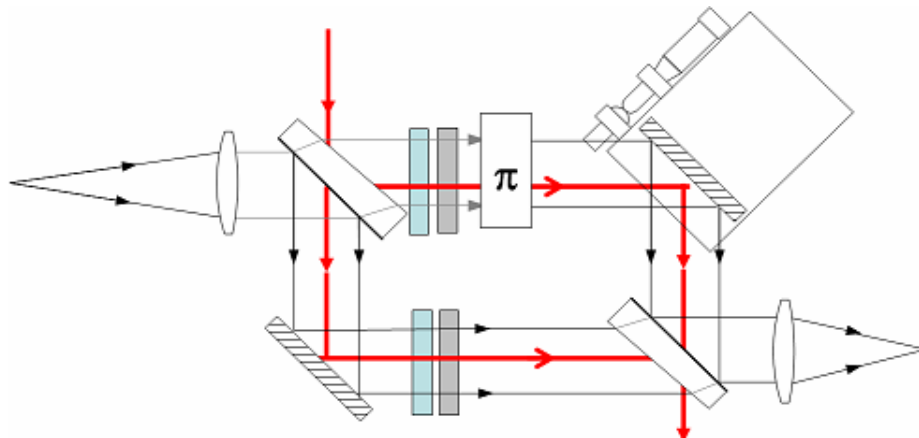


**Figure 4-16.** Schematic of a nulling interferometer: the achromatic $\pi$ phase shift in one arm converts the white-light fringe at zero optical path difference to a broad-null response. Three approaches to implementing the phase shift are being developed in parallel: (1) through-focus field inversion; (2) field counter-rotation with periscope mirrors; and (3) phase-shifts with pairs of dispersive glasses. In the above figure, the red lines show the paths of laser metrology, and the shaded boxes (blue and grey) indicate where dispersion and intensity control is included in each arm of the interferometer.

operating at room temperature, (2) test components and mounts in a simplified interferometer at 77 K, and (3) perform cryogenic testing of a nulling interferometer at 40 K.  Cryogenic testing at 40 K will be undertaken in the SIRTF test facility at JPL, previously used to test the Spitzer Space Telescope. The goal is to develop technology that will allow the TPF spectral band to be covered by only two nullers. The nulling performance at 25 % bandwidth in the 7–11 µm range will be characterized at 40 K and a model will be validated to predict the performance of a longer-wavelength (11–17 µm) nuller.

As part of this work, three different methods of implementing achromatic phase delays are first being investigated in parallel:  (1) using a through-focus field-flip of the light in one arm of the interferometer; (2) using successive and opposing field-reversals on reflection off flat optics through a periscope-like set of mirrors; and (3) using pairs of dispersive glass plates to apply a wavelength-dependent delay. Achromatic $\pi$ phase shifts are the most straightforward to accomplish and do not require pairs of glass plates.  However, in the through-focus approach a pupil-dependent polarization effect occurs, because of the changing angle of incidence on the focusing mirrors, as a function of position in the pupil.  The periscope mirrors would be ideal and truly achromatic, were it not for the difficulty of aligning the several mirrors in three dimensions.  For the more general case, requiring other phase shifts, sets of dispersive glasses are needed.  Although this latter approach is not achromatic, it may nonetheless be optimized to produce suitable broadband phase shifts to meet the null-depth requirements.  Figure 4-15 shows a view of the nuller that uses pairs of dispersive glasses to produce the phase shift.  The optical layout is shown in Fig. 4-16, and results are shown in Fig. 4-17.

Ancillary optical components and detectors are being developed and included in the testbed to meet the objectives. A new high-flux continuum light source, based on argon arcs lamps, has been implemented to improve the dynamic range of the measurements.  The low-light level limit of measurements will be improved through the development of a 10-µm camera with high dynamic range.  Components for the balancing of intensities and phases will be tested.  Spatial filters will be incorporated in the testbed as they become available.
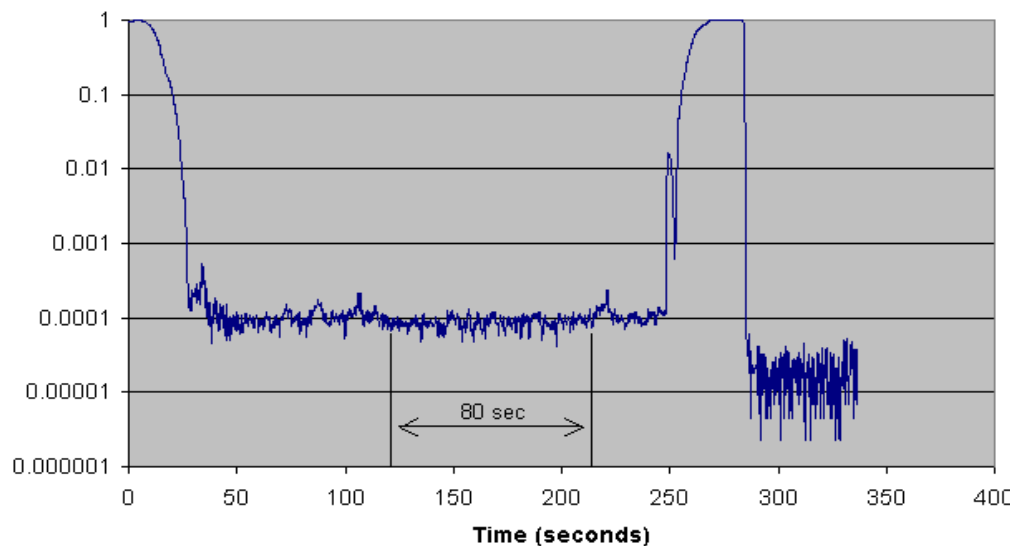


**Figure 4-17.**  Experimental data of a 10,000:1 null over a 30% bandpass centered at 9.8 microns. These results were obtained using a phase-shift with pairs of dispersive glasses.  The extra data at the end of the plot show the noise floor of the measurement.
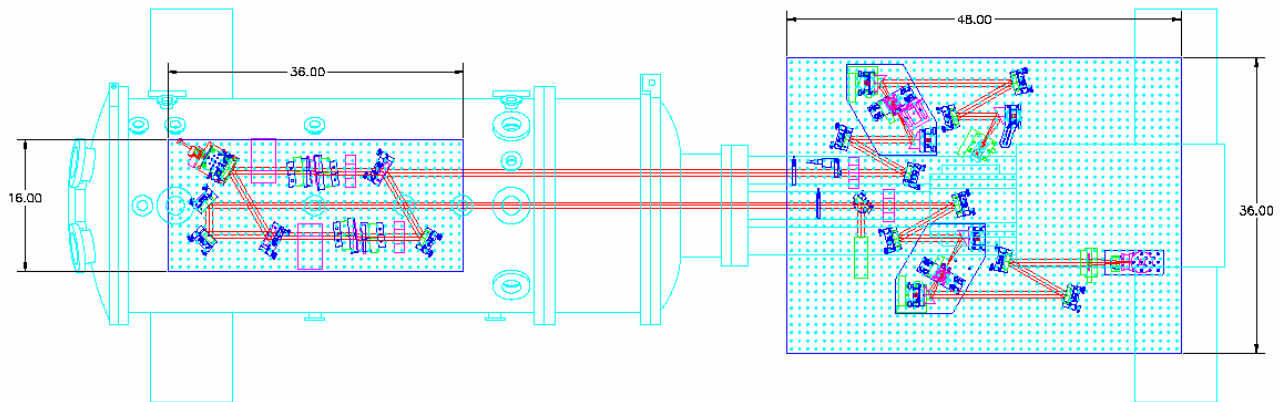
**Figure 4-18.** Top view of a schematic of the cryogenic testing facility being used to test components and a simplified interferometer at 77K. An optical table at room temperature provides the light source and detector on the right. The interferometer is within a cryogenic vacuum chamber on the left.

The Achromatic Nulling Testbed uses laser metrology and automated alignment algorithms to scan across the zero path-difference position and locate the interference null. The ANT does not use pathlength modulation for interferometric chopping, nor does it address issues related to system complexity. The algorithms that are used serve to reduce the time required for each measurement. Interferometric four-beam chopping is addressed by the Planet Detection Testbed

The principal investigator of the Achromatic Nulling Testbed is Dr. James K. Wallace at the Jet Propulsion Laboratory.

## Scope

- Infrared broadband nulling
- Off-axis faint source detection
- Performance at cryogenic temperatures

## State of the Art                                                    TRL 4

The state of the art in mid-infrared nulling is represented by the results obtained to date with the Achromatic Nulling Testbed. Pairs of glass plates have been used to provide null depths of $10^{-4}$ with a 30% bandwidth, and also a depth of $10^{-6}$ with a 10.6 μm laser. The broadband results are shown in Fig. 4-17.

## Progress to Date

Nulling has been demonstrated with the ANT using several approaches to provide the phase shifts. The most successful so far has been with the use of glass pairs, noted above. The through-focus approach has yielded nulls of 2000:1 with a 17% bandwidth. This result made use of several chalcogenide spatial filters, developed specifically for TPF. Preliminary work with the periscope mirrors is also progressing well, but with more modest null depths. A new arc source has been added to the main testbed, and should provide an increase in the dynamic range of measurements of a factor of 7. Cryogenic testing of the simplified interferometer is also proceeding well. The layout of the 77 K facility, now in use, is shown in Fig. 4-18. The schedule for the ANT development is given in Table 4-7.

**Table 4-7.  Achromatic Nuller Testbed Schedule**

| Planned Completion Date (FY) | Planned Activities | Performance Targets | TRL |
|---|---|---|---|
| **2004/Q1**<br>**Milestone** | Validation of Modified Mach-Zehnder nuller concept, narrowband | Demonstrated $10^{-6}$ null on 10-μm laser | 3 |
| **2004/Q1** | Validation of Mach-Zehnder nuller concept, broadband | Demonstrated $10^{-4}$ null with 25% bandwidth in the thermal infrared (warm) | 4 |
| **2005/Q4** | Validate cryogenic operation | Demonstrate $10^{-4}$ null with 25% bandwidth in the thermal infrared (cold) | 4 |
| **2006/Q1** | Achieve high broadband nuller performance | Demonstrate $10^{-5}$ null with 25% bandwidth in the thermal infrared | 4 |
| **2006/Q2**<br>**Milestone** | Achieve ultimate broadband nuller performance | Demonstrate $10^{-6}$ null with 25% bandwidth in the thermal infrared | 4 |
| **2007/Q1**<br>**Gate** | Detect an artificial planet with ultimate nuller performance | Null the star to $10^{-6}$ with 25% bandwidth in the thermal infrared (cold), and demonstrate detection of an artificial off-axis planet of representative flux | 5 |

## Bibliography

 J. K. Wallace, V. Babiwale, R. Bartos, K. Brown, R. Gappinger, F. Loya, D. MacDonald, S. Martin, J. Negron, T. Truong, G. Vasisht, "Mid-IR interferometric nulling for TPF," in *New Frontiers in Stellar Interferometry*, edited by Wesley A. Traub, Proceedings of SPIE Vol. 5491 (SPIE, Bellingham, WA 2004) 862–873.

## Planet Detection Testbed

### Key Technology Addressed

Cross-combination of two nullers (four apertures); planet detection by phase chopping; nulling stability

### Objectives

The Planet Detection Testbed is being developed as a nulling system testbed to demonstrate system performance requirements similar to those of proposed TPF-I flight beam-combiners. Using 10 micron laser light to provide an artificial source, the PDT has as its goal to demonstrate active control of two nulling beam combiners (four input beams in total), yielding a null depth of $10^{-6}$ that is stable to 0.1%, the detection of a planet signal that is $10^{-6}$ the brightness of the starlight, and interferometric chopping to 0.1%. The chopping and modulation of two cross-combined nulling interferometers will demonstrate mid-infrared background subtraction of simulated exozodiacal background emission.

### Approach

The Planet Detection Testbed combines four mid-infrared beams representing inputs from the four telescopes of the interferometer. In the testbed, these beams contain bright starlight and faint planet light that will then be separated by a pair of nullers and a phase-chopping cross combiner in a process that reproduces the operation of the flight beamcombiner. An important element of the testbed plan is to demonstrate control of the nullers and the cross-combiner at levels close to those needed for flight, and to show realistic faint planet detection within a period of about two hours in the presence of ambient laboratory noise



**Figure 4-19.** Beam Combiner Layout of the Planet Detection Testbed

and optical disturbances. The Planet Detection Testbed will therefore include servo loops and control systems necessary for deep and stable nulling. The testbed will address and mitigate risks associated with the need to null stably over many hours and to suppress background noise from local and exo-zodiacal light.

The simulated star and planet source combines mid-infrared laser light for nulling with broadband near-infrared thermal light for tracking the stellar fringe. A combination of near-infrared laser metrology and fringe tracking using the artificial starlight will provide the required pathlength knowledge. An additional alignment system will emulate the light of the angular and shear metrology beams. To achieve testbed goals, the phasing of the four starlight beams will be maintained at a level of 2 nm rms and the angular alignment will be maintained at 1 arcsecond rms.

**Figure 4-20.** Overview of the Optical Paths and Components in the Planet Detection Testbed

System alignment, control, and calibration techniques needed for flight are being developed and tested as necessary parts of the testbed plan. Known disturbances of the optical path will be added to aid the development of the Observatory Simulation model and to verify the ability of the control system to deliver the nulling performance predicted by the nulling stability model. By controlling the planet phase, the testbed will simulate a complete rotation of the telescope formation around the line of sight to the star over a 5000 s period and will demonstrate reconstruction of the planet signal from the data.

The Planet Detection Testbed is following a staged development plan in which the ultimate testbed is preceded by two preliminary experiments ("Fast-Start" Testbed and "4-Beam" Testbed) of progressively increasing functionality and complexity. The optical table is shown in the photograph of Fig. 4-19, and a block diagram showing the major components of the testbed is given in Fig. 4-20.

The Planet Detection Testbed uses 10-µm laser light, and does not attempt to address the goal of broadband nulling, addressed in the Achromatic Nulling Testbed. Moreover, the PDT is not a cryogenic testbed; the technology demonstrations are carried out entirely at room temperature.

The principal investigator of the Planet Detection Testbed is Dr. Stefan Martin at the Jet Propulsion Laboratory.

## Scope

- Complete full system test of a mid-infrared chopping interferometer: two nullers with cross-combiner
- Demonstrate planet detection through phase chopping to remove background light level
- Demonstrate planet detection in the presence of representative instrument noise levels
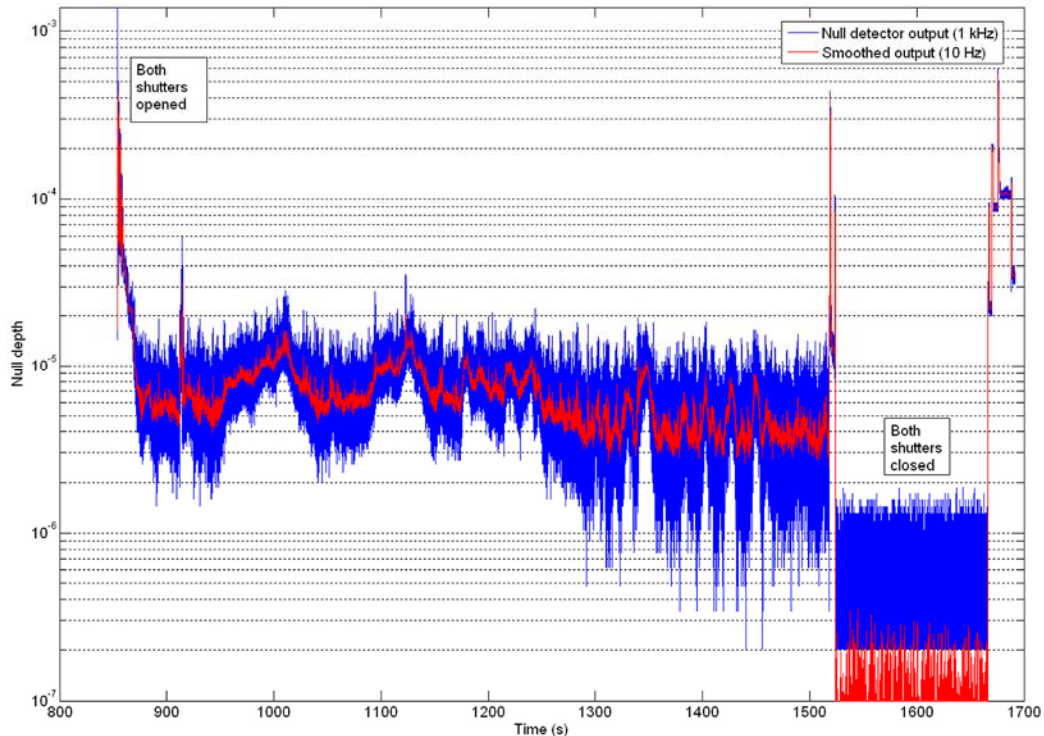
**Figure 4-21.** Four-beam nulling with the Planet Detection Testbed was achieved at a level of $10^{-5}$ in May 2005. The results are shown by the red trace in the above graph spanning the time from approximately 850 through 1520 seconds. The background level is shown for reference on the right, where the input beams are blocked (the time spanning from 1520 to 1670 seconds).

**State of the Art**                                                                                            **TRL 3**

As shown in Fig. 4-21, the PDT has demonstrated 4-beam nulling using a 10 µm laser with a null depth greater than $10^{-5}$. This is one milestone towards achieving its long-term objectives of demonstrating null stability and control. In comparison, the only other existing mid-infrared 4-beam nuller is the Keck Interferometer nuller, which achieved a null depth of greater than $10^{-3}$ using a 2-µm bandwidth during laboratory tests in 2004.

**Progress to Date**

Other progress, over and above the null depth described earlier, has included the development of a twelve-gauge laser metrology system. Initial detections of an amplitude-modulated planet signal have also been demonstrated. The 4-beam nulling results were obtained without the active tip/tilt and beam-shear control systems, which are in development on the Fast Start Testbed. These will be added in the near future. The schedule for the development of the PDT is shown in Table 4-8.

**Bibliography**

Stefan Martin, "TPF Planet Detection Testbed: a four beam infrared testbed demonstrating deep, stable nulling and planet detection," *2005 IEEE Aerospace Conference,* Big Sky, Montana (2005).

**Table 4-8 Planet Detection Testbed Schedule**

| Planned Completion Date (FY) | Planned Activities | Performance Targets | TRL |
|---|---|---|---|
| **2003/Q4** | Completed build of development breadboard | | 2–3 |
| **2004/Q1** | Defined architectures and implementations. | | 2–3 |
| **2005/Q3** | Demonstrate 4-beam nulling | Null depth of $10^{-5}$ | 3 |
| **2005/Q4**<br>**Milestone** | Demonstrate planet detection | Null depth of $10^{-5}$ | 3 |
| **2006/Q3** | Demonstrate amplitude stability of 4-beam nuller | Stable to 0.1% | 4 |
| **2006/Q4** | Demonstrate 4-beam nulling and phase chopping | Null depth of $10^{-6}$; control of chopping to 0.1% | 4 |
| **2007/Q1**<br>**Milestone** | Demonstrate planet detection at high level of nulling performance | Null depth of $10^{-6}$; strong planet signal ($10^{-4}$ of star) with fringes stationary with respect to planet. | 4 |
| **2007/Q3**<br>**Gate** | Demonstrate planet extraction at high level of nulling performance | Null depth of $10^{-6}$; with fringes rotating through the position of the planet. | 5 |

# 5   Formation Flying Technology

The principal objective of formation flying is to control the relative locations of separated spacecraft so that the beams of starlight that are sampled by each telescope travel the same distance to the beam combiner.  At the combiner, each optical beam will have its own delay line, with tens of centimeters of adjustable delay, and thus the separated spacecraft need only be controlled in their relative positions at the level of several centimeters.  Fringes can then be found on each baseline using a multi-stage pathlength servo with piezo-electric transducers, or equivalent, to provide nanometer-level control.

The formation-flying array will be launched into an orbit far from the Earth, and on-board autonomy will be essential.  Multiple spacecraft in a formation necessitates a distributed architecture for relative sensing, communications, and control; each spacecraft in the formation must sense the relative location of its neighbors and relay this information to each of the other spacecrafts.  A hierarchical and distributed precision formation control algorithm is needed to guide the maneuvers.  The maneuvers must also be orchestrated to conserve and balance the consumption of propellant amongst the elements of the array.  The overall formation system architecture needs to support a high degree of system robustness.  Specialized abilities, such as "lost in space" formation acquisition and collision avoidance, must be designed into the control algorithms to make the system fault-tolerant and to avoid a catastrophic mission failure.

## 5.1 Heritage and State of the Art

### Heritage from StarLight

TPF will benefit tremendously from the investment NASA has made in formation flying technology as part of the StarLight project.  An artist's impression of the mission is shown in Fig. 5-1.  Although the development of StarLight ceased in 2002, this work demonstrated significant progress in component, assembly, sub-system and system level technology demonstration for a precision formation flying interferometer in space.  The top-level performance requirements for the StarLight mission met or approached anticipated TPF requirements in a number of key areas.  At the completion of the StarLight project, four significant technology milestones were
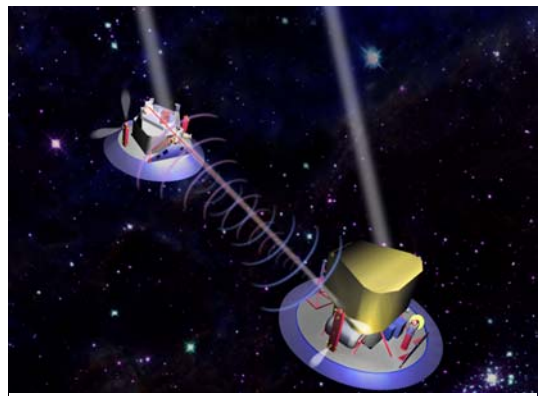


**Figure 5-1.**   Artist's Impression of the StarLight Mission

achieved that form the basis upon which the TPF Formation Flying (FF) Interferometer technology plans have been developed.

## Autonomous Formation Flying (AFF) Sensor

A Ka-band prototype of the AFF Sensor was developed and is fully functional. End-to-end system functionality has been verified through laboratory testing and operation on the 385 m JPL Outdoor Test Range (top of Fig. 5-2 at right). Performance of fundamental algorithms has been verified in a distributed spacecraft environment. Performance dependence upon the spacecraft architecture is understood. Results show that the AFF Sensor can meet the StarLight performance requirements in estimation of the range (2 cm) and bearing angles (1 arcmin), while providing a moderately wide field-of-view (±70°).

## Formation Flying Control Simulation

A high fidelity closed loop formation controls simulation testbed was developed for the Starlight two-spacecraft architecture (second image in Fig. 5-2 at right). Control algorithms were developed and demonstrated for formation acquisition, collision avoidance formation man-euvering, formation control, and observation on-the-fly. Simulation results show that the formation control performance could meet the StarLight requirements of 10 cm and 1 mrad.

## Precision Metrology Sensors

A prototype long range (600 m) dual-target laser metrology system was developed for the StarLight mission based on a ruggedized 1.32 μm space-qualifiable laser (third image in Fig. 5-2 at right). Laboratory results show that the system could meet the StarLight mission requirements. Sensitivity to 1 μm offset with precision of 11 pm over a 600 m range has been demonstrated in the laboratory.

## Formation Interferometer Testbed (FIT)

One of the challenges for a formation flying interfero-meter is to acquire and stabilize an optical system distributed over unconnected moving platforms. The StarLight mission technology development team accomplished this for the first time anywhere. The Formation Interferometer Testbed (bottom image in
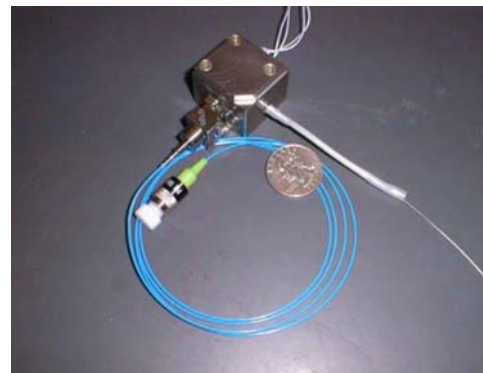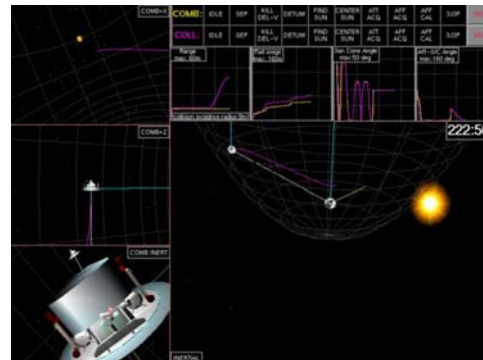








**Figure 5-2.** Technology Heritage from the StarLight Mission: AFF Sensor (top); FF Control Simulation; Precision Metrology Sensors; and Formation Interferometer Testbed (bottom)

Fig. 5-2 at right) demonstrated fringe acquisition at > 40 µm/s relative collector/combiner motion in the interferometer plane (both radial and transverse directions) and fringe lock for at least 10 seconds at relative rates of up to 30 µm/s, velocities typical of interspacecraft motion in the formation.

## Heritage from the JPL Distributed Spacecraft Technology Program

Formation flying technology is also being developed at the Jet Propulsion Laboratory for applications other than TPF-I. This work has been funded separately and organized within JPL's Distributed Spacecraft Technology Program, as described at their website http://dst.jpl.nasa.gov/. Nonetheless, specific technology being developed there, although not included in this plan, will provide useful heritage to TPF-I. The two most relevant technology efforts being conducted there are the MSTAR metrology system and the Xenon Ion thruster technology.

### MSTAR

The Modulation Sideband Technology for Absolute Metrology (MSTAR) is a concept for providing absolute range measurements to better than a millimeter. Its ties to TPF are illustrated in Fig. 5-3. MSTAR is a "bridging" sensor that closes the gap between fine interferometers and coarse pulsed RF or laser rangers. The concept uses phase modulation of a single laser. It is a handoff approach between the interferometric gauge and the long range RF sensor. The packaging promises integration of optical and RF-drive components into a small robust unit. Micron-level performance over a meter has already been demonstrated in a laboratory environment. So far, MSTAR development has been funded by other NASA technology programs. This approach might continue since MSTAR is proposed as a technology for the Space Technology 9 mission.
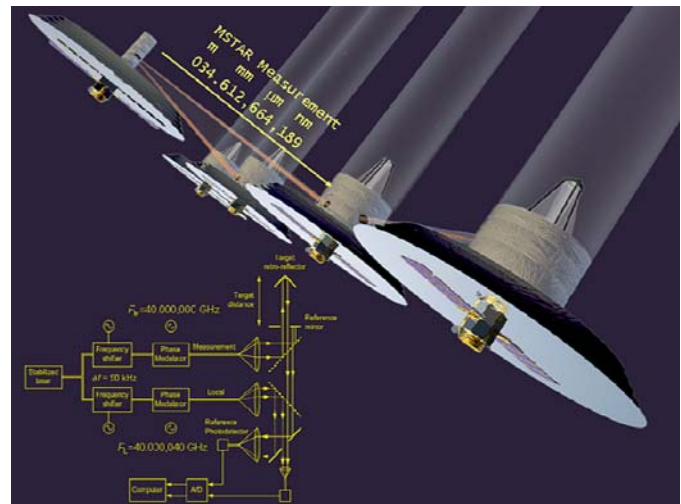


**Figure 5-3.** Schematic Overview of MSTAR Absolute Metrology Sensor

The MSTAR sensor approach implements a two-color metrology system using phase modulation of a single laser. Integrated-optics modulators operating at 40 gHz produce multiple sidebands on the output of a neodymium-doped yttrium aluminum garnet (Nd:YAG) laser operating at 1.32 µm. A simple demodulation scheme eliminates the need for high-speed photodetectors and signal processing, and the long coherence length of the narrow-linewidth laser enables operation over long distances.

87

**Miniature Xenon Ion (MiXI) Thrusters**

A number of propulsion technologies were considered for the needs of StarLight and TPF, and Ion thruster technology was considered promising given its scalability, low contamination risk and high efficiency. Ion propulsion technology, with continuous low level thrusting for the key science *uv*-plane mapping maneuvers, provides a lower risk approach to meeting the formation flying requirements, mitigating the concerns of impulsive on-off (impulse-bit) thrusting which might induce significantly higher path-length/bearing jitter/disturbances.

Opportunities were sought to fund ion propulsion technology development with specific focus to the needs of TPF-I. The NASA Code-R sponsored Distributed Spacecraft Technology (DST) research area sponsored this work for the past two years, resulting in development of Miniature Xenon Ion (MiXI) thruster. The MiXI thruster is scaled for ~3mN range, even though the basic



**Figure 5-4.** JPL Miniature Xenon Ion thruster (MiXI)

technology is scalable to much higher thrust levels. For example, the NEXIS thruster is scaled for ~450mN range. Figure 5-4 shows a photograph of a MiXI thruster, with a coin alongside to illustrate the actual scale.

One additional requirement for the MiXI thruster was the ability to mount it on a two axis gimble to enable thrust vectoring. This provides close alignment of the thrust vector with the desired motion axis regardless of the spacecraft orientation, thus providing for most efficient use of propellant without the cosine losses. Given its small size, gimbaled mounting the MiXI class thruster is considered quite feasible by the MiXI team.

In general, ion propulsion technology is considered an attractive choice for the precision-driven TPF-I mission, and there exists a viable technology development path for the TPF-I flight or other similar space science missions.

## State of the Art in Formation Flying

Although there has been, and continues to be, considerable interest in Europe and the United States in the development of formation flying technology, the technology readiness level still appears to be relatively low in areas of specific interest to TPF-I. It is somewhat difficult to judge the current state of the art in precision formation flying technology, because any coordinated hardware or software development effort outside of JPL has either been funded through national defense organizations or been undertaken at very low technology readiness levels through university research.

In France, the Office National d'Etudes et de Recherches Aerospatiales (ONERA) and the Centre National d'Etudes Spatiales (CNES) have established a common program for the development of spacecraft autonomy and formation flying technology with the use of micro-satellites. One goal has been to enable coordinated multi-satellite systems for Earth observation from low Earth orbit. These would be

radar or short-wavelength radio observations with three or more satellites, such as the Radars Orbitaux Multisatellites à Usage de Surveillance (ROMULUS) being developed at ONERA.  A second goal is to develop technology for astronomical applications.  With this in mind the CNES has funded proposals to study possible future formation-flying missions.  Most interestingly the French Ministry of Defense's procurement agency, the Délégation Générale pour l'Armement (DGA), was responsible for the ESSAIM micro-satellite system, developed by EADS Astrium, which was launched in December 2004 and has been operational since May 2005.  ESSAIM comprises four formation flying micro-satellites (120 kg Myriade satellites developed by the CNES) with receivers used to monitor ground communications.  However, there is very little information that is available concerning ESSAIM.  It is likely that the inter-spacecraft distances are much larger (many hundreds of meters or several kilometers) and that the control requirements are much looser than those needed for TPF-I.

In the United States there has also been considerable interest in the development of formation flying technology outside of JPL.  The Air Force Research Laboratory (AFRL) has had an ongoing interest in developing flight experiments to demonstrate a formation, but their TechSat-21 program (three 150-kg micro-satellites in a 550-km orbit with autonomous formation maintenance) was cancelled in early 2003.  The technology for autonomous rendezvous and docking is of interest but much less well aligned with the needs of TPF-I.  There are several efforts ongoing, including the NASA DART mission, and the Air Force's Orbital Express program.  Researchers at the Massachusetts Institute of Technology have also been developing algorithms for formation flying through their Synchronized Position Hold Engage and Reorient Experimental Satellites (SPHERES) laboratory project, previously funded through TPF.  SPHERES is intended to be tested in the zero-g environment inside the International Space Station or shuttle.  The Laser Interferometer Space Antenna (LISA), jointly sponsored by NASA and ESA, will also use a form of formation flying, but its application is vastly different than that used by TPF-I.  LISA will use micro-Newton thrusters to keep each spacecraft centered about its test mass, while relaying laser metrology between three spacecraft separated by about $5 \times 10^6$ km.

In summary, the Jet Propulsion Laboratory is continuing a coordinated and well structured program in the development of formation flying technology.  Although much of this program is directed in support of TPF-I, the program has broader applications. The needs of TPF-I specifically concern precision formation flying of a maneuverable array with elements in relatively close proximity (several tens of meters).  To the extent that it is possible to assess the state of the art in this field, the work done at JPL appears to be the most advanced and certainly the best tailored to the needs of the mission.

The formation-flying testbeds described in the following pages cover the full suite of technologies for TPF-I formation flying that need to be developed and demonstrated in a ground-technology program.  The testbeds described here will establish the viability of the formation-flying mission architecture for the TPF-I, while retiring and mitigating mission risk.

# 5.2 Formation Knowledge

## Formation Sensor Testbed

### Key Technology Addressed

Formation Sensing and Metrology

### Objectives

Formation flying interferometry will require the development of a suite of sensors to enable formation acquisition, stabilization, and precise control that will enable fringe acquisition and tracking. The formation sensor suite may consist of multiple sensing stages, namely: acquisition (coarse), handoff (medium), and tracking (fine) stages. Each finer stage provides higher precision with a narrower field of view. The Formation Sensor Testbed (FST) will develop and demonstrate the key technologies required for the formation acquisition sensor. The FST will focus on demonstrating the performance of the formation acquisition sensor (the coarse sensor). This will be a S-band sensor with the ability to measure bearing to $0.5°$ (1 $\sigma$), range to 10 cm (1 $\sigma$), and have full $4\pi$ instantaneous coverage.

### Approach

The Autonomous Formation Flying sensor was developed for the StarLight project and used an advanced reconfigurable baseband processor. It has been enhanced with a new signal structure. The new signal structure, called "ultra-BOC," will enable the sensor to operate simultaneously on multiple spacecraft, to implement passive radar operation for added protection against collisions, and to eliminate the need for time-consuming maneuvering during initial formation acquisition. These functions are achieved by resolving carrier cycle ambiguities in the differenced phase for the bearing-angle measurement. Existing RF transceivers as well as software inherited from the StarLight formation sensor design will be modified for prototype system development and demonstration.

The prototype formation acquisition sensor will be developed and demonstrated at JPL in the indoor testbed and the outdoor articulated testbed to demonstrate the sensor overall function and performance. The indoor testbed will be used for software development, hardware and software integration and test, end-to-end functional verification, and performance model validation excluding multipath error. The outdoor articulated testbed will be developed to validate end-to-end performance including the error contribution from multipath, which will be greater than expected in flight.

The principal investigator of Formation Sensor Technology is Dr. Jeff Tien at the Jet Propulsion Laboratory.

### Scope

- Design and analyze the performance of a $4\pi$-steradian acquisition sensor
- Demonstrate functionality of the acquisition sensor across three spacecraft in an indoor testbed
- Demonstrate instantaneous $4\pi$-steradian field-of-view coverage and performance of the acquisition sensor across three spacecraft in an articulated outdoor testbed

- Demonstrate integrated radar for collision avoidance

## State of the Art                                                        TRL 4

The Ka-band autonomous formation flying sensor developed for StarLight demonstrated that range measurement to 2 cm and bearing angles to 1 arcminute would be possible, while providing a moderately wide field-of-view (±70°). No prior testbed has had as its goal full 4π instantaneous coverage.

## Progress to Date

The AFF baseband processor was completed and the measurement of bearing angle was demonstrated. The new signal structure at S-band has also been developed to enable multiple spacecraft operation. The end-to-end tracking of the new signal structure was demonstrated in the indoor testbed. Work on the Formation Sensor Testbed is currently suspended, but will be restarted later in Pre-Phase A. The schedule for the development of the Formation Sensor Testbed is shown in Table 5-1.

**Table 5-1.  Formation Sensor Testbed Schedule**

| Planned Completion Date (FY) | Planned Activities | Performance Targets | TRL |
|---|---|---|---|
| 2003/Q4 | Complete AFF baseband processor | Demonstrate reconfigurable signal processing operation | 3–4 |
|  | Demonstrate bearing measurement | Demonstrate 3° bearing angle accuracy with no maneuvers required for bearing angle ambiguity calibration |  |
| 2005/Q2 | Develop new signal structure at S band to enable multiple spacecraft operation | Demonstrate end-to-end tracking of the new signal structure in the indoor testbed | 4 |
| 2009/Q1 | Implement the end-to-end indoor testbed system | Demonstrate 10-cm range and 0.5° bearing measurements (excluding error from multipath) for three spacecraft operation | 4–5 |
| 2009/Q4 | Complete outdoor testbed demonstration | Demonstrate 10-cm range (goal of 2 cm) and 0.5° bearing (goal of 1 arcmin) measurements including error from multipath for three spacecraft | 5 |
|  |  | Demonstrate 1-m range radar operation at 10-m separation. |  |
|  |  | 4π instantaneous coverage |  |

## Bibliography

J.Y. Tien J.M. Srinivasan, L.E. Young, G.H. Purcell, Jr., "Formation acquisition sensor for the Terrestrial Planet Finder," *2004 IEEE Aerospace Conference*, 2680–2690 (2004).

M. Aung, G.H. Purcell, J.Y. Tien, L.E. Young, L.R. Amaro, J. Srinivasan, M.A. Ciminera, Y.J. Chong,, "Autonomous formation flying sensor for the StarLight Mission," in *The Interplanetary Network Progress Report*, Vol. 152, 1–15 (2002).

# 5.3 Formation Control

## Formation Algorithms & Simulation Testbed

### Key Technology Addressed

Formation control algorithms, precision formation flying

### Objectives

The Formation Algorithms & Simulation Testbed (FAST) has as its goal to provide a high-fidelity end-to-end software simulation environment to demonstrate realistic mission scenarios of formation flying interferometers including formation acquisition, formation calibration, formation maneuvering, re-configuration, and nominal observation. This includes fine formation control (centimeter position and arcmin-level bearing control) and collision avoidance algorithms. An important aspect of this task is its implementation with flight-like software and CPUs in a distributed real-time system. FAST also has as an objective to provide formation flying algorithms for the FCT and use data from the FCT to validate the FAST simulation environment.

### Approach

This environment will be used to execute formation flying algorithms for a five-spacecraft formation. The work will include continued development and integration of (1) formation control architecture and algorithms; (2) models of spacecraft dynamics; (3) models of actuators; (4) models of sensors from the Formation Sensor Testbed; (5) models of inter-spacecraft communication; (6) models of ground commanding and monitoring; and (7) a simulation of the execution environment. The distributed formation control, sensing and communication architecture will be developed to maximize system robustness and performance. Figure 5-5 shows several views of the FAST development facility.

FAST uses a common modeling environment and code base to simulate both the TPF flight system and the Formation Control Testbed robots. The comparison against FCT experimental data will validate the



**Figure 5-5.** View of the FAST Realtime Processor Clusters (left), the Control Room of the FCT (middle), and Graphical Output from a Distributed Realtime Simulation (right)

FAST and bring confidence to performance predictions generated by the TPF simulation. A self-contained desktop workstation simulation of the five-spacecraft formation control system will be produced and delivered to the ObSim team for integration with the ObSim instrument simulation. The integrated simulation will provide end-to-end performance prediction for TPF.

The principal investigator of Formation Algorithms & Simulation Testbed is Dr. Matthew Wette at the Jet Propulsion Laboratory.

## Scope

- Develop formation flying (FF) control architecture and algorithms for a five-spacecraft TPF mission
- Demonstrate end-to-end TPF FF performance in a high-fidelity distributed realtime simulation testbed
- Validate FF control architecture and algorithms using the FCT hardware testbed

## State of the Art                                                    TRL 3–4

The state of the art in precision formation flying simulation is represented by the achievements of FAST. FAST has been implemented as a distributed, realtime simulation demonstrating nominal operation for two spacecraft formation flying and has demonstrated (in simulation) two-spacecraft autonomous formation flying with 5-cm range and 5-arcmin bearing control.

## Progress to Date

The Formation Algorithms & Simulation Testbed has achieved its two-spacecraft milestone, as noted above. The scenario included initial formation acquisition, formation sensor calibration maneuvers, formation collision avoidance, path planning, and nominal control including stop-and-stare observation.

Table 5-2. **Formation Algorithms & Simulation Testbed Schedule**

| Planned Completion Date (FY) | Planned Activities | Performance Targets | TRL |
|---|---|---|---|
| **2003/Q4** **Milestone** | Implement StarLight two-spacecraft formation flying algorithms into the realtime distributed environment | Demonstrate *two*-spacecraft autonomous formation flying with 5 cm range and 5 arcmin bearing control | 3–4 |
| **2005/Q4** | Implement two-robot formation flying algorithms for the FCT | Demonstrate 5 cm range and 1° bearing | 4 |
| **2006/Q4** **Milestone** | Exercise five-spacecraft formation flying algorithms into the realtime distributed environment | Demonstrate 1 cm range and 1 arcmin bearing control | 5 |
| **2007/Q1** | Validation of two-spacecraft algorithms by Formation Control Testbed | Demonstrate performance consistent with the FCT performance requirement: 5 cm range 60 arcmin bearing | 4 |
| **2007/Q4** **Gate** | Exercise five-spacecraft formation flying algorithms in realtime distributed environment with demonstrated fault recovery | Successful recovery to safe mode for all simulated fault cases | 5 |
| **2008/Q3** | Validation of three-spacecraft algorithms by FCT | FCT with 3 robots: 5 cm range, 60 arcmin bearing | 5 |

FAST was also used to provide algorithms and software for operating the first robot in the Formation Control Testbed (FCT) and is being developed to support testing with the FCT in parallel with its own development.  The schedule for the development of FAST is shown in Table 5-2.

## Bibliography

M. Wette, G. Sohl, D. Scharf, E. Benowitz, "The Formation Algorithms and Simulation Testbed," in *Second International Symposium on Formation Flying*, AIAA Proc. (2004).

M. Aung, A. Ahmed, M. Wette, D. Scharf, J. Tien, G. Purcell, M. Regehr, B. Landin, "An overview of formation flying technology development for the Terrestrial Planet Finder Mission," *2004 IEEE Aerospace Conference,* Big Sky, Montana, 2667–2679 (2004).

# Formation Control Testbed

## Key Technology Addressed

Precision formation flying

## Objectives

The Formation Control Testbed (FCT) has as its goal to demonstrate an end-to-end autonomous formation flying system in a 1-g environment. It will emulate real spacecraft dynamics and validate formation-flying algorithms using multiple mobile test robots within a ground-based laboratory to provide a realistic flight-like end-to-end demonstration. As an integrated test environment, FCT provides a system-level demonstration and validation capability for formation control technologies.
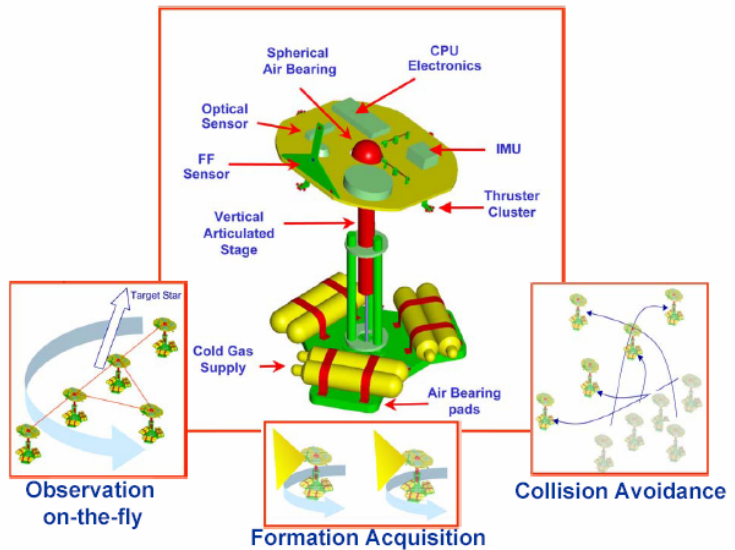


**Figure 5-6.** Simplified Drawing of a Single FCT Robot, with Illustrated Maneuvers

## Approach

The Formation Control Testbed is a ground-based laboratory consisting of three test robots in its fully deployed configuration. An early concept for the testbed is shown in Fig. 5-6. These robots, emulating three of the five TPF spacecrafts, are jointly designed with JPL's industry partners. The FCT will demonstrate formation acquisition, TPF-like formation maneuvering, and collision-free operations using the formation algorithms developed in the FAST. A high level of flight relevance was designed into the FCT avionics architecture, with on-board flight-like capabilities: (a) wireless communication emulating inter-spacecraft and spacecraft to ground communication; (b) on-board sensing and actuation using star tracker, gyros, thrusters and reactions wheels for attitude; and (c) PowerPC flight control computer on a compact PCI bus under vxWorks Realtime operating system. The on-board formation control software for the FCT is being developed by the Formation Algorithm & Simulation Testbed. With multiple FCT robots, FCT will validate the FAST algorithms and the end-to-end formation flying architecture. To emulate the real spacecraft dynamics, the FCT testbed was designed for realistic spacecraft-like dynamical behavior, mobility, and agility using linear and spherical air-bearings. With such 6 degrees-of-freedom dynamical motion and functional similarity to the TPF spacecraft, the FCT testbed will provide direct emulation of both individual spacecraft and formation behavior under autonomous on-board control. These architectural, functional, and dynamical similarities between the FCT and TPF-I will provide a direct path of development to the TPF flight system.

The requirements for the FCT have been listed in detail in Table 2-4. The layout of the FCT emulates the distribution of the formation flying telescopes, which is limited to a plane to minimize straylight from adjacent spacecrafts. The vertical air bearing has a range of ±25 cm, and the pitch and roll axes of each robot's motion is limited to ±30°, which is a physical limitation due to the spherical air bearings.

95

**Figure 5-7.** First FCT Robot Deployed and Operational, September 2004

The FCT testbed design strives to demonstrate an end-to-end system level FF control capability (functional and performance requirements) scaleable to flight, within a ground test environment. The ground operating environment for the FCT provides a more severe disturbance environment compared to the conditions in space. The net linear disturbance force due to solar pressure of ~6 $\mu$N/m$^2$ (at 1 AU) for TPF-I spacecraft (assuming a 5.7-m radius sunshade with a surface area of 102 m$^2$) is around 0.6 mN, comparable to the robot linear drift force of ~0.26N due to maximum residual floor slope of 80 $\mu$rad. Moreover, the residual center-of-gravity (CG) mass imbalance torque of 5 mN-m of the top attitude platform of the FCT robot is about 33 times worse than the expected solar pressure induced torque of 0.15 mN-m on the TPF-I spacecraft sunshade due CG to center of solar-pressure offset of ~0.25 m.

The FCT currently does not have formation sensors to directly measure the inter-robot/spacecraft range and bearing. The range and bearing for the FCT robots are currently derived from the position and attitude measurements from the star tracker on each robot — using parallax from the near-field FCT pseudo-star beacons. A laser retro-reflector system is currently under consideration as a future enhancement of the sensors of the FCT. The difference of a factor of 60 in bearing control between the flight design and FCT requirement (1 vs. 60 arcmin) arises from the greatly reduced spacing between the 'spacecraft' in the testbed. The size of the control volume within which each spacecraft is constrained at a given time is comparable for the two cases; the technology gap between testbed and flight is really the precision of the bearing sensor that is needed to maintain the formation. Bearing sensing in the flight design will be achieved with a combination of inertial star trackers on each spacecraft and encoders on the steering mirrors that direct the science and metrology beams between the spacecraft, both of which are well within the current state-of-the-art.

The principal investigator of the Formation Control Testbed is Dr. Asif Ahmed at the Jet Propulsion Laboratory.

## Scope

- Create an end-to-end multi-vehicle formation flying ground-based hardware testbed
- Demonstrate and validate FF architecture and algorithms
- Demonstrate a common sensing, communication, and formation control architecture for TPF-I

## State of the Art                                                         TRL 4

Ground-based demonstrations of formation flying have been conducted at the Massachusetts Institute of Technology.  Tests with three and five small robots on air bearings in the SPHERES testbed have demonstrated maneuvers in a plane, rotating about a center with controlled acceleration and deceleration. Further details are available at http://ssl.mit.edu/spheres/index.html.

## Progress to Date

The first of the three robots for the FCT, shown in Fig. 5-7, was deployed at the JPL Formation Flying Technology Laboratory in September 2004.  The attitude control of the first FCT robot was demonstrated in 2004 using FAST control software.  The second robot has been ordered from the supplier.  The schedule for development of the FCT is shown in Table 5-3.

**Table 5-3.  Formation Control Testbed Schedule**

| Planned Completion Date (FY) | Planned Activities | Performance Targets | TRL |
|---|---|---|---|
| 2003/Q4 | Formulation, architecture, hardware prototyping, Design Development Complete FCT System Design | Complete Critical Design Review (CDR) | 3 |
| 2004/Q4 | Develop, deploy and demonstrate first Robot | Closed-loop demonstration of first Robot | 4 |
| 2006/Q3 | Formation flying demonstration with 2 robots | Control to 5 cm position and 60 arcmin bearing | 5 |
| 2007/Q4 **Milestone** | Formation flying demonstration with 3 robots | Control to 5 cm position and 60 arcmin bearing | 5 |
| 2008/Q4 **Gate** | Formation flying demonstration with multiple robots and with fault recovery | Successful recovery to safe mode for all simulated fault cases | 5 |

## Bibliography

M.W. Regehr, A.B. Acikmese, A. Ahmed, M. Aung, R. Bailey, C. Bushnell, K.C. Clark, A. Hicke, B. Lytle, P. MacNeal, R.E. Rasmussen, J. Shields, G. Singh, "The Formation Control Testbed (FCT)" *2004 IEEE Aerospace Conference*, Big Sky, Montana,  557-564 (2004).

J.F. Shields, "The Formation Control Testbed celestial sensor: overview modeling, and calibrated performance," *2005 IEEE Aerospace Conference*, Big Sky, Montana, (2005).

# 5.4 Propulsion Systems

## Electromagnetic Formation Flying Demonstration

### Key Technology Addressed

Multi-spacecraft formation station-keeping using electromagnetic forces

### Objectives

The goal of this testbed is to demonstrate that the relative ranges and bearings of multiple spacecraft can be controlled by varying an electromagnetic field produced using orthogonal loops of high-temperature, superconducting wire. The Electromagnetic Formation Flying (EMFF) Demonstration will use electromagnetic forces from steerable magnetic dipoles plus reaction wheels to control the relative degrees of freedom within the spacecraft formation. Electromagnetic formation flying would be used in addition to the thrusters and could potentially reduce the total amount of propellant carried by each spacecraft. In so doing, it might also reduce the propellant waste and ensuing contamination of optical surfaces that would occur during reconfigurations of the telescopes. Thrusters would still be required to maneuver the entire array, for example to adjust its orbit, as EMFF would only be to adjust the relative orientations of the spacecrafts. The potential and associated risk of this technique will be evaluated.

### Approach

The approach uses two robots floated on air bearings on a test floor. A photograph of the robots is shown in Fig. 5-8. The EMFF Demonstration will use magnetic forces from three orthogonal superconducting wire coils (near 40 K temperature) supplemented by reaction wheels to control all *relative* degrees of freedom between the spacecraft. Previous studies have shown that high-temperature superconducting wire coils will exert sufficient forces to hold the TPF multi-spacecraft configuration in relative alignment during and following formation maneuvers. This approach will be implemented in hardware and control systems combining the reaction wheel and electromagnetic forces between at least two EMFF Demonstration vehicles. Current planning includes upgrading the EMFF avionics using the well-tested and modular avionics from the SPHERES program at the Massachusetts Institute of Technology (MIT).



**Figure 5-8.** Electromagnetic Formation Flying Demonstrator Units

The test data from the EMFF demonstration will be used to validate prior conceptual dynamic modeling and designs. Once validated, these models will be integrated into a spacecraft formation systems analysis

to compare EMFF performance with competing station-keeping technologies such as high-impulse thrusters.

The principal investigator for the Electromagnetic Formation Flight testbed is Dr. David Miller at MIT.

## Scope

- Develop and validate near-field electromagnetic dipole algorithms
- Confirm high angular-momentum storage and cryogenic thermal control
- Demonstrate control of non-linear dynamics between the EMFF vehicles

## State of the Art

Electromagnetic formation flying is an entirely new concept. The state of the art is represented by the achievements to date of the EMFF testbed at MIT. This includes demonstrations of maneuvers with one fixed robot and one free robot on an optical table to show closed-loop control of forward and backward relative motion, shear, and rotation.

## Progress to Date                                                       TRL 3

Closed-loop control has been demonstrated between two EMFF vehicles where one is mounted to the floor and the other is free to float on an air-bearing on the flat floor. Position hold control was performed with a separation between the vehicles of 1.875 coil diameters (or 1.5 meters). The position hold accuracy was 2 centimeters zero-peak at a control bandwidth of about 0.2 Hz (frequency at which open-loop transfer function gain drops 3db below static gain). Angular control is about 3°. This is about the precision of the measurement system. With one vehicle mounted to the floor, three degrees-of-freedom are present (one rotation and two translations). All three degrees-of-freedom were controlled simultaneously. Additionally, the same set-up was commanded to perform a step maneuver of 25 cm in size in each of the two translational degrees-of-freedom. MIT is currently preparing for larger maneuver tests involving one vehicle orbiting around the other. The schedule for the EMFF is shown in Table 5-4.

**Table 5-4.  Electromagnetic Formation Flying Demonstration Schedule**

| Planned Completion Date | Planned Activities | Performance Targets | TRL |
|---|---|---|---|
| 2004/Q4 | Demonstrate open-loop control of single robot relative to a fixed robot | Demonstrate maneuvers between robots with attraction, repulsion, shear | 2–3 |
| 2005/Q1 | Demonstrate closed-loop control of single robot relative to a fixed robot | Demonstrate recovery from disturbances in a forward, backward, shear, and rotational direction | 3 |
| 2006/Q1 | Demonstrate closed-loop control of single robot relative to a fixed robot | Demonstrate the ability to control one robot to move in a circle about a fixed robot | 4 |
| 2007/Q1 | Demonstrate array configuration and control closed-loop | Demonstrate the ability to control the orbit of three robots around a fixed center | 4 |

## Bibliography

E.M.C. Kong, D.W. Kwon, S.A. Schweighart, L.M. Elias, R.J. Sedwick, D.W. Miller, "Electromagnetic formation flight for multi-satellite arrays," *Journal of Spacecraft and Rockets*, Vol. 41, 659–666 (2004).

Daniel Kwon, *Electromagnetic Formation Flight of Satellite Arrays*, Masters of Science thesis, Massachusetts Institute of Technology (2005). Available at http://ssl.mit.edu/publications/theses/

Also see http://ssl.mit.edu/emff/testbedvideo.html

# Contamination Studies of TPF Propulsion Candidates

## Key Technology Addressed

Propulsion plume generation of visible/IR radiation and deposition on cryogenic surfaces thereby degrading instrument performance

## Objectives

The goal of this effort is to measure the potential for contamination of several candidate thruster technologies. Propulsion methodologies for TPF station-keeping must provide thrust ranges of 0.1 mN to 25 mN based on estimates provided by Lockheed Martin in related MIT research. The need for spacecraft formation station-keeping would likely require high-impulse thrusters whose ejected propellant, as in Fig. 5-9, would contaminate the optics of the telescopes and accumulate on the thermal shields, reducing their efficiency. This effort includes development of plume models that include infrared radiation signatures, direct measurement of infrared radiation of thruster plumes in the wavelength band from 8–16 microns, and direct measurement of deposition on quartz crystal microbalances at temperatures less than 40 K. The thruster technologies currently planned for these studies include Hall thrusters using xenon, helium, neon, and perhaps argon and RF ion thrusters. The information thus generated will be used for a preliminary selection of propulsive technology for the TPF Interferometer mission.

## Approach

This study effort includes three components: (a) extension of existing numerical models of propulsive plumes (both plasma and charged colloids) to address radiation and deposition; (b) experimental measurement of the visible and IR emission by selected micro-thrusters; (c) experimental measurement of deposition and evaporation of propulsive gases from cryocooled surfaces.

The existing plume models will be further developed by incorporating radiation emission into the MIT AQUILA code with the focus on predicting selected spectral lines of interest/ concern to TPF instrumentation. Deposition and condensation on cryogenic surfaces will be addressed by first determining the sticking coefficient (and other adsorption properties) of potential propellant gases then constructing a surface model for tracking the balance of adsorption and thermal re-emission on each surface.

Experimental Measurements of visible and infrared emission will be compared to existing model predictions with emphasis on plasma thrusters. Extension to the mid-IR range (7–20 micro-meter wavelengths) of interest to TPF instrumentation is being considered.

Materials considered for the Adsorption/Desorption measurements include Xenon for Hall and Ion thrusters, ionic liquids for colloid thrusters, and nitrogen for cold-gas thrusters, etc. Results will be compared to existing databases.

The principal investigator of the Contamination Studies of TPF Propulsion Candidates is Dr. Manuel Martinez-Sanchez at the Massachusetts Institute of Technology.

**Figure 5-9.** Schematic of Thruster Plume Interference with Cooled Surfaces of a Neighboring Collector Spacecraft

## Scope

- Extend existing plume models to predict emission spectra and propellant deposition on cryogenic surfaces
- Conduct experimental measurement of propellant visible and near-IR and mid-IR emission and plume deposition/ adsorption to extend existing databases
- Conduct experimental measurements of deposition and evaporation on cryogenic surfaces
- Compare experimental results and existing database information to extended plume model results to guide TPF thruster selection and development

## State of the Art                                                    TRL 2

The state of the art for plasma thruster plume simulation is represented by the MIT AQUILA code, developed for studies of Hall thrusters with support from the Air Force Office of Scientific Research (AFOSR). Characterization of thrusters in terms of their infrared signatures and rates of deposition at 40 K has never before been undertaken. There is very little information available to assess what adverse effects the TPF observatory will experience from plume radiated visible/near infrared IR emissions and/or propellant deposition.

## Progress to Date

An existing vacuum chamber has been instrumented to detect radiative spectra in the visible and near-IR parts of the spectrum. Experiments are ongoing that measure the radiation spectra and intensity from direct observation of representative thruster plumes. The existing vacuum chamber is also being used to characterize surface contaminations either by direct adsorption or impingement of the thruster propellant. Deposition measurement use a quartz microbalance cooled to cryogenic (~ -40 K) temperatures to detect actual deposition. Current measurements are limited to above 90 K by the electronics in the quartz crystal microbalance, but an upgrade to 40 K is planned. Modeling of these effects and experimental information on propellant adsorption are at TRL 2 as proposed here. The intent of this MIT program is to raise the relevant technologies to TRL 4. The schedule for the contamination studies is shown in Table 5-5.

**Table 5-5. Contamination Studies Schedule**

| Planned Completion Date (FY) | Planned Activities | Performance Targets | TRL |
|---|---|---|---|
| **2006/Q2** | Complete 600 W Hall Thruster with Ne/Ar and Xe | Conduct chamber testing at 40 K temperature with upgraded micro-balance and candidate propellants | 3–4 |
| **2006/Q3** | Complete data gathering for simulated hydrazine model, and complete RF ion engine plume data gathering | Compare experimental results and existing database information to upgrade model performance and experimental techniques | |
| **2006/Q4** | Complete final report | Integrate results from model development and experimental data and make recommendations to guide TPF thruster selection and development | 4 |

## Bibliography

L. Trevisani, F. Negrini, M. Martinez-Sanchez., "Material deposition measurements from a Hall Thruster using a Quartz Crystal Microbalance," Proceedings of the *4th International Spacecraft Propulsion Conference,* ESA Publication SP-555 (CDROM), Edited by A. Wilson, p. 122.1 (2004).

M. Santi, S. Cheng, M. Celik, M. Martinez-Sanchez and J. Peraire, "Further development and preliminary results of the AQUILA Hall thruster plume model," 39th *AIAA Joint Propulsion Conference and Exhibit*, Huntsville, AL, 20–23 July 2003. AIAA, 2003–4873.

# 6   Cryogenic Technology

TPF-I is being designed as a mid-infrared observatory with the ability to detect planet light over the wavelength range of 7–13 μm and possibly over the extended range of 7–17 μm. At mid-infrared wavelengths every warm object emits radiation, and warm surfaces within the observatory, such as the telescope and interferometer mirrors, can appear far brighter than the distant astronomical sources. The optics must therefore be cooled, shielded from direct sunlight, and provided with baffling and protection against scattered light. Using a multi-layered thermal shield, passive cooling to 40 K seems feasible with technology developed for JWST and should be adequate for TPF-I. Although adequate thermal shielding will be crucial to the success of the mission, it is not addressed in this technology plan. Numerous related issues, such as mission design, scattered light between spacecraft, reflected light from the Moon, and the design of optical baffles, are also important but will be addressed separately as part of future TPF-I Design Team activities.

Unlike most cryogenic observatories, that are designed to have very few moving parts and actuators, the TPF Interferometer will have numerous active systems. These will likely include movable mirrors for alignment and star acquisition, multi-stage delay lines for pathlength control, piezoelectric actuators for pathlength modulation, and shutters for alignment and calibration. Each of these devices will dissipate heat and induce vibrations in the structure. Many of the strategies that are currently used to limit vibrations in room-temperature interferometers will also be adapted and used at cryogenic temperatures. Each device will need to meet a global heat-dissipation error budget if the interferometer is to remain within operational temperature limits. As well, the structural behavior and damping properties of the observatory will change at extremely low temperatures, offering a challenge for a system that is particularly susceptible to vibration. The cryogenic structures technology, described in this chapter, addresses these concerns. The error budget related to structural and thermal design has not yet been developed and will be closely tied to the design team efforts in modeling the observatory.

TPF-I will also need state-of-the-art coolers for its detectors. Over the last two decades, NASA, often in collaboration with the US Air Force, has funded cryocooler technology development in support of a number of missions. The largest use of coolers is currently in Earth Science instruments operating at medium to high cryogenic temperatures (50 K to 80 K), reflecting the current state-of-the-art cryocooler technology. Since 2002, two new long-life cryocooler systems have been launched into space to support NASA missions: the Northrop Grumman Space Technology (NGST) pulse tube coolers on the Atmospheric Infrared Sounder (AIRS) instrument, and the Creare NCS turbo Brayton cooler (on the Hubble Space Telescope's Near Infrared Camera and Multi-Object Spectrometer (NICMOS) instrument. This chapter describes progress with the Advanced Cryocooler Technology Development Program, which has been funded through TPF to develop the next generation of cryocoolers.

# Cryogenic Structures Technology

## Technology Need Addressed

Characterization and modeling of microdynamic behavior of precision structures at cryogenic temperatures

## Objectives

This goal of this work is to test the variation of damping of more than 10 materials over a temperature range from room ambient to 40 K. Detailed analytical and experimental studies of critical microdynamic properties at low temperatures will be carried out to ensure proper functioning of interferometer structures in the mission environment. Key studies include model development, test validation, mechanical precision and stability, and sensitivity to on-orbit environment.

## Approach

The microdynamic behavior of cryogenic structures will be investigated through a combination of numerical modeling and experimental tests. Material properties characterization, component and sub-system tests will be designed and conducted to validate the system-level modeling approach. These activities will be conducted both through outside contracts and in-house work at JPL.

Existing data in the literature will be collected, reviewed, and assessed. This process will include heritage from IRAS, Spitzer, WMAP, and data from JWST as it becomes available. The experience of these mission in



**Figure 6-1.** Cryogenic Damping Facility

how they addresses macro (system-level) issues, and what problems occurred as a result of repeated cooling and warm-up cycles will be extremely informative to assess how well predictions and data will match up. It would furthermore provide an enduring legacy to future efforts to archive this data in one central location.

The Cryo Structures effort will go far beyond that to produce the reliable database of knowledge on cryogenic material properties essential to flight. Numerical models will be constructed and then test-validated in hardware. Models will simultaneously address regimes of small physical scales and low temperatures ("nano/cryo"). Out of this will come guidelines and recommendations for the modeling, testing, and validation of high-precision, stable cryogenic structures. In particular, a detailed model will describe the Formation Flying Interferometer (FFI), and assess its sensitivity to on-orbit environment. Also modeled will be the precision and stability of large mechanical structures with multiple nonlinear hinge/latch interfaces, such as the booms supporting FFI sunshields.

Dominant design and performance parameters will be studied within the ppb ($10^{-9}$) strain regime. The parameters of interest include, but are not limited to, damping, stiffness, friction coefficient, nonlinear hysteresis, dynamic response, and thermal-mechanical stability.

The principal investigator of the Cryogenic Structures Technology is Chia-Yen Peng at the Jet Propulsion Laboratory. Working with the JPL Cryogenic Structures Technology team, the University of Colorado (CU) and MIT will support research in the areas of microdynamic modeling, test validation, and model uncertainty.

## Scope

- Conduct damping experiments to find highly damped materials
- Compile a comprehensive database of material damping properties at cryogenic and room temperatures
- Validate cryo/nano friction models with a cryogenic tribometer
- Establish Cryogenic Structures Precision Stability Lab to test structural components at cryogenic temperature
- Build a Microdynamics System Verification Testbed at CU to validate nonlinear microdynamic modeling tools and to evaluate the various parameters contributing to microdynamic stability
- Develop IMOS-compatible tools for the modeling and test-validation of cryogenic structures with multiple nonlinear hinge/latch interfaces (IMOS, Integrated Modeling of Optical Systems, combines optical, structural, and thermal modeling in a unified software package)
- Develop guidelines for test and analysis of cryogenic structures for flight

## Cryogenic Material Properties

TPF-I will not be able to achieve high precision modeling prediction without incorporating into the models highly accurate material properties. To measure material damping and coefficient of thermal expansion (CTE) properties to the highest precision possible, the TPF-I technology team will use the Cryogenic Damping Facility and Cryogenic Dilatometer Facility, as shown in Fig. 6-1 and Fig. 6-2, respectively. Both facilities were initially developed at JPL for JWST.

To gain insight into the material damping levels at cryogenic temperatures and to search for materials with high cryogenic damping, the Cryogenic Damping Facility, Fig. 6-1, will be used to assess material damping by measuring the decay rate of the fundamental modes of rectangular sample bars.

The damping test will be performed inside a 0.6 m diameter thermal vacuum chamber equipped with a Gifford-McMahon cycle cryocooler. The system is
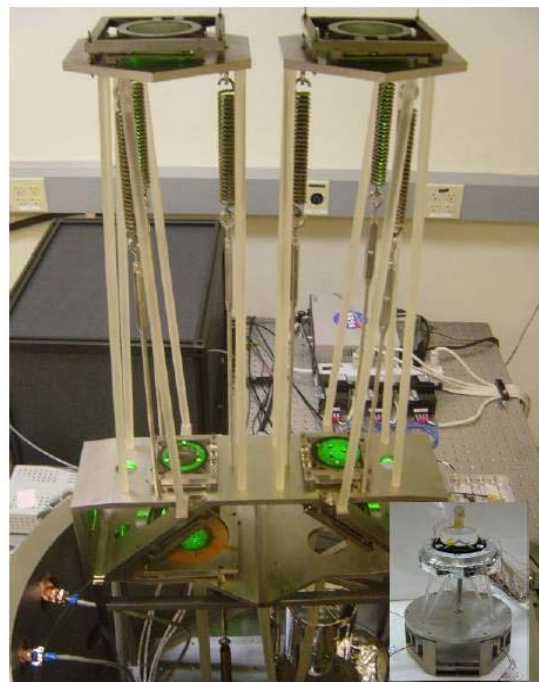


**Figure 6-2.** Cryogenic Dilatometer Facility

capable of maintaining the cold finger at any arbitrary temperature between 11 K and 293 K, but for various practical reasons the minimum specimen temperature achieved is 17 K.

During the heating or cooling process, the specimen temperature will be closely monitored through the Lakeshore 340 Temperature Controller. Pressure inside the chamber was maintained between $10^{-5}$ and $10^{-6}$ Pa. A number of materials have already been measured, and data are shown below in Fig. 6-3 for Titanium 15-3-3-3. The figure shows damping for Ti 15-3-3-3 as a function of temperature and modal frequency (sample bar thickness). Whereas Al damping decreases monotonically to levels as low as $10^{-4}$ % damping at 30 K, Ti fluctuates to damping as high as 0.1% at 20 K, possibly making it a good candidate for stable cryogenic applications. Based on these data, the accuracy of cryogenic damping measurement is approximately $10^{-5}$ of critical damping.

The TPF-I technology team will take advantage of the Cryogenic Precision Dilatometer Facility, as shown in Fig 6-2, to characterize the thermal strains, material variability and long term dimensional stability of relevant precision optical materials, at any temperature between 20 K and 305 K.

This facility has been calibrated using a sample of single crystal silicon. The CTE data collected on the sample matches almost exactly, to within 5 ppb/°C, the data measured on another extreme precision facility in Australia by K. G. Lyon over 30 years ago. The data shows that the accuracy in the instantaneous CTE is approximately 2 ppb/°K, at least an order of magnitude better than other existing test facilities in the US typically used for this kind of measurement. Examples of materials to be tested include ULE and Zerodur for optical mirrors, PMN for the deformable mirrors, as well as Titanium and various metals for mechanical components or flexures. Other mechanical and thermal properties will also
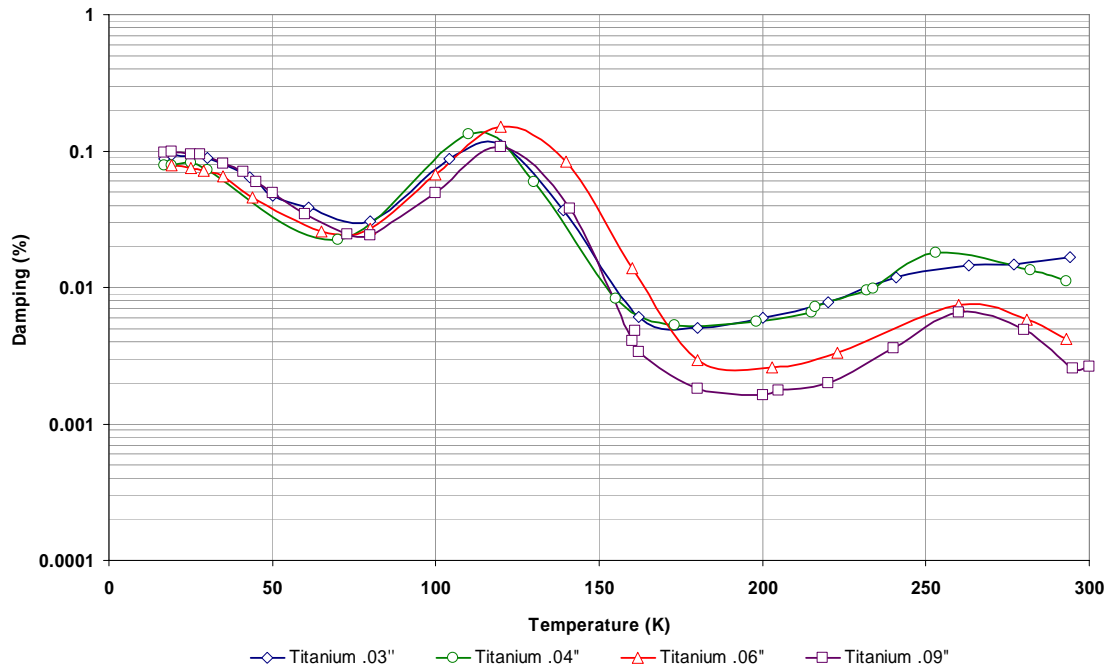


**Figure 6-3.** Cryogenic Damping for Ti-15-3-3-3

108

be gathered from the literature or tested when necessary. It will be important to also capture the accuracy with which these data have been measured, such as to propagate the measurement uncertainties within the analytical predictions. This implies that all facilities from which data are collected will require a validated error budget — note that test repeatability only highlights random errors, and does not evaluate systematic errors.

Material property measurements will not be limited to damping and CTE alone. The Project will establish a list of all material properties required for assessing performance stability using the integrated thermal, structural, and optical models. Included in this material property list are all elements in the dynamic and thermal load paths, including joints, and cables. Data will be needed for these properties as a function of temperature, wavelength, frequency, and load cycle as appropriate. Published literature data will be reviewed, and if it is established that the quality of the published data does not meet TPF-I accuracy requirements, then additional materials testing will be performed. Accuracy requirements on material property data will be defined later as more analysis is performed to understand the sensitivity of material data error on predicted performance. Allocations for material data error will eventually be folded into the Modeling Uncertainty Factor allocation. Ultimately, all material property data assembled under this endeavor will be gathered within a project controlled database for use on all TPF-I modeling activities.

## Cryogenic Microslip Characterization

The Cryogenic Tribometer Microslip Characterization Facility, as shown in Figure 6-4, will measure the coefficient of friction in the microslip regime well below the onset of gross Coulombic slip. This information is required as a physical parameter within established microslip hysteresis model forms that combine both stress-induced and roughness-induced microslip. Data need to be collected for representative materials of frictional interfaces, such as hinges and latches, with varying surface roughness specifications and over the temperature range of 20 K to 305 K to investigate thermal sensitivities. The tribometer is designed, built and calibrated at room temperatures by Dr. Jason Hinkle at
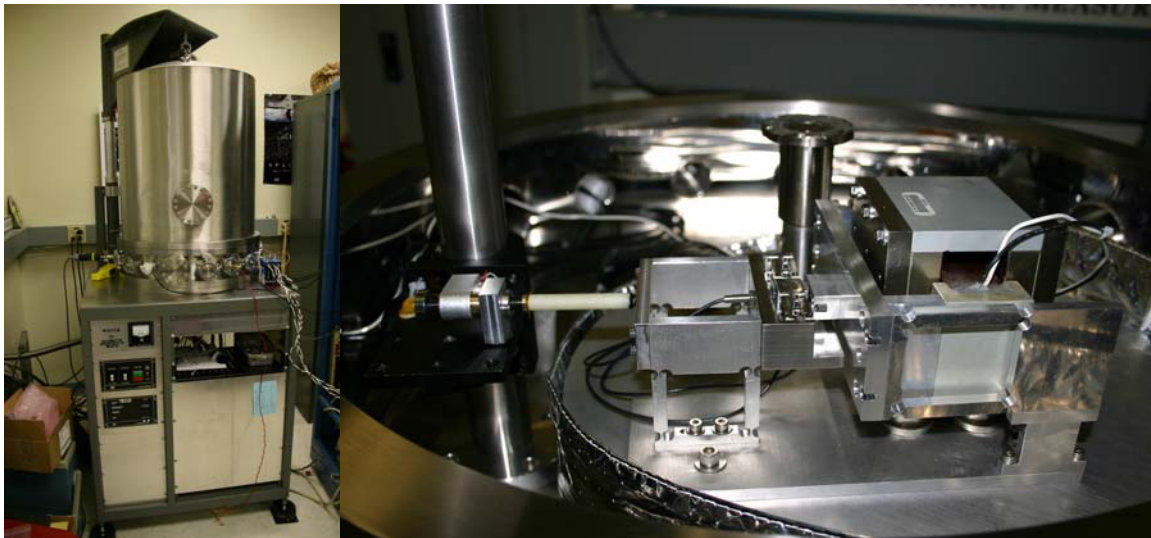


**Figure 6-4.** Cryogenic Tribometer Facility

the University of Colorado. The apparatus has been delivered to JPL to be integrated with a thermally controlled cryogenic vacuum chamber. The current accuracy requirement of microslip measurement is 10–100 nm. Data collected on this facility will be enclosed in a project material database.

## Cryogenic Micro-Mechanics System Technology

Current efforts related to cryogenic component behavior for TPF-I focus on very small-scale disturbances, as described in the following. This should eventually include the broader field of thermal cycling on joints as well as orthotropic material, mechanical disturbances (due to vibration and other noise sources), and larger-scale effects such as the repeatability of damping and dynamic responses after a simulated launch environment and the effect of self weight preload on these responses (the difference between one-g laboratory and zero-g operational conditions). These are all effects which may ultimately eclipse classical micro- to nano-mechanics.

The **Cryogenic Sub-Assembly Precision Test Facility** will be developed at JPL to characterize the thermo-mechanical stability of composite materials, composite structure sub-assemblies, and eventually actual flight hardware including hinges and latches. The facility will derive experience gained on the Cryogenic Precision Dilatometer test facility to incorporate a sub-nm interferometric metrology system within a thermally controlled vacuum chamber to enable distortion and strain measurements for these mechanical sub-assemblies. The current requirement goal is to achieve 5–10 nm measurement accuracy over a 1 minute time interval. Better measurement performances have already been achieved on the Cryogenic Precision Dilatometer test facility and the Space Interferometer Mission (SIM) Thermo-Optical Mechanical (TOM) testbeds, so the measurement capability itself is not seen as a risk.

The immediate goal will be to collect property data for non-optical materials. The focus will be on measuring and understanding the thermal strain, CTE, material variability, microdynamics and dimensional stability of proposed composite materials on TPF-I. Of special interest are the materials forming the primary mirror support structure, the secondary mirror tower and the optical bench.

Over time the facility will be used to investigate the dimensional stability and thermal sensitivity of critical sub-assemblies such as bonded composite parts, bearings, hinges and latches, and parasitic effects of cables through pivot or latch joints. Other areas of potential concern include micro-cracking and residual stress behavior of ULE segments joined through a low-temperature fusion process — especially as they relate to non-recoverable launch-induced deformations — or geometric misalignment of sub-assembly elements due to initial fabrication imperfections. This test facility could also be used to investigate active or passive structural damping technologies, should there be a need in the future. Details and test plans for the sub-assembly test articles will be developed as the design and analysis of TPF-I mature, and as the understanding of these risks with respect to the error budget improve.

The test facility will be multi-functional and will be capable of measuring nm-level motions due to thermal or mechanical disturbances. Tests will range from long-term stability observations to high frequency measurements, all of which are required to investigate a variety of nonlinear mechanical physics. For instance, test articles will be tested for quasi-static thermal or mechanical cyclic loads to identify hysteresis, and for steady-state dynamic loads to characterize harmonic distortion of the frequency response. When testing hinge and latch assemblies, the specimens will be turned around in various orientations to investigate and model the effects of 0-gravity. Alternative means to artificially

change the pre-load on the frictional interfaces will be implemented. The facility will be required to provide extreme thermal stability and control, as well as accurate means to decouple the response of the test article itself from external error sources typically attributed to instrument misalignment, load path parasitics, nonlinear responses, and interactions with mounting the hardware, etc.

Material data and validated sub-structure/sub-assembly component models gained from this activity will be collected within the project controlled material and model databases and used by the modeling team for prediction of flight performance.

The **System Microdynamics Verification Facility** will be developed at the University of Colorado by Prof. Lee Peterson and Dr. Jason Hinkle to evaluate, on a generic frictional interface, the various parameters contributing to microdynamic stability. The facility will be a simplified representation of the primary mirror to secondary mirror telescope assembly with an interchangeable frictional interface whose parameters, such as preload, stiffness, and surface roughness, can be varied to study the impact of the microdynamic stability at the simulated optics positions. These parameters are those included in existing models for frictional nonlinearities, and the measurements will be used to validate the sensitivity of these parameters to the microdynamic requirements on TPF-I. In particular, performance analysis models which bound the microdynamic performance will be developed and validated, and nonlinear analysis tools to model localized nonlinear behavior of hinges and latches will also be validated. A secondary goal of this test facility is to define the parameters and mechanical performance requirements of hinges and latches which will be levied on the actual TPF-I flight mechanisms.

## Integrated System Dynamics Modeling Tool

High and low intensity dynamic environments, experienced by a TPF-I spacecraft during on-orbit operations, induce structural loads and motions, which are difficult to reliably predict. Structural dynamics in low- and mid-frequency bands are sensitive to component interface uncertainty and non-linearity as evidenced in laboratory testing and flight operations. Analytical tools for prediction of linear system response are not necessarily adequate for reliable prediction of mid-frequency band dynamics and analysis of measured laboratory and flight data. A new MATLAB toolbox, designed to address the key challenges of mid-frequency band dynamics, will be developed. Finite-element models of major sub-assemblies will be defined following rational frequency-wavelength guidelines. For computational efficiency, these subassemblies will be described as linear, component mode models. The complete structural system model will be composed of component mode subassemblies and linear or non-linear joint descriptions. Computation and display of structural dynamic responses will be accomplished employing well-established, stable numerical methods, modern signal processing procedures and descriptive graphical tools. Parametric sensitivity and Monte-Carlo based system identification tools will be developed to reconcile models with experimental data and investigate the effects of uncertainties. Models and dynamic responses will be exported for employment in applications, such as detailed structural integrity and mechanical-optical-control performance analyses. The integrated system dynamics modeling tool developed by this effort will also be incorporated into an IMOS-compatible multi-disciplinary system simulation environment.

## State of the Art                                                              TRL 2–3

Currently, the methods to simulate the microdynamic behavior of precision structures at cryogenic temperature are not fully developed and are not validated at the level required by TPF-I.

## Progress to Date

The Cryo Tribometer Microslip Testbed has been integrated and is ready for preliminary testing. The mechanical design of the Cryo Sub-Assembly Stability Testbed is proceeding well, and its optical layout is being prepared. The requirements definition for the System Microdynamics Verification Testbed is being refined. The Cryo Material Damping Testbed has completed tests of silicon foam and silicon carbide foam, which are now being prepared for publication. The schedule for cryogenic structures technology is shown in Table 6-1.

**Table 6-1.  Cryogenic Structures Technology Schedule**

| Planned Completion Date (FY) | Planned Activities | Performance Targets | TRL |
|---|---|---|---|
| 2003/Q3 | Generic cryogenic/microdynamic test plan for model validation of cryogenic structures | | 2 |
| 2003/Q4 | Deliver IMOS-compatible nonlinear analysis process | | 3 |
| 2005/Q2 2005/Q4 | Compile material damping database (cryo & room temp.) Deliver nonlinear joint model interface and system parameters identification process | Test data and models shall allow resolution of structural motions to 10 nm and 10 arcsec with a goal of 0.1 nm and 0.1 arcsec. | 2 3 |
| 2006/Q1 | Report of cryo/nano friction experiments to validate models | | 3 |
| 2007/Q1 2007/Q1 | Deliver room-temperature microdynamics system verification testbed data, validated models and report Deliver final cryogenic structures test/analysis guidelines | Deliver validated models with resolution of structural motions to 10 nm and 10 arcsec with a goal of 0.1 nm and 0.1 arcsec. | 4 5 |

## Bibliography

C.-Y. Peng, M.B. Levine, L. Shido, and R.S. Leland, "Experimental Observations on Material Damping at Cryogenic Temperatures," in *Space Systems Engineering and Optical Alignment Mechanisms*, edited by Lee D. Peterson and Robert C. Guyer, Proceedings of. SPIE Vol. 5528, (SPIE, Bellingham, WA, 2004) 44–62.

P.B. Karlmann, M.J. Dudik, P. G. Halverson, M.B. Levine, M.R. Marcin, R.D. Peters, S.B. Shaklan, and D. Van Buren, "Continued Development of a Precision Cryogenic Dilatometer for the James Webb Space Telescope," in *Space Systems Engineering and Optical Alignment Mechanisms*, edited by Lee D. Peterson and Robert C. Guyer, Proceedings of. SPIE Vol. 5528, (SPIE, Bellingham, WA, 2004) 63–71.

M.B. Levine and C. White, "Material Damping Experiments at Cryogenic Temperatures," in *Optical Materials and Structures Technologies*, edited by William A. Goodman, Proceedings of. SPIE Vol. 5179, (SPIE, Bellingham, WA, 2003) 165–176.

# Advanced Cryocooler Technology Development Program

## Technology Need Addressed

Cryocooler technology

## Objectives

The objective of this development program is to develop low vibration, long life, development model coolers and test them through competitively awarded contracts to demonstrate the critical cryocooler technologies and performance needed by the TPF mission and other NASA astrophysics missions such as Constellation X. Cryocooler technologies identified as critical for the Advanced Cryocooler Technology Development Program (ACTDP) effort include efficient cooling to below 6 K, resistance to efficiency variations caused by parasitic thermal loads from gettered water vapor or other contaminants, launch survivability, lifetime requirements (avoiding plugging of the JT nozzle in the case of the Joule-Thomson cycle), electrical efficiency, and thermal stability of the work surface. The main objective is to provide at least 20 mW of cooling at 6 K for all coolers and for JWST-specific coolers to provide 30 mW of cooling at 6 K and 150 mW of cooling at 18 K. The program has as its objective to provide the technology base to initiate flight cooler procurements around 2007 to enable delivery of flight hardware in 2009–2010.

## Approach

To develop the needed cryocooler technology, NASA initiated the ACTDP in 2001 under the leadership of the TPF project at JPL and in collaboration with the NASA Goddard Space Flight Center. The ACTDP effort began with generation of detailed requirements and specification in summer 2001 and the awarding of four parallel study-phase contracts in April 2002. The four contractors, Ball



**Figure 6-5.** Illustrations of the Designs Proposed for the Four Parallel Study Contracts Awarded in April 2002

Aerospace, Creare, Inc., Lockheed Martin, and Northrop Grumman, proposed designs including Joule-Thomson, turbo-Brayton, and pulse tube coolers, all for use at 6 K and 18 K. Three concepts, by Ball, Lockheed Martin, and Northrop Grumman, were selected in December 2002 to advance into the Demonstration Phase. These early concepts are shown in Fig. 6-5.

During FY03, detailed design requirements for the three chosen ACTDP approaches were updated to reflect the rapidly developing mission concepts for TPF, Constellation-X, and the Mid Infrared Instrument (MIRI) of the James Webb Space Telescope (JWST).

In FY2004, JWST selected an open-cycle cryostat for MIRI. As a result, ACTDP adopted a greater focus on development of critical closed-cycle technologies, such as Stirling and pulse-tube efficiencies and

**Figure 6-6.** Development-Model Cryocoolers from Ball Aerospace, Lockheed Martin, and Northrup-Grumman, at the Time of Testing in 2004

overall cryocooler reliability, rather than detailed system design specific to one mission. The primary objective became the delivery of a working, tested Development Model (DM) cooler with laboratory drive electronics to NASA/JPL by the end of September 2006, with the pursuit of multiple technologies to reduce programmatic risk. Figure 6-6 shows photographs of the three coolers as they were in 2004.

### Scope

- Deliver Development Model (DM) mechanical cryocooler and laboratory cooler electronics
- Deliver Ground Support Equipment for system testing
- Document cooler system test results

### State of the Art                                                                    TRL 5

The state of the art in cryocooler technology is represented by the cooler developed by Lockheed Martin Advanced Technology Center through the ACTDP. Their development cooler demonstrated breakthrough success, shown in Fig. 6-7, by achieving the performance specification of 20 mW at 6 K with 150 mW at 18 K.

### Progress to Date

In 2005 all three contractors are in the testing phase with their testbed coolers. As noted above, the Lockheed-Martin cooler has achieved notable success far in advance of schedule. Ball and NGST are testing their Joule-Thompson (J-T) cooler stages, complete with recuperative heat exchangers, to demonstrate gas flow and cooling capability at 6 K. The Ball 3-stage Stirling precooler cold head was designed, fabricated, and successfully
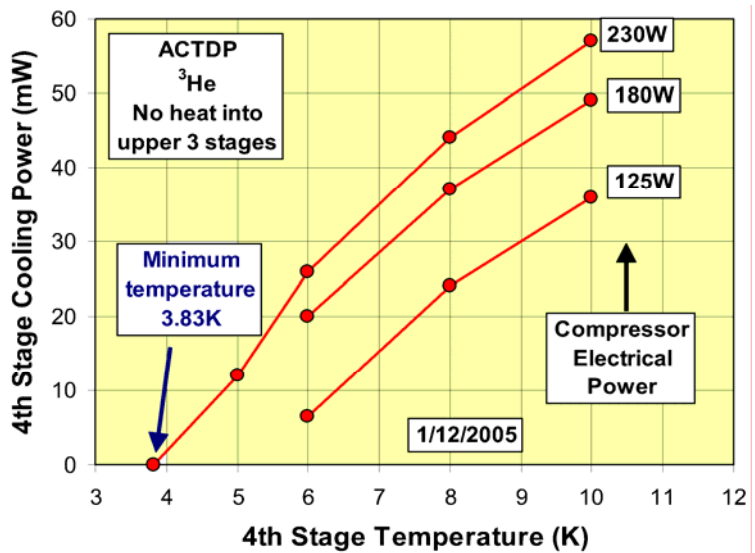


**Figure 6-7.** The Lockheed Martin four-stage pulse tube cryocooler achieved a no-load of 3.83 K using 3He as the working fluid and achieved the specification of 20 mW at 6 K, and 150 mW at 18 K with about 250 W of input power.
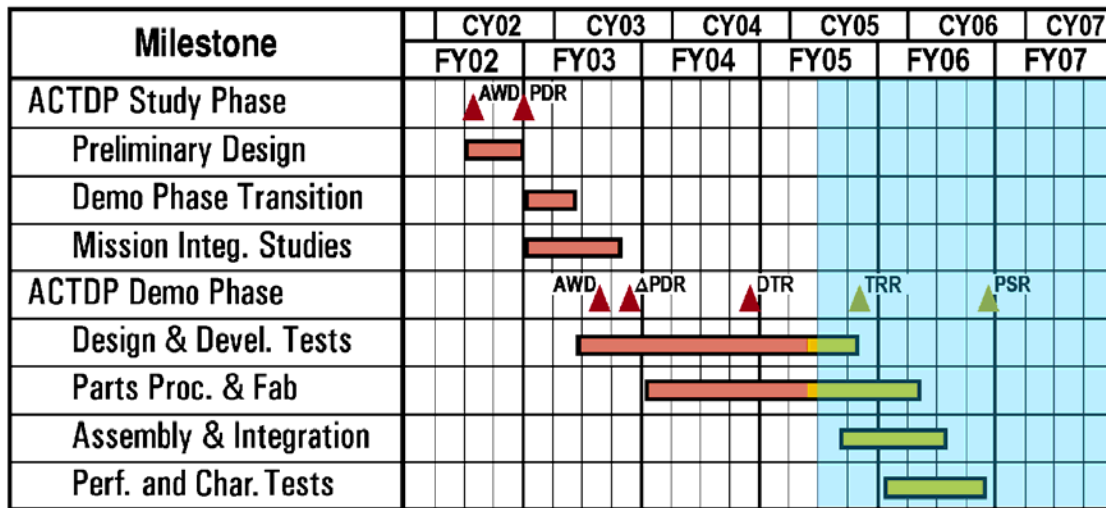
**Figure 6-8.** The ACTDP Schedule, with the Transition to Management by JWST Noted by the Shading on the Right

passed launch vibration tests. Ball is conducting design iterations on the precooler to increase its 18 K performance to the level needed to precool the J-T cooler stage. NGST is conducting design iterations to increase the 18 K cooling efficiency of their 3-stage pulse tube coldhead to a level needed to precool the J-T cooler stage. Lockheed-Martin Advanced Technology Center has also integrated their 4-stage pulse tube cooler and began performance testing.

For programmatic reasons, support by TPF for the ACTDP ended in 2005. The JWST Program reassessed their requirements, and responsibility for the continuation of the ACTDP was transferred to JWST as a part of the development of MIRI. The planned schedule, shown in Fig. 6-8 and Table 6-2, has transitioned from TPF to JWST. Ongoing efforts are now focused on JWST and in resolving the technical challenges prior to the Technology Readiness Review in September 2005.

## Bibliography

*Cryocoolers 13*, edited by Ronald G. Ross, Jr., ISBN: 0-387-23901-4 (Springer, New York, 2005).

**Table 6-2. Advanced Cryocooler Technology Development Program Schedule**

| Planned Completion Date | Planned Activities | Performance Targets | TRL |
|---|---|---|---|
| 2004 | Design DM Cryocoolers and Fab Critical-component Testbeds | Fab and test Lockheed risk reduction cooler, Design Ball, and NGST DM coolers and fabricate and initiate testing of PT and Stirling precooler testbeds | 3 |
| 2005/Q4 | Technology Readiness Review | Demonstrate that all individual critical technologies are sufficiently advanced to provide a high probability that the integrated DM cryocooler will meet its requirements | 4 |
| 2006/Q4 Gate | Development Model Cooler Performance Demonstration | Demonstrate that the development model coolers meet or exceed their performance requirements to provide 150 mW at 18 K and 20 mW of cooling a 6 K, with JWST coolers being capable of providing 30 mW at 6 K. | 5 |

# 7   Integrated Modeling and Model Validation

It will likely be impossible to test the entire observatory under flight-like conditions prior to launch. Predictability of success and minimization of risk are therefore paramount. Verification of TPF-I testbed, brassboard, and flight hardware performance will be accomplished by subsystem and component testing at the most detailed level. The results of these tests will be used to confirm analytic models, and these models will then be linked together to estimate the overall performance of TPF-I. By comparing the interaction of individually tested elements (represented by verified independent models) confidence in the overall systems model will be obtained. The fidelity of the models and their analytic interfaces will be verified. Proof that these tolerances can be achieved in a repeatable and robust manner will be completed prior to the start of Phase C/D. This proof will be obtained by measurements of appropriately scaled testbeds and components and by correlating these results with models whose scalability and linearity can be verified.

There are considerable challenges to evaluating system performance in the presence of uncertainty in nonlinear dynamical systems. The desire is to build an end-to-end simulation wherein some of the subsystem models are verified from the testbeds. The tolerances are so high that the analysis of small noises passed through nonlinear functions, or dynamic systems, must preserve the non-Gaussian stochastic character of the outputs. Since not all system models can be verified by testbeds, parameter uncertainty in these models must be included in the stochastic analyses.

To significantly reduce the computation time, a covariance analysis may ultimately be used. This effective approximation to a Gauss-Markov system would need to be verified through a nonlinear simulation. This means that the statistical approximations to the system nonlinearities must be made. Moreover, it will be important to ensure that the covariance tool reflects the performance generated from a similar Monte Carlo analysis and captures any worst-case analysis associated with the choice of system parameters.

# Model Uncertainty Evaluation of TPF-I Structure

## Key Technology Addressed

Methodologies to model high-performance spacecraft structural systems in the presence of uncertainty

## Objectives

The objective of this work is to use modeling of parametric uncertainty and propagation of uncertainty to generate a range of performance predictions for the structural model of the JPL Terrestrial Planet Finder spacecraft. Several techniques are currently being used to address this class of problem. Structural optimization can be performed using integrated models in order to get the greatest possible performance out of a system. Uncertainty modelling and propagation are used to quantify uncertainty and propagate its effects through the model to generate a range of performance predictions. Robust design techniques can then be used to make a system less sensitive to uncertainty.

## Approach

Previous model verification work at MIT was performed using the Disturbance, Optics, Controls and Structures (DOCS) modeling and analysis framework within a MATLAB environment. This work was based on a JPL-provided single-spacecraft model that included performance predictions and functional dependencies for the orbital environment of the TPF mission (Masterson and Miller, 2005). The model was in the form of NASA Structural Analysis Program (NASTRAN) bulk data files. One file described the main spacecraft structure, and a second file described the sunshield. Only the main telescope and bus structure is being examined in the current work. A NASTRAN finite element model of a TPF-I collector is shown in Fig. 7-1.

Key components of the spacecraft include modeled components such as the telescope mirror, light trays and sunshade booms, as well as concentrated masses that represent the secondary mirror or spacecraft control assembly. A broadband reaction wheel model, which models the disturbances over a range of speeds, is also implemented. A simple Attitude Control System (ACS) is included using DOCS to control the spacecraft rigid body rotations. The translational rigid body modes are truncated. Although additional performance metrics are desired, the rotation of the secondary mirror is currently the only output. Its selection was based on the typical dominance of secondary mirror tip and tilt motion on image jitter, but can be changed if desired. No optical control is used at this point. A parametric uncertainty analysis will be performed. To investigate which parameters contribute most to the total performance uncertainty, all of the following parameters are identified in the model:

- Secondary tower supports modulus
- Primary mirror plate modulus
- Primary mirror plate bending inertia ratio
- Sunshade booms modulus
- Mass at end of sunshade boom
- Light trays CBUSH stiffness, translational & rotational
- Leaf radiator's CBUSH stiffness, translational & rotational
- Secondary mirror mass
- Primary mirror mount masses
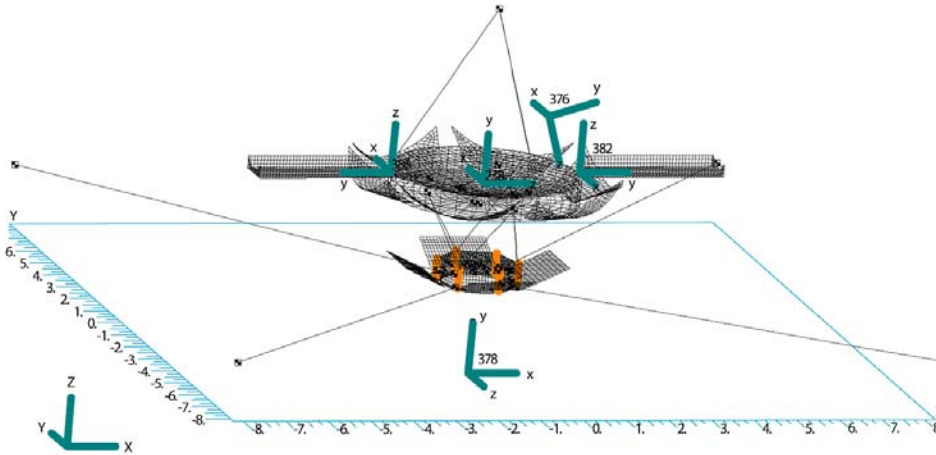
**Figure 7-1.** NASTRAN Finite Element Model of TPF-I

After initial simulations are run and the largest contributors to model uncertainty are identified, those major contributors will be used in an uncertainty propagation routine to provide worst-case model uncertainty bounds on the outputs. The selection tool that will be examined is computational simulation using parameters at low and high values, with results compared using the Analysis of Variance tools. This simulation-based approach potentially would allow much greater flexibility for non-linearity or a thermal effect to be investigated since it does not necessitate a linear state-space system (although that will be used in this work).

The MIT DOCS modeling framework within the MATLAB computational environment has been reliably demonstrated on other programs and design tasks. Application of the MIT DOCS modeling framework to the JPL TPF model and bounding parametric uncertainty is at a TRL 2 as proposed here. The intent of the MIT Model Validation task is to raise the relevant structural uncertainty modeling technologies for the TPF application to TRL 4.

The principal investigator of the Model Uncertainly Evaluation is Professor David Miller at the Massachusetts Institute of Technology.

## Scope

- Identify the list of essential parameters to be included in the uncertainty evaluation of the JPL FFI model
- Perform a frequency-based uncertainty analysis of the JPL FFI model evaluating the essential parameters
- Deliver modeling code to JPL ensuring that all developed MATLAB tools are compatible with JPL IMOS tools
- Produce a report and include all MATLAB scripts implementing the TPF model to permit JPL to replicate and link the MIT modeling methodology to the JPL TPF spacecraft modeling activity

## State of the Art

The discipline of model uncertainty evaluation has not previously been applied to the study of the structural vibrations of TPF-I. Consequently, this work is at a low TRL level.

## Progress to Date                                                    TRL 2–3

Additions to the formation flying integrated model are complete, allowing the critical parameter identification and uncertainty routines to be performed on a more realistic system. The additions include several stages of isolation modeled as low pass filters. There is a reaction wheel disturbance isolator with a nominal 10 Hz corner frequency, and an isolator between the bus and the optics with a nominal 2 Hz corner frequency. Both isolator models have 5% damping. Optical control is modeled using a high pass filter on the outputs, with a nominal 10 Hz bandwidth. Both the isolator corner frequencies and the optical control bandwidth can be varied in the DOCS model. Current work involves re-running and expanding upon the critical parameter identification techniques and uncertainty propagation tools using this new model. In addition to this tool development, the MATLAB codes are being re-written to be more easily integrated with tools developed at JPL. The schedule of development is shown in Table 7-1.

**Table 7-1. Model Uncertainty Evaluation of TPF-I Structure Schedule**

| Planned Completion Date (FY) | Planned Activities | Performance Targets | TRL |
|---|---|---|---|
| **2005/Q1** | MIT receives initial formation flying collector model from JPL | Deliver modeling code with all developed MATLAB tools shown to be compatible with JPL IMOS tools | 2–3 |
| **2005/Q2** | MIT receives final formation flying model from JPL | | |
| **2005/Q2** | Description of MUF methodology/process delivered | | |
| **2005/Q3** | MUF software, tools, descriptions delivered | | 3 |
| **2006/Q1** | Deliver MIT findings for TPF-I formation flying model | Provide alternative design, control, or operations schemes where necessary. | 4 |
| **2006/Q2** | Deliver a frequency-based uncertainty analysis of formation flying model | | 4 |

## Bibliography

R.A. Masterson and D.W. Miller, "Dynamic tailoring and tuning for precision optical space structures," AIAA 2004-1600, 45th *AIAA Structures, Structural Dynamics and Materials Conference*, Palm Springs, California, 19–22 April 2004.

S.A. Uebelhart, D.W. Miller, and Carl Blaurock, "Uncertainty Characterization in Integrated Modeling." AIAA 2005-2142, in the *13th AIAA Adaptive Structures Conference,* Austin, Texas, 18–21 April 2005.

C. Blaurock, S.A. Uebelhart, D.W. Miller, "Identification and propagation of probabilistic uncertainties for flexible space structures," in *Space Systems Engineering and Optical Alignment Mechanisms*, edited by Lee D. Peterson and Robert C. Guyer, Proc. SPIE Vol. 5528, 215–226 (2004).

## Note

The DOCS modeling and analysis framework has been developed by the MIT Space Systems Laboratory and takes the form of a MATLAB toolbox — a collection of algorithms. MATLAB (Matrix Laboratory, a MathWorks product) is a high-level technical computing language and interactive development environment. The environment provides the user access to high performance numerical computing with matrices and vectors.

# Observatory Simulation

## Key Technology Addressed

End-to-end modeling, testbed validation, and simulation

## Objectives

Concerns that are central to the demonstration of a TPF interferometer are the characterization of the interferometer's null, and its amplitude and phase stability to the level of 0.13% and 1.5 nm over long periods of time in the presence of numerous system perturbations. Since the interferometer will be a large multi-spacecraft system much too large to test as a whole in any cryogenic vacuum chamber that now exists, it will be necessary to develop a trusted and validated end-to-end simulation of the observatory. The TPF interferometer requirements necessitate the integration of structural, thermal, control, and optical models into the overall Observatory Simulation, as shown in Fig. 7-2.

The resulting tool will be used to model the testbeds for validation against measured performance and, once convinced of the models' fidelity, to model and evaluate various architectures and missions.

## Approach

JPL will use the Next-Generation Integrated Modeling of Optical Systems (NG-IMOS) tool as the framework for the Observatory Simulation. The individual models developed in the course of designing
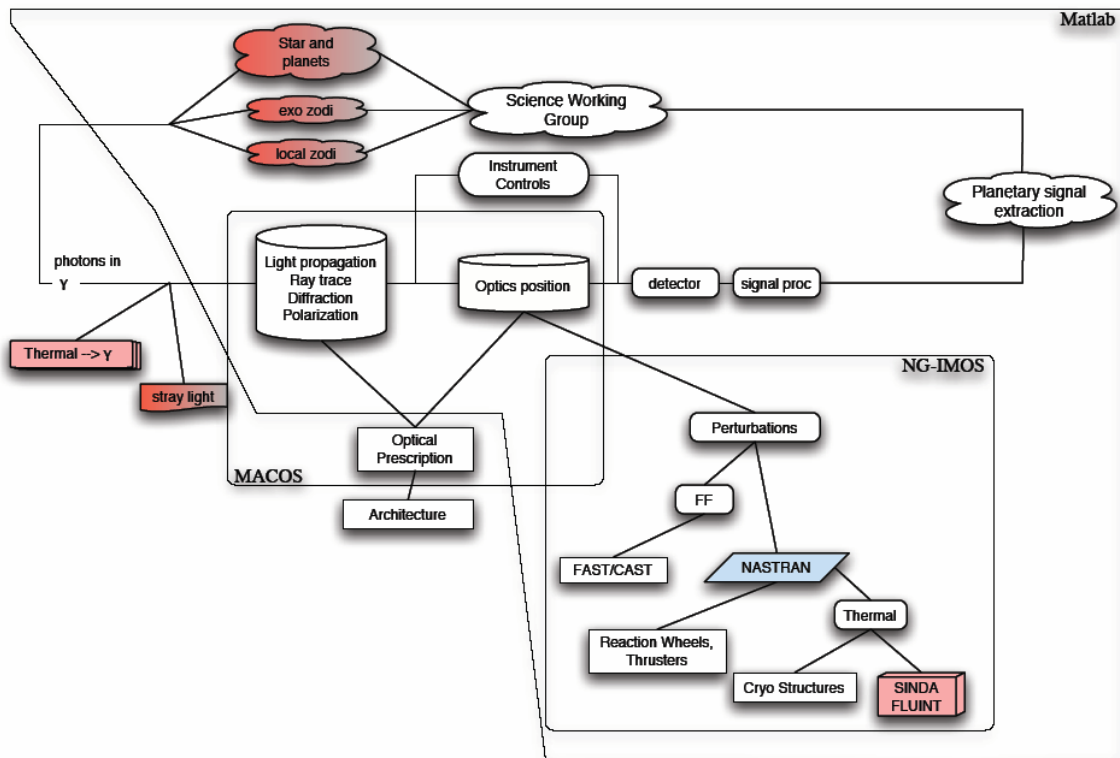


**Figure 7-2.** Schematic of the Observatory Simulation Activities, Including the Planetary Signal Extraction

the interferometer will be incorporated into the ObSim. Representative disturbances from reaction wheels, cryogenic pumps, thrusters, etc., will be used as inputs to the physical models, which will in turn cause optical disturbances that affect the null stability. The performance of the system will then feed back into the error budget and the structures, controls, thermal, and optical designs. The performance of the system can be optimized by studying the integrated performance of the end-to-end simulation.

This effort includes the development of methods to extract planetary signals from noisy data. Methods, new code, and models will be validated through a range of tests that include theoretical, closed-form solutions and comparisons of predicted performance to measured results from the Planet Detection Testbed. Test architectures will also be available for participants in the interferometer community to model with independent tools for performance comparison purposes. This should result in a uniquely qualified tool for interferometer system development. In future phases, the models will be developed to insure that the simulations can be used to diagnose various hardware anomalies should they occur in flight.

The Observatory Simulation task also oversees the work done by the Planetary Signal Extraction science working group whose members include scientists from the University of Arizona, JPL, and the U.S. Naval Observatory and members of the TPF-I Science Working Group. This group studies methods of detecting planets from the signals generated by the interferometer (and its simulation).

## Scope

- Use NG-IMOS to build an end-to-end model of the formation flying interferometer
- Design sensitivity and optimization of the separate physical design models
- Correlate methodologies and code implementation for comparison to measured performance of the Planet Detection Testbed


## State of the Art                                                           TRL 2–3

Current integrated analysis requires the use of separate codes for radiation exchange, heat transfer, structural analysis, structural/optical interpolation, and optical analysis, incurring the penalties and errors associated with separate model descriptions. There is no combination of either commercial off-the-shelf or internally developed toolsets currently available that will allow for analysis of all multidisciplinary (structural, thermal, controls, and optical) aspects of TPF.

## Progress to Date

A single wavelength simulator was completed for ObSim that generated star and planet signals with the appropriate amount of noise. In the past year most of the time was spent on the planetary signal extraction task. For this work, several existing algorithms were tested and some new algorithms were developed. Blind tests were performed, and feedback from this exercise was used to help the design team used to rule out certain array architectures. Results of the planetary signal extraction work have been submitted for publication. Preparations are ongoing to integrate thermal, optical, and structural models for a demonstration in NG-IMOS. Models of the interferometer are being included in ObSim from Ball Aerospace, GSFC, and JPL. The schedule for the development of ObSim is shown in Table 7-2.

**Table 7-2.  Observatory Simulation Schedule**

| Planned Completion Date (FY) | Planned Activities | Performance Targets | TRL |
|---|---|---|---|
| **2007/Q3** | Demonstration of Integrated structural and optical models into NG-IMOS model of FFI | Initial validation of ability to reach 1.5 nm and 0.13% stability | 3 |
| | Use reaction wheels and cryopump inputs to study optical sensitivities | PDT validation correlation of simple cases to $>10^5$ null depth prediction | |
| | Build initial model of PDT | | |
| **2008/Q1 Milestone** | Demonstrate a simulation of the flight observatory concept that models the observatory in a *static* condition (no dynamic disturbances) | Validate the model with experimental results from at least the Achromatic Nulling and Planet Detection testbeds at discrete wavelengths | 4 |
| **2009/Q4 Gate** | Demonstrate a simulation of the flight observatory concept that models the observatory subjected to *dynamic* disturbances (e.g., from reaction wheels) | Validate the model with experimental results from at least the Planet Detection Testbed at discrete wavelengths | 5 |

## Bibliography

M.B. Levine, G. Moore, S.A. Basinger, A. Kissil, E. Bloemhof, and S. Gunter, "Integrated modeling approach for the Terrestrial Planet Finder (TPF) mission," Proc. SPIE 5497, 181 (2004).

B. Ware, C. Henry, "Modeling the TPF Interferometer," *Optimizing Scientific Return for Astronomy through Information Technologies*, Edited by Peter J. Quinn, Proc. SPIE Vol. 5497, 193–201 (2004).

D.W. Draper, N.M. Elias II, M.C. Noecker, P.J. Dumont, O.P. Lay, B. Ware, "Planetary signal extraction for the interferometric Terrestrial Planet Finder," submitted to *Astrophysical Journal* (2005).

O.P. Lay, "Imaging properties of nulling interferometers," submitted to *Applied Optics* (2005).

# Appendices

# Appendix A
# Organization

Figures A-1 through A-4 show the organization of the TPF-I element.  The pale blue box shows the GSFC partnership.  The tan boxes show where industry collaboration occurs.    Green boxes indicate collaborations with universities.  The instrument and cryo structure technologies of this document are managed by the Instrument Engineering element of the organization.  The formation flying technologies are managed by Spacecraft Engineering.  The modeling technologies are managed by either the TPF-I Systems Manager or Instrument Engineering.

```
                   ┌─────────────────────────────┐
                   │  TPF Interferometer Project  │
                   │    Dan Coulter Proj Mgr      │
                   │    Chas Beichman Proj Sci    │
                   └─────────────────────────────┘
                                 │
                   ┌─────────────────────────────┐
                   │       Systems Manager        │
                   │         Curt Henry           │
                   └─────────────────────────────┘
                                 │
      ┌──────────────────┐       │        ┌──────────────────────────┐
      │   Architecture   ├───────┼────────┤  Observatory Engineering │
      │   Oliver Lay     │       │        │     Louise Hamlin        │
      └──────────────────┘       │        └──────────────────────────┘
                                 │        ┌──────────────────────────┐
                                 ├────────┤  Observatory Simulation  │
                                 │        │       Brent Ware         │
                                 │        └──────────────────────────┘
      ┌──────────────────┬───────┴────────┬──────────────────────────┐
┌──────────────────┐ ┌──────────────────┐ ┌──────────────────────────┐
│ Instrument Eng   │ │ Spacecraft Eng   │ │  Telescope Engineering   │
│  Steven Gunter   │ │   Asif Ahmed     │ │   GSFC – Neil Martin     │
└──────────────────┘ └──────────────────┘ └──────────────────────────┘
```
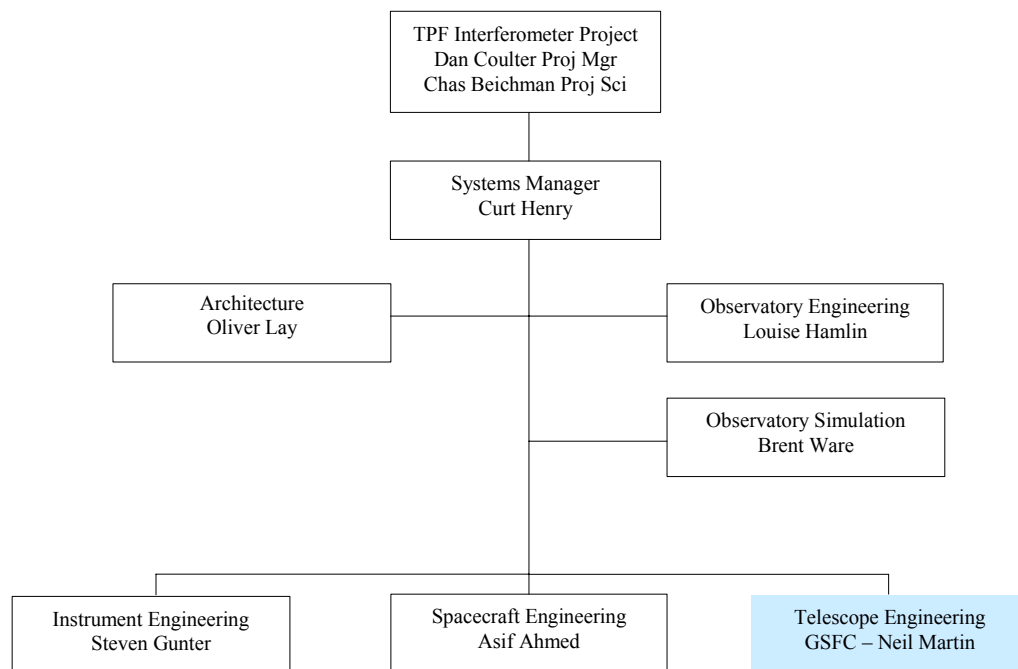
**Figure A-1.**  High-Level Organization Chart for TPF-I

Spacecraft Engineering
Asif Ahmed

FF Flight Design
George Purcell

Formation Sensor
Jeff Tien

Formation Algorithms
Asif Ahmed

Formation Control
Asif Ahmed

FF System Studies
Steve Mitchell
Ball - Fischer

Univ. Contracts
John Treichler

Robots/Floor
Allan Eisenman
GDC - Rasmussen

EMFF
MIT - Miller

Propulsion Plumes
MIT – Martinez-Sanchez
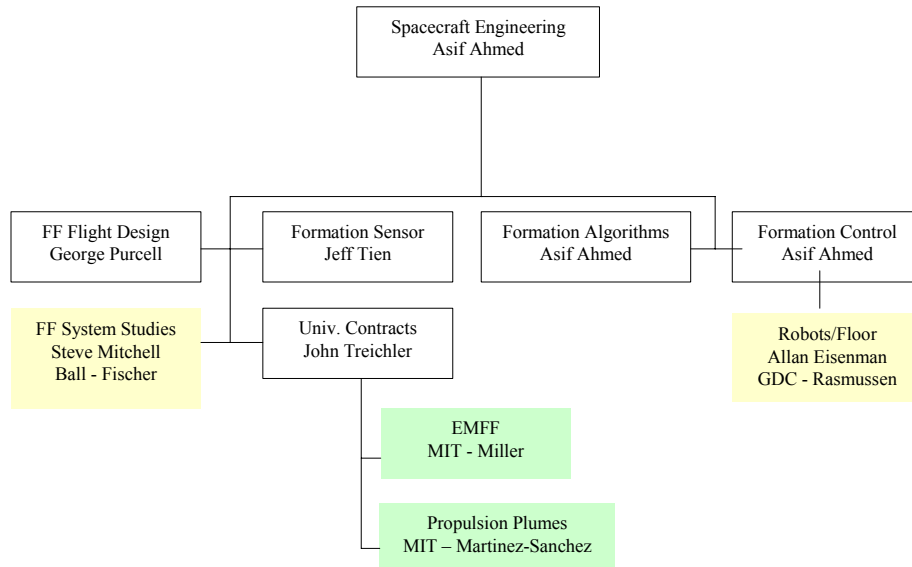
**Figure A-2.** Organization Chart of Formation Flying Activities for TPF-I

Instrument Engineering
Steven Gunter

Achromatic Nulling
Kent Wallace

Planet Detection
Stefan Martin

Adaptive Nuller
Robert Peters

Cryo Delay Line
Robert Smythe

Optical Elements
Alex Ksendzov

Optical Contracts

Flight Instrument
Stefan Martin

Cryo Structures
Chai-Yen Peng

Integrated Optics
U of Az - Walker

Phasing
John Treichler
U of Az - Hinz

Cryo Structures
CU - Peterson

Spatial Filters
Tel Aviv U – Katzir
U of Az – Walker
NRL - Sanghera

Beamsplitter
John Treichler
U of Az - Hinz

Modeling Uncertainty
John Treichler
MIT - Miller

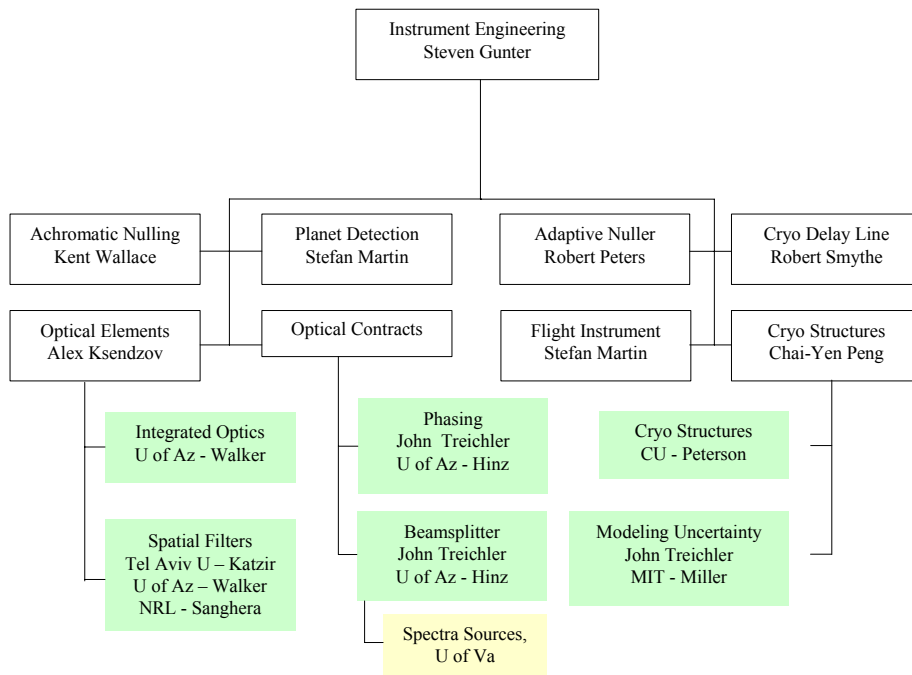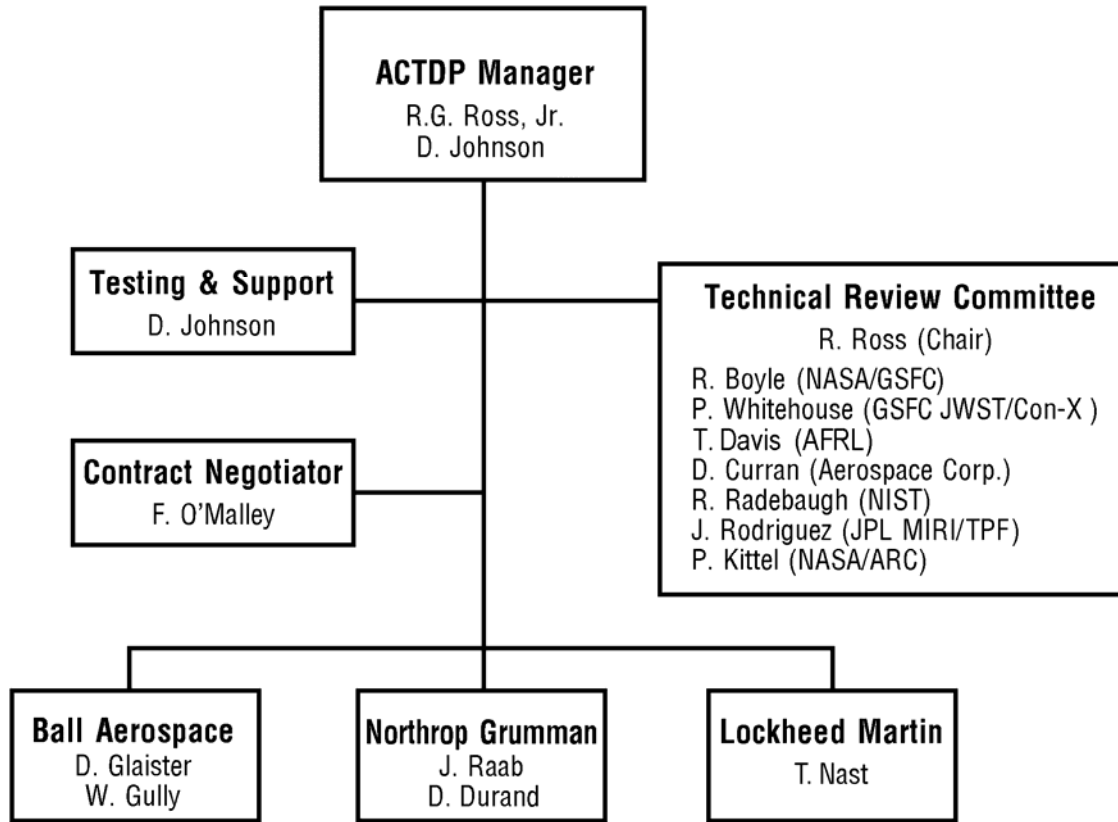Spectra Sources,
U of Va

**Figure A-3.** Organization Chart of Optics and Starlight Suppression and Instrument Engineering Activities for TPF-I

**Figure A-4.** Organization Chart of the Advanced Cryocooler Technology Development Program, Managed by the TPF Project until March 2005

# Appendix B
# Technology Summary Table

**Table B-1.  Summary of Technology Activities**

| Technology Testbed or Task | PI / Cog-E | Institute | Page Refs | |
|---|---|---|---|---|
| **Optics and Starlight Suppression** | | | | |
| Beamsplitter Development | Ph. Hinz | Univ. of Arizona | 48–49 | **62** |
| Mid-Infrared Spatial Filter Tech | A. Ksendov | Jet Propulsion Lab | 48–49 | **64** |
| Hollow Waveguides | C. Walker | Univ. of Arizona | 48–49 | **64** |
| Chalcogenide Fibers | J.S. Sanghera | Naval Research Lab | 48–49 | **64** |
| Polycrystalline Silver Halide Fibers | A. Katzir | Univ. Tel Aviv, Israel | 48–49 | **64** |
| Integrated Optics | A. Ksendov | Jet Propulsion Lab | 48–49 | **67** |
| Hollow Waveguides | C. Walker | Univ. of Arizona | 48–49 | **67** |
| Cryogenic Delay Line | R. Smythe | Jet Propulsion Lab | 48, 50 | **69** |
| Common Path Phase Sensing Testbed | Ph. Hinz | Univ. of Arizona | 48–49 | **71** |
| Adaptive Nuller | R. Peters | Jet Propulsion Lab | 22–23, 48–49, 56 | **73** |
| Achromatic Nulling Testbed | J.K. Wallace | Jet Propulsion Lab | 22–23, 48–49, 57 | **76** |
| Planet Detection Testbed | S. Martin | Jet Propulsion Lab | 22–23, 48–49, 57 | **80** |
| **Formation Flying Technology** | | | | |
| Formation Sensor Technology | J. Tien | Jet Propulsion Lab | 31, 51–52 | **90** |
| Formation Algorithms & Simulation | M. Wette | Jet Propulsion Lab | 25, 51–52, 58 | **92** |
| Formation Control Testbed | A. Asif | Jet Propulsion Lab | 34, 51–52, 58 | **95** |
| Electromagnetic Formation Flying | D. Miller | MIT | 33, 51–52 | **98** |
| Contamination Studies of Propulsion | M. Martinez-Sanchez | MIT | 33, 51–52 | **101** |
| **Cryogenic Technology** | | | | |
| Cryogenic Structures Technology | C. Peng (JPL) | Univ. Colorado | 36, | **106** |
| Advanced Cryocooler Technology Prog. | Ron Ross (JPL) | Ball, Lockheed-Martin, NGST | 37, 59 | **114** |
| **Integrated Modeling** | | | | |
| Model Verification | D. Miller | MIT | 39, 52–53 | **118** |
| Observatory Simulation | L. Hamlin | Jet Propulsion Lab | 52–53, 59 | **121** |
| Planetary Signal Extraction | B. Ware | Jet Propulsion Lab | 52–53 | **121** |

# Appendix C
# Detailed Schedules

Figures C-1 through C-4 show detailed schedules that were current in May and June 2005.
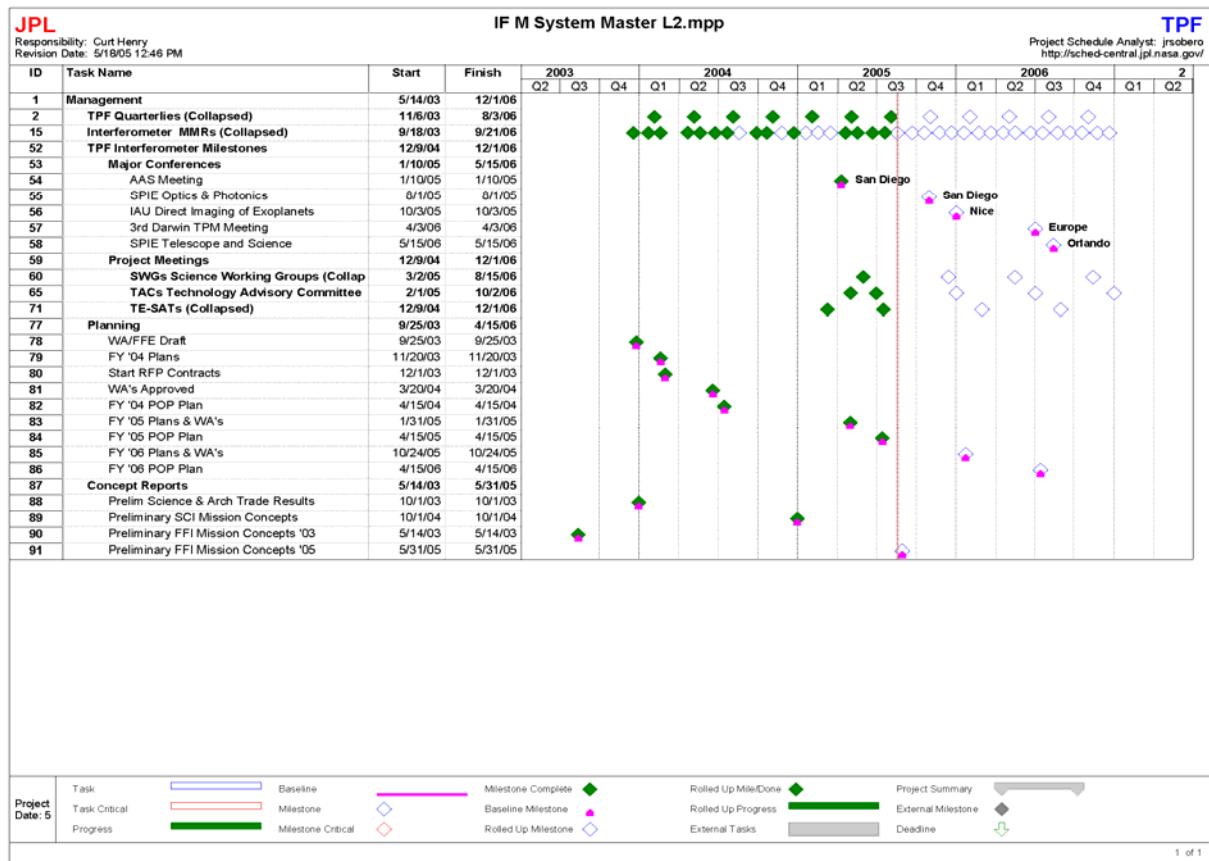


**Figure C-1.** Schedule of Project-Level Activities
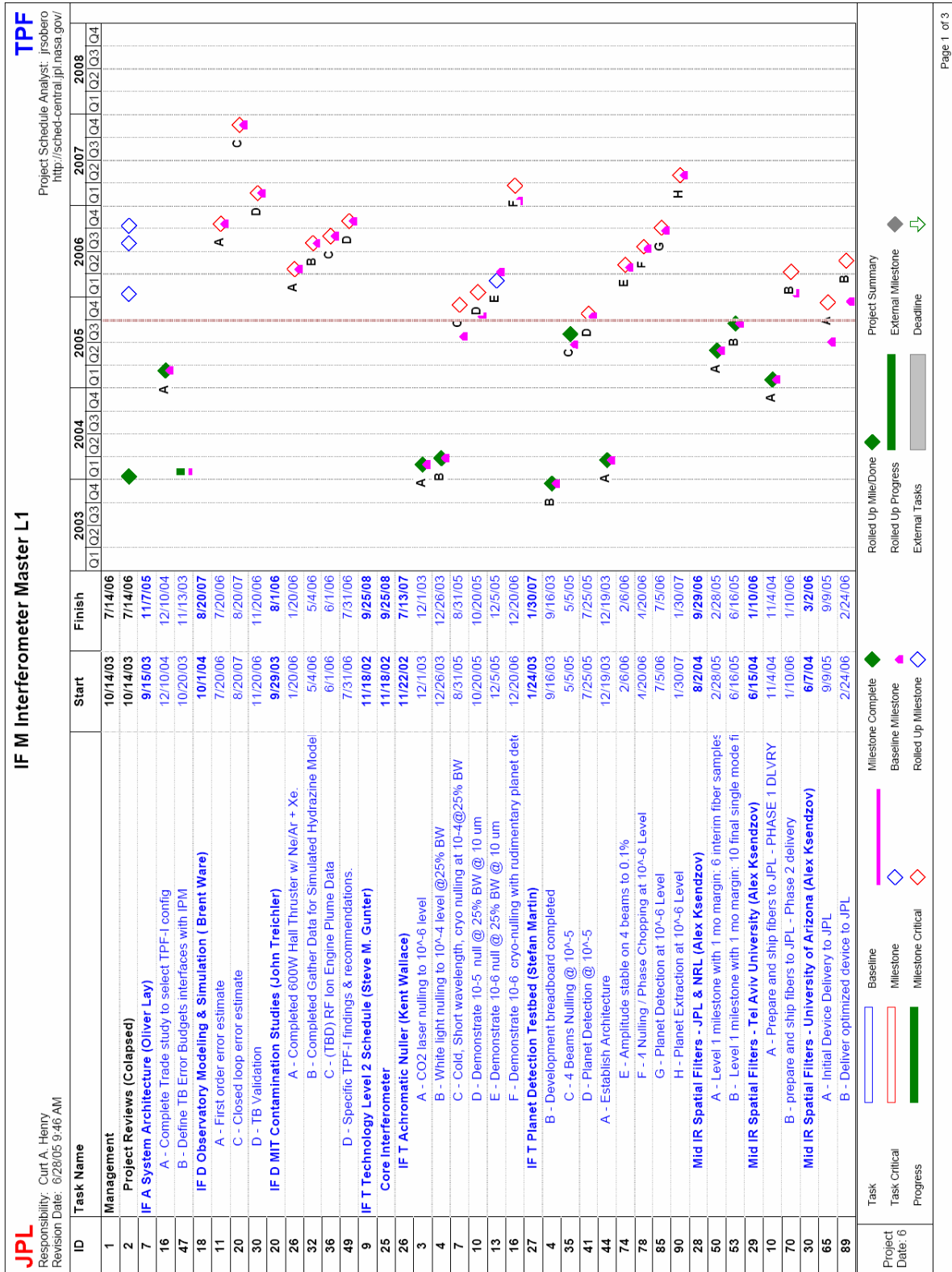
**Figure C-2.** Schedules of TPF-I Testbeds and Tasks (First of Three Charts)
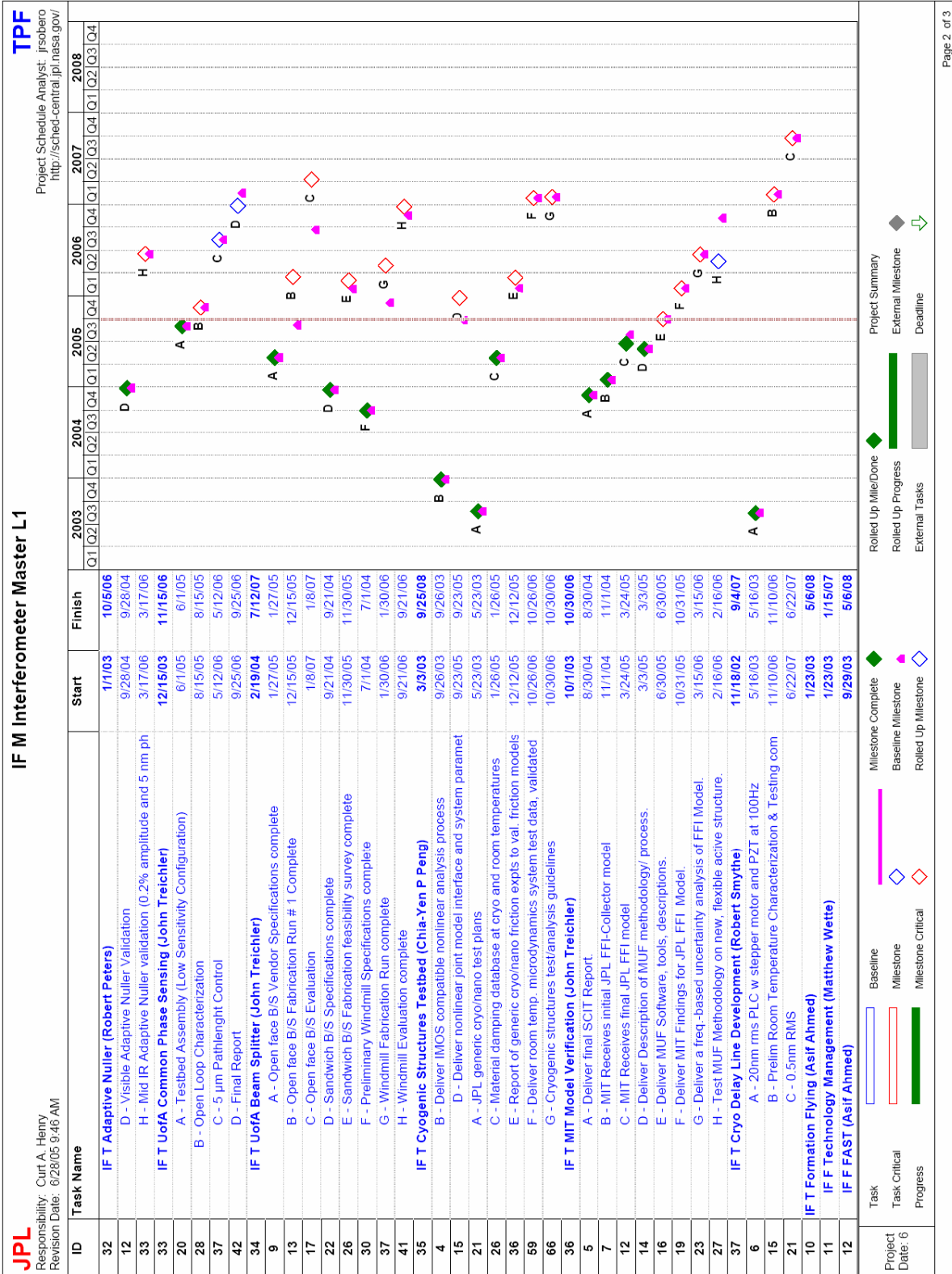
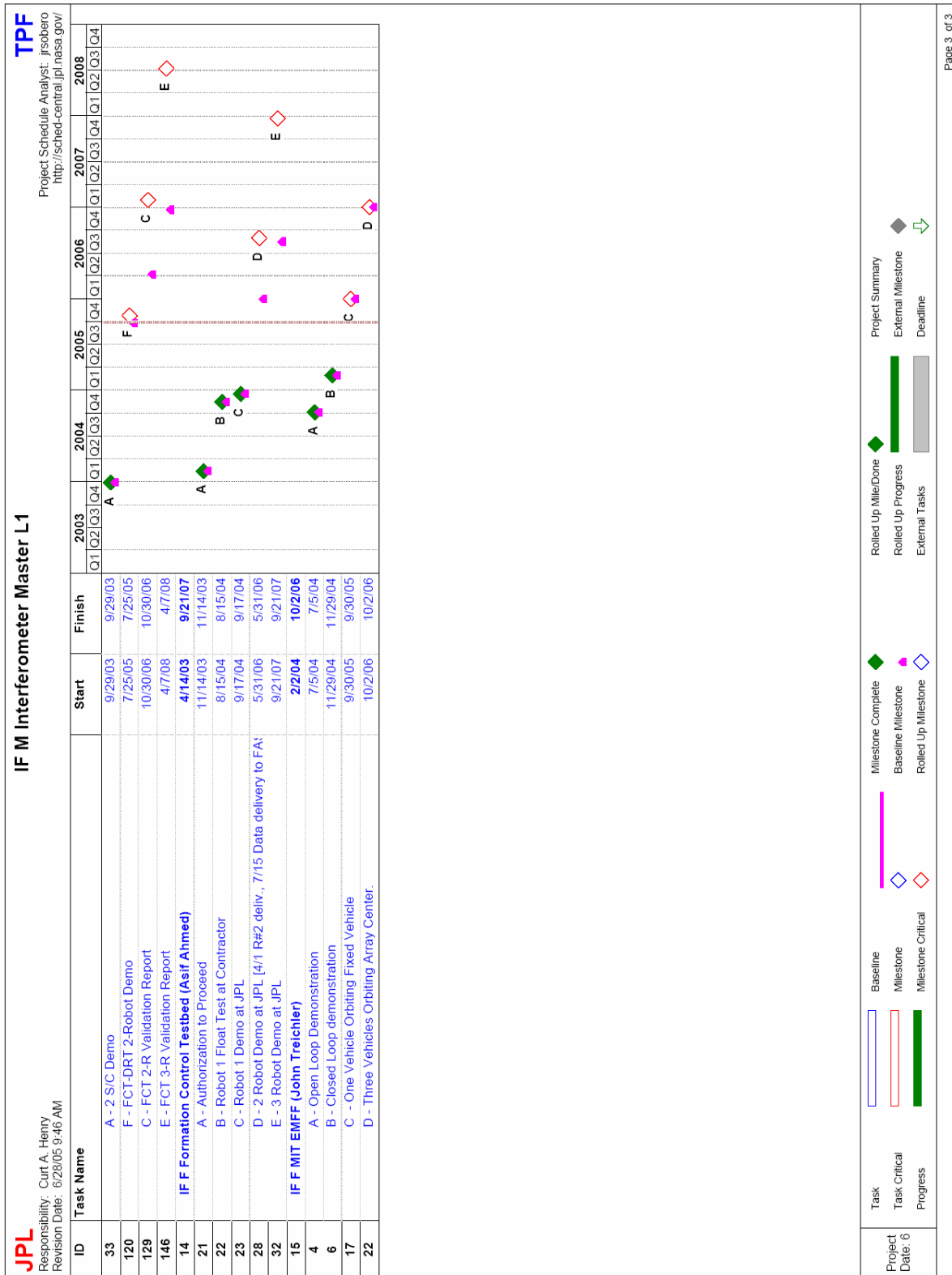**Figure C-3.** Schedules of TPF-I Testbeds and Tasks (Second of Three Charts)

**Figure C-4.** Schedules of TPF-I Testbeds and Tasks (Third of Three Charts)

# Appendix D
# Science Working Group

Table D-1 lists the members of the TPF-I Science Working Group.  Twenty-two representatives from the astronomical community and one ex officio member were named to the TPF-Interferometer Science Working Group (TPF-I SWG). They will work closely with the TPF project to develop science rationale for the mid-IR observing program, help guide the appropriate technology, and interface with their counterparts on the European Space Agency's Terrestrial Exoplanet Science Advisory Team and Darwin project. As representatives of the broad astronomical community, the TPF-I SWG is expected to act as the science conscience of the project, ensuring that the broad TPF-I science goals are worthy of the mission and that the mission will be able to fulfill them. Specific tasks of the TPF-I SWG may include, but are not limited to:

1. Refining, as necessary, TPF-I science goals, as embodied in the Design Reference Mission, and assessing the impact of altering mission design parameters (orbit, mission duration, telescope size, instrument complement, etc.) on these science goals.

2. Assessing design concepts, technology and implementation plans relative to the overall scientific performance of the mission.

3. Assisting NASA in explaining the goals of TPF-I to the larger astronomy community and in preparing materials for review by external scientific advisory groups and oversight committees.

4. The TPF-I SWG will produce a Science Requirements document. This document will include the prioritized science objectives and requirements for the planet finding and characterization and general astrophysics aspects of the TPF-I mission.

The duration of the appointments is approximately three years.

**Table D-1.  Members of the TPF-I Science Working Group (2005-2008)**

| Name | Institution |
|---|---|
| Akeson, Rachel | Michelson Science Center, CalTech |
| Bally, John | University of Colorado |
| Beichman, Charles (ex officio) | Michelson Science Center, CalTech |
| Crisp, David | Jet Propulsion Laboratory |
| Danchi, William | GSFC |
| Falkowski, Paul | Rutgers University |
| Fridlund, Malcolm | ESA/ESTEC |
| Hinz, Phil | University of Arizona |
| Hollis, Jan M. (Mike) | GSFC |
| Hyland, David | Texas A&M University |
| Johnston, Kenneth (chair) | US Naval Observatory |
| Lane, Ben | MIT |
| Laughlin, Gregory | UC Santa Cruz |
| Liseau, Rene | Stockholm Observatory, Sweden |
| Mennesson, Bertrand | Jet Propulsion Laboratory |
| Monnier, John | University of Michigan |
| Noecker, Charley | Ball Aerospace |
| Quillen, Alice | University of Rochester |
| Röttgering, Huub | Leiden University, Netherlands |
| Serabyn, Gene | Jet Propulsion Laboratory |
| Wilner, David | Harvard-Smithsonian Center for Astrophysics |
| Woolf, Nick | University of Arizona |

# Appendix E
# Technology Advisory Committee

**Table E-1.  TPF Technology Advisory Committee**

| Name | Institution |
|---|---|
| Peter Lawson (Co-Chair) | Jet Propulsion Laboratory |
| Jennifer Dooley (Co-Chair) | Jet Propulsion Laboratory |
| Ron Allen | Space Telescope Science Institute |
| Chris Burrows | Metajiva |
| Rich Capps | Jet Propulsion Laboratory |
| Dick Dyer | Schafer Corporation |
| Mike Krim | Perkin-Elmer, retired |
| Bruce MacIntosh | Lawrence Livermore National Laboratory |
| Pete Mason | California Institute of Technology |
| Dave Mozurkewich | Seabrook Engineering |
| Jason Speyer | UCLA |

# Appendix F
# Flight System Configuration

Tables F-1 through F-5 describe the flight-system configuration studied by the TPF-I design team. The interferometer under consideration was a 4-telescope dual-Bracewell interferometer.

**Table F-1.  Mission Summary**

| Parameter | Preliminary Requirements |
|---|---|
| Number of collector spacecraft | 4 |
| Number of combiner spacecraft | 1 |
| Design life | 5 years |
| Mission orbit | L2 Halo |
| ΔV (TCM's and L2 injection) | 105 m/s |
| Launch vehicle | Delta 4050H |
| Lift mass | 9408 kg |
| Margin | 30 % |

**Table F-2.  Design Team Power Allocations**

| DC Power | Collector | Combiner |
|---|---|---|
| Payload | 75 W | 475 W |
| Downlink | 58 W | 78 W |
| Housekeeping | 537 W | 557 W |
| Reserve | 192 W | 335 W |
| Total | 862 W | 1445 W |

**Table F-3.  Design Team Mass Allocations**

| Mass | Collector | Combiner |
|------|-----------|----------|
| Payload (each) | 550 kg* | 461 kg |
| Spacecraft (each) | 605 kg | 684 kg |
| Reserve (each) | 276 kg | 268 kg |
| Total (each) | 1431 kg | 1413 kg |
| Launch mass | 5724 kg | 1413 kg |

*Collector payload includes 391 kg primary mirror with aerial density of 30 kg/m$^2$

**Table F-4.  TPF-I Combiner Spacecraft Design Summary**

| Parameter | Design Team Allocation |
|-----------|------------------------|
| Architecture | Modular, process-driven, fully redundant |
| Attitude control | 3-axis, zero-net-momentum |
| Attitude determination | Star trackers, inertial reference unit |
| Attitude control actuators | 4 reaction wheels, 16 RCS thrusters |
| Formation acquisition sensors | S-band and sensors |
| Propulsion / RCS | Ion thrusters, Isp = 2500–3500 s |
| Delta-V capability | 750 m/s |
| Solar array type / size | Rigid panel, 9.0 m$^2$ |
| Solar cell type | Cascade multi-junction, 28% efficiency (BOL) |
| Array power (EOL) | 1455 W (45° off-point) |
| Battery type / Capacity | Li-ion, 72.7 A-h |
| Thermal shield | 5-layer, deployable sunshade |
| Telecommunications | X-band up / Ka and X-band down |
| Data rates up/down | 2 Kpbs / 1 Mbps (Ka-band) 16 Kbps (X-band) |
| Inter-spacecraft telecommunications | UHF full-duplex, 2.0 Mbps |

**Table F-5.  TPF-I Collector Spacecraft Design Summary**

| Parameter | Design Team Allocation |
|---|---|
| Architecture | Modular, process-driven, fully redundant |
| Attitude control | 3-axis, zero-net-momentum |
| Attitude determination | Star trackers, inertial reference unit |
| Attitude control actuators | 4 reaction wheels, 16 RCS thrusters |
| Formation acquisition sensors | S-band and sensors |
| Propulsion / RCS | Ion thrusters, Isp = 2500–3500 s |
| Delta-V capability | 750 m/s |
| Solar array type / size | Rigid panel, 5.4 m$^2$ |
| Solar cell type | Cascade multi-junction, 28% efficiency (BOL) |
| Array power (EOL) | 862 W (45° off-point) |
| Battery type / Capacity | Li-ion, 19.8 A-h |
| Thermal shield | 5-layer, deployable sunshade |
| Telecommunications | X-band up/down (contingency mode) |
| Data rates up/down | 2 Kpbs / 16 Kpbs |
| Inter-spacecraft telecommunications | UHF full-duplex, 2.0 Mbps |

# Appendix G
# Technology Readiness Level Definitions

Technology Readiness Levels (TRLs) are a systematic metric/measurement system that supports assessments of the maturity of a particular technology and the consistent comparison of maturity between different types of technology. The TRL concept is based on a general model for technology maturation that includes: (a) research in new technologies and concepts (targeting identified goals, but not necessarily specific systems), (b) technology development addressing specific technologies for one or more potential identified applications, (c) technology development and demonstration for each specific application before the beginning of full system development of that application, (d) system development (through first unit fabrication), and (e) system launch and operations.

### TRL 1: Basic principles observed and reported

Transition from scientific research to applied research. Essential characteristics and behaviors of systems and architectures. Descriptive tools are mathematical formulations or algorithms.

### TRL 2: Technology concept and/or application formulated

Applied research. Theory and scientific principles are focused on specific application area to define the concept. Characteristics of the application are described. Analytical tools are developed for simulation or analysis of the application.

### TRL 3: Analytical and experimental critical function and/or characteristic proof-of-concept

Proof of concept validation. Active Research and Development (R&D) is initiated with analytical and laboratory studies. Demonstration of technical feasibility using breadboard or brassboard implementations that are exercised with representative data.

### TRL 4: Component/subsystem validation in laboratory environment

Standalone prototyping implementation and test. Integration of technology elements. Experiments with full-scale problems or data sets.

**TRL 5: System/subsystem/component validation in relevant environment**

Thorough testing of prototyping in representative environment. Basic technology elements integrated with reasonably realistic supporting elements. Prototyping implementations conform to target environment and interfaces.

**TRL 6: System/subsystem model or prototyping demonstration in a relevant end-to-end environment (ground or space)**

Prototyping implementations on full-scale realistic problems. Partially integrated with existing systems. Limited documentation available. Engineering feasibility fully demonstrated in actual system application.

**TRL 7: System prototyping demonstration in an operational environment (ground or space)**

System prototyping demonstration in operational environment. System is at or near scale of the operational system, with most functions available for demonstration and test. Well integrated with collateral and ancillary systems. Limited documentation available.

**TRL 8: Actual system completed and "mission qualified" through test and demonstration in an operational environment (ground or space)**

End of system development. Fully integrated with operational hardware and software systems. Most user documentation, training documentation, and maintenance documentation completed. All functionality tested in simulated and operational scenarios. Verification and Validation (V&V) completed.

**TRL 9: Actual system "mission proven" through successful mission operations (ground or space)**

Fully integrated with operational hardware/software systems. Actual system has been thoroughly demonstrated and tested in its operational environment. All documentation completed. Successful operational experience. Sustaining engineering support in place.

# Appendix H
# IR Optics Materials and Coatings

This appendix describes the approach that has been used for the suballocation of requirements to the nulling interferometer optics. The description is an extract of a Request for Information (RFP) that was sent to potential vendors, and is based on the flow down of allowable errors for an interferometer that can correct a range of phase and intensity errors using an Adaptive Nuller. A 7% intensity capture range leads to a residual null requirement of only $10^{-3}$, while a 1-µm phase capture range leaves a residual $10^{-1}$ null requirement. To provide performance margin and a challenge to the prospective coatings vendors (but not an overwhelming challenge), the beamsplitter performance was specified for a $10^{-5}$ null depth.

Future instrument system risk and reliability considerations might drive the design to more challenging requirements. The ability to recover from failure or degradation in the Adaptive Nuller may lead to near full performance nulling capabilities required of the remaining system. These trades would be performed in Phase A or B where the technology capabilities are better understood.

Current baseline design for TPF-I calls for covering the wavelength rage of 7–17 µm with two or more sets of bulk-optics nullers, each dedicated to a certain spectral region. An effort was initiated to procure beamsplitters and optics materials and coatings from various industry and university sources that would enable one or two nullers to cover the entire observation spectrum. This included investigation of coatings and materials issues necessary for cryogenic operation. One specific goal was to evaluate the feasibility of a beamsplitter that is sufficiently symmetric to allow the replacement of the dual-beamsplitter modified Mach-Zehnder approach with a single beamsplitter, which in turn allows simplifications to the optical layout.

A Request for Information was sent to a number of industry optical vendors to determine the current state of the art in fabrication and testing of optics and coatings suitable for use as nulling beam combiners (beamsplitters). As funds are available, the RFI would be followed by the purchase of a prototype nulling beamsplitters.

A Request for Information was released from JPL, that specified the desired optical quantities. Nullers require a highly symmetric layout of components that are very closely matched in their optical properties (power reflection and transmission coefficients R and T; phase shifts on reflection and transmission $\varphi_r$ and $\varphi_t$). Again, these properties must match in both S and P linear polarizations (independently) and at each wavelength over one of the two broad spectral bands planned for TPF-I: "Short-$\lambda$" (7–11 µm) or "Long-$\lambda$" (11–17 µm). The following quantities are to be matched between any pair of beamsplitters in a set of 4:

1. **Reflection coefficient R**   (power/intensity reflection coefficients)
   a.   must match in S polarization and in P polarization (but S need not match P)
   b.   must match at every λ in design band Short-λ (7–11 μm) or Long-λ (11–17 μm)
2. **Transmission coefficient T, T'** (power/intensity transmission coefficients)
   a.   must match in S polarization and in P polarization (but S need not match P)
   b.   must match at every λ in design band Short-λ (7–11 μm) or Long-λ (11–17 μm)
   c.   NOTE:  we require equality of T to T', the transmission in back-to-front direction to within $9.0 \times 10^{-4}$ and will need measurements of T and T' on all 4 beamsplitters.
   d.   NOTE:  it is permissible to match the transmission through a complete traverse of the optic, including beamsplitter coating, glass, and AR coating, rather than addressing individual layers
3. **Phase shift $\varphi_r$ on reflection**  (phase refers to electric field, not intensity)
   a.   must match in S polarization and in P polarization (but S need not match P)
   b.   must match at every λ in design band Short-λ (7–11 μm) or Long-λ (11–17 μm)
4. **Phase shift $\varphi_t$, $\varphi_{t'}$ on transmission**  (phase refers to electric field, not intensity)
   a.   must match in S polarization and in P polarization (but S need not match P)
   b.   must match at every λ in design band Short-λ (7–11 μm) or Long-λ (11–17 μm)
   c.   NOTE:  we require equality of phase shifts from transmission in forward and reverse directions to within $9.0 \times 10^{-4}$ and will need measurements of $\varphi^t$ and $\varphi^{t'}$ on all 4 beamsplitters
   d.   NOTE:  it is permissible to match the transmission through a complete traverse of the optic, including beamsplitter coating, glass, AR coating, rather than addressing individual layers

A full verification that the beamsplitters in a set of 4 are matched according to our specifications might consist of obtaining 48 independent data plots that are instances of the following 6 basic curves:

$R(\lambda)$ = reflection coefficient
$T(\lambda)$ = transmission coefficient (beam enters at front, at beamsplitter coating)
$T'(\lambda)$ =          "              "         (beam traverses backwards, entering at AR coating)
$\varphi_r(\lambda)$ = phase shift on reflection
$\varphi_t(\lambda)$ = phase shift on transmission (beam enters at front, at beamsplitter coating)
$\varphi_{t'}(\lambda)$ =   "       "  "       "          (beam traverses backwards, entering at AR coating)

i.e., a plot of each of these 6 quantities would be required, as a function of wavelength, for each of the 4 matched beamsplitters and for each linear polarization S and P.

The wavelength span of the plots would be either 7 to 11 μm or 11 to 17 μm, depending on whether the beamsplitters were intended for the Short-λ or Long-λ band of TPF-I.  Spectral resolution should be 0.25 μm or finer.

The tolerances are met when the matched beamsplitters show curves that are identical at every wavelength within the targeted spectral band, to within $9.0 \times 10^{-4}$ in each of the following: (power) reflection coefficient; (power) transmission coefficient (back to front transmission pass); phase shift on reflection; and phase shift on transmission (back to front transmission pass).  The above requirement is beam-averaged over a 35-mm diameter beam for a matching pair of optics to achieve a null depth of $10^{-5}$ in S and P polarizations independently.

# Appendix I
# Acronyms

ACS         Attitude Control System
ACTDP       Advanced Cryocooler Technology Development Program
AdN         Adaptive Nuller Testbed
AFF         Autonomous Formation Flying
AFOSR       Air Force Office of Scientific Research
AFRL        Air Force Research Laboratory
AIRS        Atmospheric Infrared Sounder
ANT         Achromatic Nulling Testbed
ARR         Assembly Readiness Review
ASO         Astronomical Search for Origins
ASTER       Advanced Spaceborne Thermal Emission and Reflection Radiometer
ATLO        Assembly, Test, and Launch Operations
CDR         Critical Design Review
CNES        Centre National d'Etudes Spatiales
CTE         Coefficient of Thermal Expansion
CU          University of Colorado
DCB         Dual Chopped Bracewell
DGA         Délégation Générale pour l'Armament
DM          Development Model
DOCS        Dynamics Optics Controls Structures
DOD         Department of Defense
DST         Distributed Spacecraft Technologies
EIRB        External Independent Readiness Board
EM          Engineering Model
EMFF        Electromagnetic Formation Flying
ESA         European Space Agency
ExNPS       Exploration of Neighboring Planetary Systems
FACS        Formation Algorithms & Control System software
FAST        Formation Algorithms & Simulation Testbed
FCT         Formation Control Testbed
FDDS        Formation Dynamics & Devices Simulation software
FF          Formation Flying
FFI         Formation Flying Interferometer
FFTL        Formation Flying Technology Laboratory
FIT         Formation Interferometer Testbed
FST         Formation Sensor Testbed
FWHM        Full Width at Half Maximum
FY          Fiscal Year
HIRDLS      High Resolution Dynamics Limb Sounder

| | |
|---|---|
| HST | Hubble Space Telescope |
| HQ | Headquarters |
| HZ | Habitable Zone |
| Hz | Hertz |
| IHZ | Inner Habitable Zone |
| IMOS | Integrated Modeling of Optical Systems |
| IO | Integrated Optics |
| IPM | Interferometer Performance Model |
| IR | Infrared |
| ISAMS | Improved Stratospheric and Mesospheric Sounder |
| JPL | Jet Propulsion Laboratory |
| J-T | Joule-Thomson |
| JWST | James Webb Space Telescope |
| kHz | Kilo Hertz (1000 Hz) |
| L2 | Sun-Earth Lagrange-2 point |
| LAMP | Laser-Augmented Mobility Power |
| LADAR | Laser Detection and Ranging |
| LBT | Large Binocular Telescope |
| LBTI | Large Binocular Telescope Interferometer |
| LISA | Laser Interferometer Space Antenna |
| LRR | Launch Readiness Review |
| MSTAR | Modulation Sideband Technology for Absolute Metrology |
| MATLAB | Matrix Laboratory |
| MIR | Mid-Infrared |
| MIRI | Mid-Infrared Instrument (for JWST) |
| MIT | Massachusetts Institute of Technology |
| MiXI | Miniature Xenon Ion thruster |
| MMZ | Modified Mach-Zehnder |
| MOPITT | Measurements of Pollution in The Troposphere |
| MUF | Modeling Uncertainty Factor |
| NAR | Non-Advocate Review |
| NASA | National Aeronautics and Space Administration |
| NASTRAN | NASA Structural Analysis Program |
| NGST | Northrop Grumman Space Technology |
| NICMOS | Near Infrared Camera and Multi-Object Spectrometer |
| nm | nanometer ($10^{-9}$ meters) |
| NRA | NASA Research Announcement |
| NRL | Naval Research Laboratory |
| ObSim | Observatory Simulation model |
| OPD | Optical Path Difference |
| ONERA | Office National d'Etudes et de Recherches Aerospatiales |
| OSS | Office of Space Science |
| PAL | Present Atmospheric Level |
| PCI | Peripheral Communications Interconnect local bus |
| PDR | Preliminary Design Review |
| PDT | Planet Detection Testbed |
| PLRA | Program Level Requirements Appendix |
| PMSR | Preliminary Mission Systems Review |
| POP | Program Operating Plan |
| ppb | Parts per Billion |
| PSD | Power Spectral Density |

| | |
|---|---|
| PSR | Pre-Ship Review |
| P-V | Peak to Valley |
| QE | Quantum Efficiency |
| R&A | Research & Analysis |
| RFI | Request For Information |
| RHESSI | Ramaty High-Energy Solar Spectroscopic Imager |
| RMS | root mean-square |
| ROMULUS | Radars Orbitaux Multisatelittes à Usage de Surveillance |
| SBIR | Small Business Innovative Research |
| SIRTF | Space Infrared Telescope Facility |
| SIM | Space Interferometry Mission |
| SNR | Signal-to-noise ratio |
| SPHERES | Synchronized Position Hold Engage and Reorient Experimental Satellites |
| SPIE | International Society for Optical Engineering |
| SWG | Science Working Group |
| TAU | Tel Aviv University |
| TES | Tropospheric Emission Spectrometer |
| TOM | Thermo-Optical Mechanical |
| TPF | Terrestrial Planet Finder |
| TPF-C | Terrestrial Planet Finder Coronagraph |
| TPF-I | Terrestrial Planet Finder Interferometer |
| TRL | Technology Readiness Level |
| TRP | Technology Review Panel |
| UA | University of Arizona |
| V&V | Verification and Validation |
| WFE | Wavefront Error |
| WFS | Wavefront Sensor |
| WFS&C | Wavefront Sensing and Control |

# Appendix J
# Further Reading

*Terrestrial Planet Finder — News*
>  Edited by R. Jackson (Jet Propulsion Laboratory)
>  http://planetquest.jpl.nasa.gov/TPF/tpf_news.cfm

*The Vision for Space Exploration*
>  Sean O'Keefe, NASA Administrator (February 2004)
>  http://www.nasa.gov/pdf/55584main_vision_space_exploration-hi-res.pdf

*A Renewed Spirit of Discovery*
>  President George W. Bush (January 2004)
>  http://www.whitehouse.gov/space/renewed_spirit.html

*General Astrophysics and Comparative Planetology with the Terrestrial Planet Finder Missions*
>  Edited by M.J. Kuchner
>  Jet Propulsion Laboratory, Pasadena, CA: JPL Pub 05-01 (2005)
>  http://planetquest.jpl.nasa.gov/documents/GenAst28b.pdf

*Precursor Science for the Terrestrial Planet Finder*
>  Edited by P.R. Lawson, S.C. Unwin, and C.A. Beichman
>  Jet Propulsion Laboratory, Pasadena, CA: JPL Pub 04-014 (2004)
>  http://planetquest.jpl.nasa.gov/documents/RdMp273.pdf

*New Frontiers in Stellar Interferometry*
>  Edited by Wesley A. Traub
>  SPIE Press: Bellingham, WA: Proc. SPIE 5491 (2004)

*Techniques and Instrumentation for Detection of Exoplanets*
>  Edited by Daniel R. Coulter
>  SPIE Press: Bellingham, WA: Proc. SPIE 5170 (2003)

*Towards Other Earths (Darwin/TPF)*
>  Edited by B. Battrick
>  European Space Agency: ESA SP-539 (2003)

*Technology Plan for the Terrestrial Planet Finder*
>  Edited by C.A. Lindensmith
>  Jet Propulsion Laboratory, Pasadena, CA: JPL Pub 03-007 (2003)
>  http://planetquest.jpl.nasa.gov/Navigator/library/TechPlan_4-4-03RevA.pdf

*Summary Report on Architecture Studies for the Terrestrial Planet Finder*
       Edited by C.A. Beichman, D.R. Coulter, C.A. Lindensmith, and P.R. Lawson
       Jet Propulsion Laboratory, Pasadena, CA: JPL Pub 02-011 (2002)
       http://planetquest.jpl.nasa.gov/TPF/arc_index.cfm


*Origins Roadmap 2003*
       Origins Science Subcommittee
       Jet Propulsion Laboratory, Pasadena, CA: JPL Pub 400-1060 (2002)
       http://origins.jpl.nasa.gov/library/roadmap03/


*Astronomy and Astrophysics in the New Millennium*
       National Academies Press (2001)
       http://www.nas.edu/bpa2/nsindex.html


*Biosignatures and Planetary Properties to be Investigated by the TPF Mission*,
       D.J. Des Marais et al,
       Jet Propulsion Laboratory, Pasadena, CA: JPL Pub 01-008 (2001)
       http://planetquest.jpl.nasa.gov/TPF/TPFrevue/BioJun02.pdf


*TPF: A NASA Origins Program to Search for Habitable Planets*
       Edited by C.A. Beichman, N.J. Woolf, and C.A. Lindensmith
       Jet Propulsion Laboratory, Pasadena, CA: JPL Pub 99-3  (1999)
       http://planetquest.jpl.nasa.gov/TPF/tpf_book/index.cfm


*A Road Map for the Exploration of Neighboring Planetary Systems*
       Jet Propulsion Laboratory, Pasadena, CA: JPL Pub 96-22 (1996)
       http://origins.jpl.nasa.gov/library/exnps/index.html